Connectivity within a metapopulation of the foundation species, *Ridgeia piscesae* Jones (Annelida, Siboglinidae), from the Endeavour Hydrothermal Vents Marine Protected Area on the Juan de Fuca Ridge

by

Lara Puetz
BSc., Dalhousie University, 2010

A Thesis Submitted in Partial Fulfillment
of the Requirements for the Degree of

MASTER OF SCIENCE

in the Department of Biology

Supervisory Committee

Connectivity within a metapopulation of the foundation species, *Ridgeia piscesae* Jones (Annelida, Siboglinidae), from the Endeavour Hydrothermal Vents Marine Protected Area on the Juan de Fuca Ridge

by

Lara Puetz
BSc., Dalhousie University, 2010

Supervisory Committee

Dr. Verena Tunnicliffe (Department of Biology, and School of Earth and Ocean Sciences)
Co-Supervisor

Dr. John Taylor (Department of Biology)
Co-Supervisor

Dr. John Volpe (School of Environmental Studies)
Outside Member

Abstract

Supervisory Committee

Dr. Verena Tunnicliffe (Department of Biology, and School of Earth and Ocean Sciences)
Co-Supervisor

Dr. John Taylor (Department of Biology)
Co-Supervisor

Dr. John Volpe (School of Environmental Studies)
Outside Member

The natural instability of hydrothermal vents creates variable environmental conditions among habitat patches. Habitat differences correspond to phenotypic variation in *Ridgeia piscesae*, the only 'vent tubeworm' on the spreading ridges of the Northeast Pacific. *Ridgeia piscesae* that occupy high fluid flux habitats have rapid growth rates and high reproductive output compared to tubeworms in habitats with low rates of venting fluid delivery. As recruitment occurs in all settings, worms in the "optimal habitat" may act as source populations for all habitat types. *Ridgeia piscesae* is a foundation species in the Endeavour Hydrothermal Vents Marine Protected Area of the Juan de Fuca Ridge.

The objective of this thesis was to assess fine scale population structure in *Ridgeia piscesae* within the Endeavour vent system using genetic data. Population structure was assessed by analysis of the mitochondrial *COI* gene in 498 individuals collected from three vent sites of the Juan de Fuca Ridge; Middle Valley (n=26), Endeavour Segment (n=444) and Axial Volcano (n=28). Genotyping using microsatellite markers was attempted but all loci developed for closely related tubeworm species failed to amplify microsatellites in *Ridgeia piscesae*.

Sequence analysis identified 32 mitochondrial *COI* haplotypes; one dominant haplotype (68%), three common haplotypes (4%-7%) and the remainder were rare (<2%). Axial Volcano was differentiated from Middle Valley and Endeavour. Within Endeavour, genetic sub-structuring of *Ridgeia piscesae* occurred among vent fields (Clam Bed, Main Endeavour and Mothra) and habitat types < 10 km apart. Patterns of genetic variation and coalescent based models suggested that gene flow among vent fields moved in a north to

south direction in individuals from high flux habitat but from south to north in individuals from low flux habitat. Tubeworms from low flux habitat had more nucleotide polymorphisms and haplotypes than those from high flux habitats. Estimates of the number of immigrants per generation moving from high flux to low flux subpopulations was four times higher than in the reverse direction. The effective population size was estimated to be three times greater in high flux habitat when the generation times for individuals from each habitat type were considered. Demographic tests for population equilibrium identified a recent and rapidly expanding metapopulation at Endeavour.

Models of gene flow in *Ridgeia piscesae* reflected the general oceanographic circulation described at Endeavour. Genetic data illustrate that dispersing larvae exploit the bi-directional currents created through plume driven circulation within the Endeavour axial valley and suggest that adult position on or near chimneys may influence larval dispersal trajectories upon release. Building on known ecological and biological features, this study also showed that *Ridgeia piscesae* from limited and ephemeral high flux habitat act as sources to the overall metapopulation and that asymmetrical migration and habitat stability sustain high genetic diversity in low flux sinks. The overall metapopulation at Endeavour experiences frequent extinction and recolonization events, differences in individual reproductive success, and source-sink dynamics that decrease the overall effective size and genetic diversity within the population. These factors have important implications for the conservation of a foundation species.

Table of Contents

List of Tables

List of Figures

Acknowledgments

First and foremost I would like to thank my supervisors Verena Tunnicliffe and John Taylor for their guidance, patience, encouragement and most of all their shared knowledge. I appreciate all of the opportunities you both made possible over the last two years. I would also like to thank my committee member John Volpe for your words of wisdom and support throughout the process of this degree. It would be impossible not to thank Jon Rose for his undying day to day support, to not only myself, but to all SEOS graduate students. A special thanks to Sarah Cockburn for helping me through those early days in the lab, your calm confidence and shared laughter went a long way. I would also like to thank Jessica Mackenzie for your help with the microsatellite work. It was fun working with you. Thank you to all my fellow Tunnicliffe and Taylor lab mates, Jackson Chu, Jessica Nephin, Cherisse Du Preez, Emily Morris and Tom Iwanicki whom have been both friends and support systems throughout this degree. Your questions, interests and suggestions allowed me to look at things from a different perspective and communicate my research more effectively. I am grateful to Belaid Moa from Compute Canada for his assistance with running my data on the Nestor computer cluster, taking the time explain high performance computing to me and helping me write my program scripts. Thank you to Peter Beerli for walking me through MIGRATE. Thanks to CHONe for their funding support and incredible learning opportunities. I would also like to thank NEPTUNE Canada for taking me out to Endeavour. Thanks to the Perlman and Hintz labs for your shared knowledge in the lab. Finally, I would like to thank Jean-Pierre Desforges for your editing skills and most of all your support.

Dedication

I dedicate this thesis to the wilderness that still remains untouched and to those who diligently fight to preserve it.

Also, to my family. Their love, laughter and support remind me to appreciate and enjoy even the simplest moments throughout the day.

Chapter 1 -
General Introduction

1.1 Background

1.1.1 Motivation for this study

The nature of fluid delivery through hydrothermal conduits creates ephemeral and naturally fragmented habitat patches hosting productive communities of vent-endemic species. The mosaic of highly variable habitats provides an interesting opportunity for studying metapopulation processes including source-sink dynamics (Jollivet *et al.* 1999). Habitat differences correspond to phenotypic variation in *Ridgeia piscesae* (Phylum: Annelida, Class: Polychaeta, Family: Siboglinidae) (Tunnicliffe *et al.* in review; Southward *et al.* 1995; Black *et al.* 1998; Carney *et al.* 2002), the only 'vent tubeworm' and a foundation species at the Endeavour Hydrothermal Vents Marine Protected Area (Southward *et al.* 1995; Tsurumi & Tunnicliffe 2003; Urcuyo *et al.* 2003). *Ridgeia piscesae* that occupy high fluid flux habitats have rapid growth rates and high reproductive output compared to worms in low flux habitats (Tunnicliffe *et al.* in review; St. Germain 2011). Venting delivers reduced compounds dissolved in hydrothermal fluids; such compounds fuel chemoautotrophic microorganisms that provide the primary energy source for *Ridgeia piscesae* (Corliss *et al.* 1979; Karl *et al.* 1980; Jannasch & Wirsen 1981; Cavanaugh *et al.* 1981). As recruitment occurs in all settings, worms in the "optimal habitat" may act as source populations to all habitat types (Tunnicliffe *et al.*, in review; St. Germain 2011). The goal of this thesis was to estimate population connectivity by linking patterns of genetic variability and gene flow data to our current understanding of the ecology and biology of *Ridgeia piscesae.* Genetic data have the potential to identify signatures of metapopulation processes and source-sink dynamics.

1.1.2 Dispersal and connectivity

Dispersal strategies, especially for spatially separated subpopulations, are critical to the persistence and resilience of any population. For many marine organisms, dispersal occurs at the earliest life history stage (spore, egg, larvae) prior to settlement and

metamorphosis into a benthic adult life. Early life history traits, seafloor topography and oceanographic currents play important roles in determining the success of planktonic larval dispersal, where larvae are vulnerable to starvation and predation or lost by transport via currents to inhospitable environments (Palumbi 2003; Cowen & Sponaugle 2009). The extent to which a species is linked by the successful dispersal and survival of individuals within its range is a measure of population connectivity (Palumbi 2003; Cowen & Sponaugle 2009). Larval quality and behaviour, pelagic larval duration, and current patterns determine the distance over which larvae can travel away from its source and therefore influence how marine populations are connected (Cowen 2000; Kinlan & Gaines 2003; Shanks *et al.* 2003).

1.1.3 Metapopulation dynamics

Metapopulations are generally defined as a mosaic of subpopulations with frequent local extinction and recolonization events that facilitate the survival of the overall population (Hanski & Gilpin 1991, 1997; Hanski & Thomas 1994). The fundamental assumption is that the environment consists of discrete habitat patches with independent local dynamics and that the inhabitants are connected through migration (Hanski & Gilpin 1997; Hanski 1999). Metapopulations persist only when the rate of extinction is less than the rate of colonization into available habitat patches therefore, when connectivity is low, the viability of the overall population is threatened (Hanski & Gilpin 1997). Typically, there is a compromise between patches being close enough together to facilitate rapid colonization, and thus rescue the population, but far enough apart that their dynamics are not synchronized (Hanski & Gilpin 1997; Hanski 1999). The stability of the overall demographic system therefore relies on effective dispersal for rapid colonization. Metapopulation persistence is also positively correlated with the frequency of habitat patches, which decreases the chances of all populations going extinct at once, increases the overall number of available migrants, and allows more time for rescue (Hanski & Gilpin 1997).

1.1.4 Source-sink metapopulations

Within a metapopulation there may be differences in the quality of suitable habitats, which introduces the concept of source-sink dynamics in a patchy heterogeneous environment (Pulliam 1988). A source-sink metapopulation is a special case of a metapopulation structure in which one or more source populations, occupying optimal habitat, yield a net demographic excess of individuals that migrate into sink populations (Dias 1996; Hanski & Gilpin 1997). Individuals in source populations generally have higher fitness and reproductive success, due to better quality habitat, causing local births on average to exceed local deaths (Pulliam 1988). Sink populations have intrinsic growth rates less than zero because they reside in poorer quality habitats, where resources are scarce, and reproduction is insufficient to balance out local mortality (Pulliam 1988). As a result, sink populations are maintained through immigration from the surplus of individuals in source habitats (Pulliam 1988; Dias 1996).

Sources are generally thought of as larger and more persistent populations however, sinks can have higher densities than sources if optimal habitats are rare and immigration rates into sinks exceed local mortality rates (Pulliam 1988; Purcell & Verner 1998). Source-sink dynamics are common in populations where dispersal is driven by abiotic factors, such as wind or currents and, in fact, evolve from either passive dispersal or intraspecific competition in heterogeneous environments (Pulliam 1988; Loreau *et al.* 2013). Which sites will be a source or a sink is governed by the extent of variability between habitats and how they are connected through dispersal (Mathias *et al.* 2001; Parvinen 2002). In reality, populations within a metapopulation likely fall along a continuum from sources to sinks and it is not uncommon for one to switch to the other due to temporal fluctuations within the system (Thomas & Kunin 1999; Loreau *et al.* 2013).

1.1.5 Genetic approaches to measure connectivity

Estimating connectivity depends on quantifying dispersal however, this is extremely challenging, especially for many marine organisms. Genetic methods have become key tools in population and conservation biology as molecular variation has the

ability to detect and retain historical and current patterns of variation within populations. Genetic indices can be used to estimate rates of migration among subpopulations and therefore play an important role in studying connectivity and the evolutionary consequences of dispersal (Hedgecock *et al.* 2007a; Lowe & Allendorf 2010). Gene flow among populations can be measured by both indirect and direct methods depending on how you sample the population and the molecular markers and statistical tools you use (Lowe & Allendorf 2010). Indirect methods estimate gene flow from the amount of genetic differences among subpopulations and are based on population genetic theory, therefore generally assume population equilibrium (Slatkin 1993; Hedgecock *et al.* 2007a). Genetic differentiation among subpopulations has traditionally been measured by the fixation index (F_{ST}) with values ranging from 0-1; 0, when subpopulations are genetically identical and 1, when subpopulations share no alleles (Hedgecock *et al.* 2007a). Estimates of the number of migrants per generation among subpopulations are generally formed by $N_em = (1–F_{ST})/(4F_{ST})$, where N_e is the effective population size and m is the proportion of migrants entering a population each generation (Hedgecock *et al.* 2007a). When $N_em = 0$ and $F_{ST} = 1$, absence of connectivity is inferred. Recent progress in population genetics theory proposes measures of gene flow indirectly through coalescent-based approaches that generally tend to be more reliable and less biased than the traditional methods mentioned above (Beerli & Felsenstein 2001). Coalescent based models use genealogical information from raw sequence data that generally provide more reliable and less biased estimates of genetic exchange among subpopulations than summary statistics, such as F_{st} values (Beerli & Felsenstein 2001). Direct genetic methods (e.g., assignment tests) are conceptually similar to non-genetic approaches to estimating connectivity (e.g., marking individuals) as they use multiple genotypes to assign individuals sampled from across a species' distribution to their place of origin (Paetkau *et al.* 1995; Manel *et al.* 2005; Hedgecock *et al.* 2007a; Lowe & Allendorf 2010).

1.2 Study System

1.2.1 Chemosynthetic ecosystems at hydrothermal vents

It is difficult to understand the ecology of hydrothermal vents without first considering the geological processes that drive these systems. Deep sea hydrothermal venting occurs along the seafloor where the youngest crust is being formed (Corliss *et al.* 1979); active spreading centers along mid ocean ridges, back-arc basins and seamounts (Figure 1.1). Seawater is superheated as it percolates down through the oceanic crust near rising magma (reviewed in Van Dover 2000). The chemical composition of the fluid is altered as it extracts metals, minerals and reduced compounds from the crust, prior to being expelled from the seafloor through focused hydrothermal plumes or milder diffuse fluid flow venting (reviewed in Tunnicliffe *et al.* 2003). Fluid flows vary depending on the local permeability of the rock, pressure and temperature characteristics within the system, which are dynamic and change as the system ages (Davis *et al.* 2001; Fisher & Harris 2010). The rate of venting fluid delivery increases as temperature increases.

Focused venting can reach temperatures greater than 400°C and when these fluids mix with cold ambient seawater, their pH is altered, causing minerals to precipitate out of solution (reviewed in Tunnicliffe *et al.* 2003). These precipitates may form tall sulphide structures, such as columnar chimneys, along the seafloor that can grow 10-30 m in height (reviewed in Van Dover 2000). Diffuse venting occurs when hydrothermal fluids mix with ambient seawater below the surface of the seafloor prior to escaping from cracks in the basalt. As a result, diffuse venting fluids are much more dilute and have lower temperatures, generally between 2-10°C. Venting delivers reduced compounds dissolved in hydrothermal fluids; such compounds fuel chemoautotrophic microorganisms that provide the primary energy source for vent communities (Corliss *et al.* 1979; Karl *et al.* 1980; Jannasch & Wirsen 1981; Cavanaugh *et al.* 1981).

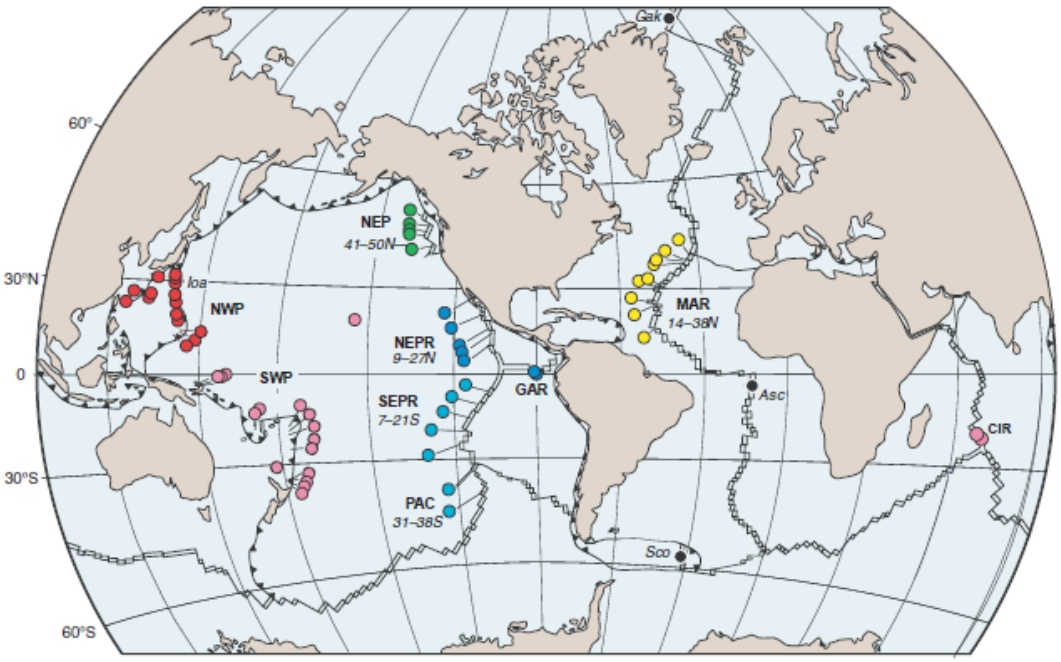

Figure 1-1: Worldwide distribution of deep-sea hydrothermal vents known to support chemosynthetic communities. Spreading centres are indicated with double lines, and subduction zones are indicated with directional arrowheads. Figure taken from (Vrijenhoek 2010). Green dots are vent sites in the Northeast Pacific where a distinct biogeographic province exists.

Some species have adapted to thrive in the extreme conditions of hot vent systems which form communities of endemic species in low diversity but very high biomass (Jollivet 1996; Juniper & Tunnicliffe 1997; Tsurumi & Tunnicliffe 2003). In the absence of sunlight, productivity is fueled by chemosynthetic microbes that metabolize dissolved gases, mainly hydrogen sulfide, in vent fluids to produce the energy to fix inorganic carbon (Corliss *et al.* 1979; Karl *et al.* 1980; Jannasch & Wirsen 1981; Cavanaugh *et al.* 1981). The diversity of microbial life and abundance of unique animals rivals some of the most productive areas on earth and are often referred to as the "oases" of the deep sea (Corliss & RD 1977). Invertebrate species represent a large proportion of the overall biomass at vents, many of which access productivity through mutualistic symbiosis with chemolithoautotrophic microbes (e.g. Cavanaugh *et al.* 1981; reviewed in Dubilier *et al.* 2008). The relationship is mutualistic as both parties benefit. Chemosynthetic bacteria produce organic carbon that provides nutrition to its invertebrate host and in return

receives a regulated environment and supply of reducing substrates (e.g. HS^-) required for chemosynthesis (Felbeck & Somero 1982; Stewart *et al.* 2005; Dubilier *et al.* 2008).

Invertebrate hosts have a variety of life history strategies and morphological adaptations for exploiting the energy rich environment at vents. For example, vestimentiferan tubeworms lack a gut as adults and rely solely on their obligate endosymbionts for all of their nutrition (Cavanaugh et al., 1981; Felbeck 1981; Rau 1981). The extent to which individual host species rely on their symbionts, and consequently the venting fluids that support their symbionts, will shape their distribution around the vents (Van Dover 2000; Neubert *et al.* 2006).

1.2.2 Source-sink metapopulation dynamics at hydrothermal vents

The instability of hydrothermal vents creates variable environmental conditions between habitat patches defined by their differences in temperature, fluid flux and chemical composition of surrounding environments. It is not surprising to observe very different vent assemblages, sometimes within only meters of each other on the seafloor, due to the nature of fluid delivery through hydrothermal conduits (Sarrazin *et al.* 1997; Sarrazin & Juniper 1999). Variation across gradients of venting fluid flux affects chemosynthetic productivity, population structure and species interactions due to differences in physiological tolerances and nutritional requirements for a given vent species (Neubert *et al.* 2006). The patchy distribution of habitats varying in quality combined with the ephemeral nature of vents make them a well suited ecosystem for studying source-sink metapopulation dynamics in a marine setting (Neubert *et al.* 2006). Rapid colonization through migration is essential to the persistence of metapopulations and we therefore expect to see rapid growth rates, high reproductive output and effective dispersal capabilities in species at hydrothermal vents (Vrijenhoek 2010).

1.2.3 Dispersal patterns at hydrothermal vents

Many, but not all, vent organisms are sedentary or have limited migratory capabilities as adults therefore dispersal occurs during free-living larval stages. Rapid colonization into new habitat indicates that many species of vent larvae can promptly and effectively disperse between vent habitats (Tunnicliffe *et al.* 1997; Marcus *et al.* 2009).

Vent species display a range of reproductive strategies, even within a taxon, that influence the timing and number of larvae in the water column and how they interact with the surrounding currents at varying depths (Tyler & Young 1999, 2003). Generally, breeding tends to be continuous throughout the year for most vents species; however, reproductive periodicity occurs in some taxa, such as the *Bathymodiolus azoricus* bivalve and the *Paralvinella palmiformis* polychaete (Tyler & Young 1999).

How long larvae remain in the water column depends on their physiology, behaviour and mode of development; for example, longer pelagic larval duration may be expected from larvae that feed in the water column or from species with non-feeding larvae that can arrest their development in cooler temperatures while dispersing (e.g. the polychaete *Alvinella pompejana*) (Tyler & Young 1999; Pradillon *et al.* 2001; Adams *et al.* 2012). Strong-swimming vent larvae can migrate high up into the water column, where they feed on photosynthetic-based food sources before settling back to vents (e.g. shrimp and crabs) (Figure 1.2) (Dittel et al. 2008). Other species have weak swimming non-feeding larvae that are benthic and remain close to the vents (e.g. limpets) or can be transported above the seafloor passively through differential buoyancy (e.g. tubeworms) (Figure 1.2) (Adams et al. 2012; Mullineaux et al. 2005). Planktonic larval duration, timing of their release and larval position in the water column will determine when and how larvae interact with oceanic currents and ultimately how far they disperse away from their source (Cowen & Sponaugle 2009).

Connectivity of vent species is also influenced by a number of physical processes including ridge geomorphology, oceanographic currents patterns, and the temporal stability of the vents (reviewed in Vrijenhoek 2010). Spreading rates vary among mid-ocean ridge systems and determine habitat longevity, the frequency of newly created vents, and how far apart vent fields are located from one another (Tsurumi & Tunnicliffe 2003; reviewed in Vrijenhoek 2010). Faster spreading centers are less stable, have shorter distances between vent fields and rapid habitat turnover times, whereas, the opposite is true for slower spreading centers (Vrijenhoek 2010).Valley relief is also defined by spreading rates which in turn influences circulation within the region (reviewed in Van Dover 2000). Slow to intermediate rate spreading centers have higher axial walls that

dampen external oceanographic currents within the axial valley and allow plume driven circulation to dominate currents within the system (Thomson *et al.* 2003).

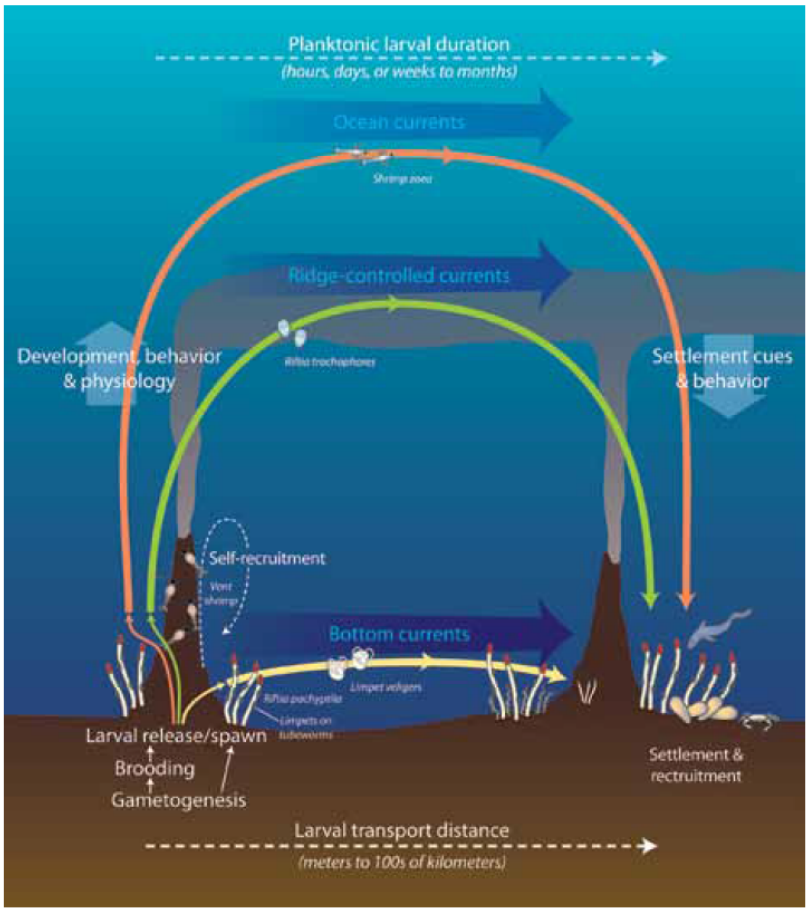

Figure 1-2: A simple model depicting how the interaction between larval biology and currents may affect dispersal among hydrothermal vent communities. Strong swimming larvae can migrate high up into the water column far away from the vents. Weak swimming buoyant larvae may be transported above the bottom whereas other larvae generally remain near bottom and close to the vents. Figure taken from (Adams *et al.* 2012).

Rising hydrothermal plumes set up a circulation cell that may retain larvae near source populations and although this may inhibit dispersal, chances of colonizing suitable habitat within the region may increase (Humphris *et al.* 1995; Thomson *et al.* 2003). Faster spreading centers have lower axial walls which allow physical processes in the overlying water column to have a greater influence on currents, and consequently larval

transport, within the region (Adams et al. 2012). In such systems, passively dispersing larvae are at risk of being exposed to oceanic currents outside the ridge system due to lower valley relief and are potentially advected away from suitable habitat at the vents (Marsh *et al.* 2001; Thomson *et al.* 2003). Gene flow data show little evidence for isolation by distance in most vent species, except on larger spatial scales (thousands of kms), suggesting that vent larvae potentially exist as well-mixed larval pools capable of extensive dispersal within mid-ocean ridge segments but not across transform faults of other large topographic features (Vrijenhoek 1997; Tunnicliffe *et al.* 1998; Black *et al.* 1998).

1.2.4 Study site: Endeavour hydrothermal vents

The unique habitat and high productivity found at the Endeavour Hydrothermal Vents are one of many reasons why it was established as Canada's first marine protected area in 2003 (Tunnicliffe 2000; DFO 2009). The Endeavour segment of the Juan de Fuca Ridge is a hydrothermally active intermediate-rate spreading center located approximately 250 km SW of Vancouver Island (Figure 1.3) (Thomson *et al.* 2003; DFO 2009). With over 800 individual extinct and active chimneys and numerous diffuse flow sites, Endeavour displays a fragmented and dynamic setting, hosting dense biological communities (Kelley *et al.* 2012). The region has five main vent fields, located 2-3 km apart along the axial rift valley (Kelley *et al.* 2001; Thomson *et al.* 2003). The northern vents are older and less hydrothermally active (Sasquatch and Salty Dog) compared to the younger southern vent fields (High Rise, Main Endeavour and Mothra) within axial valley (Kelley *et al.* 2001; Thomson *et al.* 2003). Depth varies from 2170 m in the north to 2300 m in the south (Kelley et al. 2001). Valley relief is between 100-150 m and buoyant plumes may rise approximately 50-350 m off the valley floor and spread laterally (Thomson *et al.* 2003, 2005). Based on observational and modelling data, hydrothermal venting initiates a circulation cell that dominates currents within the system (Thomson *et al.* 2003, 2009).

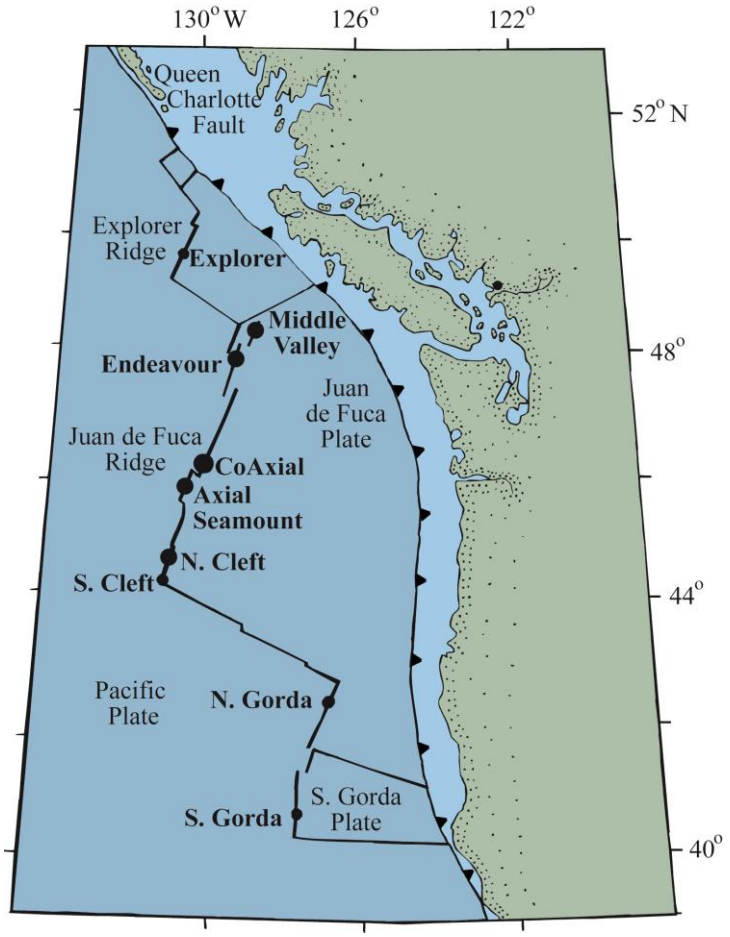

Figure 1-3: Hydrothermal vent sites of the North East Pacific Ridge system. The Endeavour segment is a part of the Juan de Fuca Ridge.

Plume driven circulation at Endeavour creates a cold, near bottom inflow at both ends within the axial valley (Thomson *et al.* 2003, 2005, 2009). Inflow is strongest and predominantly northward at southern and central sectors (~5-10 cm s^{-1}), where the valley is the deepest and hydrothermal activity is most intensive, compared to weaker and predominantly southward inflow in the north (~1 cm s^{-1})(Thomson *et al.* 2003, 2005; Garcia Berdeal *et al.* 2006). At elevations greater than 75 m above the seafloor mean flow in the valley is predominantly southward (Thomson *et al.* 2003, 2005). Based on the highest abundance of multi-species larvae near bottom and close to vent sources at fast spreading centers in the East Pacific Rise, it has been suggested that larvae may preferentially exploit bottom currents at Endeavour (Kim & Mullineaux 1998; Mullineaux *et al.* 2005, 2013; Garcia Berdeal *et al.* 2006). However, slower to

intermediate spreading regions, like Endeavour, have higher axial walls that may allow for the transport of larvae downstream in currents higher off the seafloor but still within the valley (Thomson *et al.* 2003). A larval transport model at Endeavour has been proposed where near bottom northward flow may aggregate and retain larvae near central buoyancy sources prior to being exported downstream in a southward current, greater than 75-100 m above the valley floor (Thomson *et al.* 2003).

1.3 Study Species

Ridgeia piscesae is the only 'vent tubeworm' on the Juan de Fuca Ridge. It lacks a digestive tract once it becomes sessile and relies solely on obligate microbial symbionts for all nutrition (Bright & Lallier 2010). Tubeworm symbionts are acquired from the environment during late larval stages, which are eventually incorporated within an internal organ called the trophosome (Figure 1.4) (Southward 1988). *R. piscesae* actively takes up dissolved gases (e.g. HS^-, CO_2, O_2) through their branchial plume, a specialized organ efficient in gas exchange. These metabolites are transported via the vascular system (in dissolved form or attached to hemoglobins that have a high affinity for sulphide) to endosymbionts (Figure 1.4) (Fisher et al. 1997; Childress 1988; Arp & Childress 1983).

Ridgeia piscesae is capable of colonizing many different habitats at hydrothermal vents (Figure 1.5) (Sarrazin et al. 1997; Sarrazin & Juniper 1999). The limited high flux habitat supports a small proportion of the overall tubeworm population, with the remainder supported by the abundant diffuse flow habitat on basaltic substrata (Sarrazin *et al.* 1997; Sarrazin & Juniper 1999; Urcuyo *et al.* 2007). Habitat differences typically occur within meters of one another at the vents, and generally there is a gradient among these differences (Southward *et al.* 1995; Sarrazin *et al.* 1997; Sarrazin & Juniper 1999). High flux, ephemeral habitats are generally characterized by vigorous high temperature venting around sulphide structures, high sulphide concentrations (~200 µM) and rapid turnover rates that can be less than two years (Sarrazin *et al.* 1997; Tunnicliffe *et al.* 1997; Sarrazin & Juniper 1999). Low flux habitats are generally more stable on the basaltic substrata or at the base or flanks of chimneys and are characterized by weak fluid flux venting and therefore low temperature and sulphide concentrations (<0.1µM) at the

plume level of a tubeworm (Tsurumi & Tunnicliffe 2001, 2003; Urcuyo *et al.* 2003). The habitat differences correspond to notable phenotypic variation in tubeworms that has led to studies that confirmed that only one species is present (Southward *et al.* 1995; Black *et al.* 1998; Carney *et al.* 2002). Distance data of allozymes, restriction fragment length polymorphisms (RFLPs) and mitochondrial cytochrome c oxidase subunit I gene revealed no substantial genetic differences among *Ridgeia piscesae* morphotypes (Southward *et al.* 1995; Black *et al.* 1998; Carney *et al.* 2002).

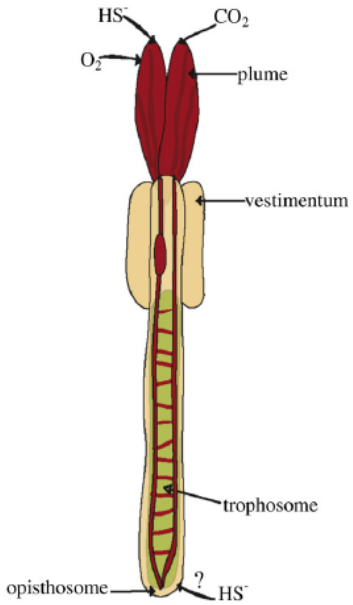

Figure 1-4: Basic morphological body plan of the vestimentiferan tubeworm *Ridgeia piscesae* without the tube. Normally, the plume is the only region visible outside of the tube. Endosymbionts are housed within the trophosome. Figure taken from Carney et al. 2007.

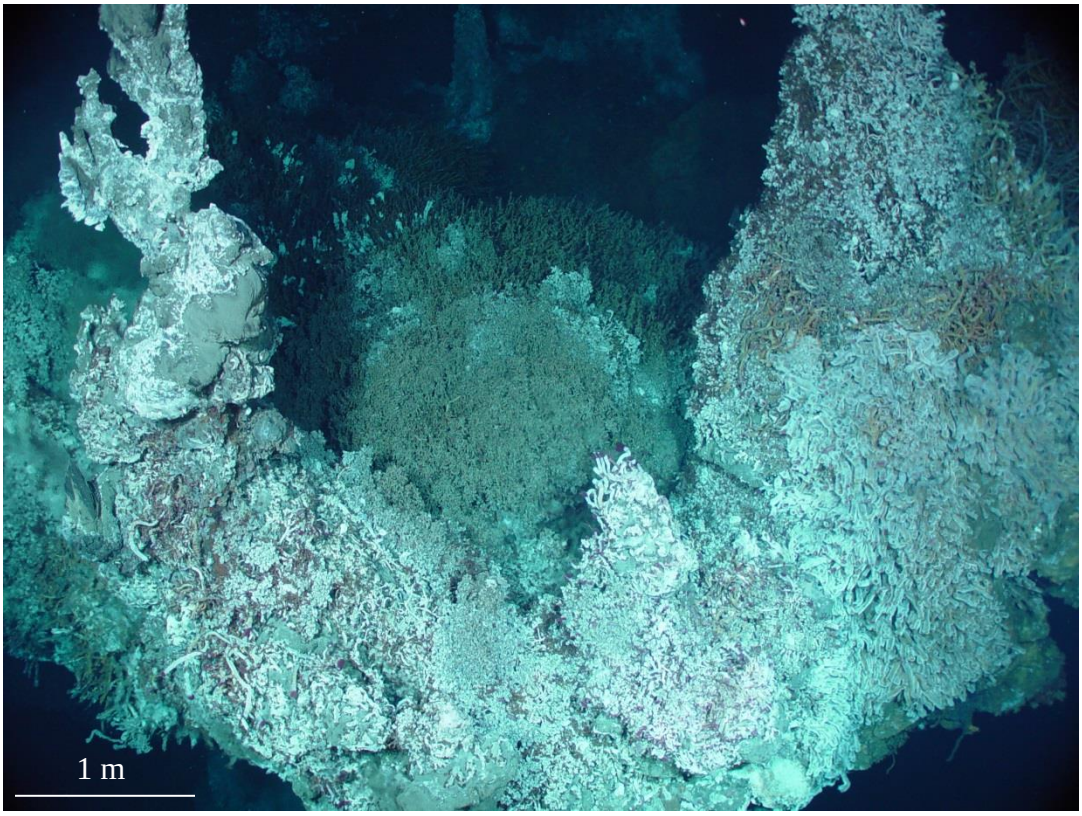

Figure 1-5: Image depicts *Ridgeia piscesae* colonizing variable habitats within meters of one another at the Endeavour Hydrothermal Vents. Image from Tunnicliffe/Juniper 2008 cruise.

Overall, reproductive output is high for *Ridgeia piscesae* and breeding is continuous throughout the year, however, this varies among tubeworm assemblages occupying different habitats at the vents (Tunnicliffe *et al*, in review.; MacDonald *et al.* 2002; St. Germain 2011). Reproductive activity is concentrated in the rare tubeworm assemblages occupying high flux habitats (MacDonald *et al.* 2002; St. Germain 2011). Within a tubeworm cluster, sperm bundles are entangled in the branchial filaments of the anterior portion of the worm and are transferred from the male to the female plume by direct contact with the female (Tunnicliffe *et al.*; MacDonald *et al.* 2002). The proximity of adults and the receptivity of the females will determine the success of fertilization and, factors, such as the reduction or loss of plume branchial filaments due to predation, will likely decrease the probability of sperm transfer (Tunnicliffe *et al.* 1990; MacDonald *et al.* 2002). Successful delivery and attachment of sperm packets to the female vestimentum is followed by internal fertilization before eggs are released into the water column (MacDonald *et al.* 2002; Hilário *et al.* 2005). The female to male sex ratio in

Ridgeia piscesae is 1:1 (Tunnicliffe *et al.* in review; Urcuyo *et al.* 2003; St. Germain 2011).

Tubeworm recruitment occurs in all habitats examined at Endeavour (St. Germain 2011). If we apply observations from other vestimentiferan species, then genetic exchange and colonization is facilitated through slightly buoyant eggs that develop into non-feeding, pelagic trochophore larvae that remain in the water column for several weeks to a month prior to settlement (Marsh et al. 2001; Young et al. 1996). *Riftia pachyptila*, a close relative within the same Family of *R. piscesae*, have a larval stage estimated to disperse over 100 km in 38 days, with a 3-week passive and 2-week active dispersal strategy (Marsh *et al.* 2001). Although these estimates were based on external fertilization, typical for *Riftia pachyptila*, they may remain valid for *Ridgeia piscesae* as embryogenesis does not begin until after fertilized eggs are released in to the water column (Hilário *et al.* 2005). Internal fertilization prior to zygote release is thought to increase the level of fertilization without reducing dispersal potential, which may be ideal for a species living in such variable environments at vents (Hilário *et al.* 2005).

1.4 Research Objectives

The focus of this thesis was to explore fine scale population structure, genetic diversity and genetic connectivity in hydrothermal vent tubeworms within the Endeavour MPA. The tubeworm *Ridgeia piscesae* is a foundation species and has highly variable morphotypes depending on its local habitat (Southward et al. 1995; Tsurumi & Tunnicliffe 2003). Reproductive activity is concentrated in few tubeworm assemblages located in optimal habitat at the vents however, recruitment occurs in all habitat types (MacDonald *et al.* 2002; St. Germain 2011). Regional currents likely influence the transfer of larvae among habitats and sites however, it is uncertain how larvae exploit these currents at Endeavour. Specifically, I hoped to identify whether all individuals contribute equally to the gene pool or whether some areas or worm types have a greater genetic contribution to the overall population by addressing the following two objectives:

1. Assess if patterns of genetic variation and connectivity are consistent with the general oceanographic circulation described at Endeavour.

2. Assess genetic variability and gene flow data at small spatial scales within the Endeavour MPA for genetic signatures of metapopulation processes and source sink dynamics.

Considering the above objectives; one of my thesis goals was to assess genetic connectivity using two different molecular markers; mitochondrial cytochrome oxidase subunit I gene (mtDNA *COI*) and microsatellites. The mitochondrial *COI* gene was previously isolated in *Ridgeia piscesae* and showed considerable genetic variation, therefore it was chosen as an appropriate molecular marker to assess indirect measures of genetic connectivity (Southward *et al.* 1995; Young *et al.* 2008).

My goals for Chapter 2 were first, to determine whether tubeworm phenotypes at habitat extremes had differences in corresponding genotypes. Secondly, I wanted to assess different models of gene flow using a coalescent based approach to address the two objectives of this thesis. Coalescent based models use genealogical information from raw sequence data that generally provide more reliable and less biased estimates of genetic exchange among subpopulations than summary statistics, such as F_{st} values (Beerli & Felsenstein 2001). Wright's F_{ST} based methods assume that populations are in equilibrium (Slatkin, 1993), all subpopulations are of equal size and that migration rates are all symmetric (Beerli & Felsenstein, 2001). When one or all of these assumptions are violated, F_{ST} based methods will deliver wrong population parameter estimates (see Beerli & Felsenstein, 2001).

The goal of Chapter 3 was to amplify microsatellites in *Ridgeia piscesae* to augment *COI* data and to assess genetic connectivity using direct genetic methods. Microsatellites are short tandem repeats that are often used in fine-scaled population genetic studies due to their rapid mutation rates, which generate a large number of alleles (Schlötterer 2000; Estoup *et al.* 2002; Balloux & Lugon-Moulin 2002; Avise 2004; Ellegren 2004; Selkoe & Toonen 2006; Barbará *et al.* 2007).

In the final chapter of my thesis, I provide an overview of the anthropogenic threats to hydrothermal vents and why we need to establish effective conservation strategies prior to industrial exploitation of these vulnerable marine ecosystems. My main goal of Chapter 4 was to address the implications of genetic connectivity identified in

Ridgeia piscesae, an ecologically significant species at Endeavour, for future management plans within the MPA.

Chapter 2 -
Identifying source-sink dynamics and metapopulation processes: Genetic variation and substructure among tubeworms from the Endeavour Hydrothermal Vents Marine Protected Area (Juan de Fuca Ridge)

Introduction

The natural instability of hydrothermal vents creates non-equilibrium conditions between habitat patches defined by their differences in temperature, fluid flux and chemical composition of surrounding environments. Sporadic tectonic and volcanic events episodically destroy local habitats while creating new ones (Johnson *et al.* 2000); thus, hydrothermal vents provide an interesting opportunity for studying metapopulation processes (Jollivet *et al.* 1999). Patterns of genetic variability are influenced by the frequency of local extinction and recolonization events and the extent of connectivity among subpopulations (demes) within the metapopulation (Pannell & Charlesworth 2000). The number, and sources, of successful recruits and rates of gene flow among demes influence the distribution of genetic diversity and differentiation in demographically unstable populations (Pannell & Charlesworth 2000; Hanski & Gaggiotti 2004). Surprisingly, fragmented populations can persist with only a small number of immigrants per year, therefore, insights into patterns of successful dispersal and recruitment are valuable for guiding management polices (Hanski 1991; Stacey & Taper 1992; Beier 1993; Botsford *et al.* 2003; Lubchenco *et al.* 2003; Palumbi 2003). Population parameters, however, are often poorly understood for most marine species (Cowen *et al.* 2007). Genetic tools are useful for understanding demographic history and, when combined with ecological, biological and oceanographic data, may provide reliable estimates of genetic and demographic connectivity of marine species (Cowen & Sponaugle 2009; e.g. Thomas & Bell 2013). For example, extensive oceanographic modeling studies for the New Zealand rock lobster, *Jasus edwardsii*, suggested that source-sink dynamics exist within the overall population that was later confirmed with genetic data (Thomas & Bell 2013).

Few hydrothermal vent studies have focused on fine-scale (meters to 10's of kilometers) population genetics to understand the effects of local dynamics within a habitat patch on the genetic properties of the overall metapopulation. In general, a metapopulation may appear to be panmictic despite substructure among individual patches (Swearer *et al.* 2002; Balloux & Lugon-Moulin 2002). Several studies at vents have assessed genetic differentiation at multiple spatial scales and identified a lack of genetic structure among populations, except at larger spatial scales (100's to 1000's of kilometres) (e.g. Thaler *et al.* 2011; Beedessee *et al.* 2013). However, reduced genetic diversity and demographic instability due to metapopulation processes has been inferred in many hydrothermal vent species (e.g. Hurtado *et al.* 2004; Coykendall *et al.* 2011; Teixeira *et al.* 2012). A rare example of fine scale population structure occurs in the hydrothermal vent tubeworm, *Riftia pachyptila,* which appeared to reveal significant levels of genetic differentiation among tubeworm assemblages less than 400 m apart on the East Pacific Rise using amplified fragment length polymorphisms (AFLP) (Shank & Halanych 2007). However, sample sizes were small and other studies failed to detect similar patterns of small scale structure in *R. pachyptila* using nuclear and mitochondrial DNA, however, (Black *et al.* 1994; Coykendall *et al.* 2011).

Ridgeia piscesae (Class: Polychaeta, Family: Siboglinidae) is the only vestimentiferan tubeworm, and a major foundation species, on the Juan de Fuca Ridge of the northeast Pacific (Figure 2.1). This ecosystem-structuring annelid provides the primary substratum and, in some cases, physical, chemical and predatory protection for many vent species (Southward *et al.* 1995; Tsurumi & Tunnicliffe 2003; Urcuyo *et al.* 2003). As recruits become sessile, siboglinids acquire obligate nutritional endosymbionts that require chemical compounds to synthesize organic carbon (Corliss *et al.* 1979; Karl *et al.* 1980; Jannasch & Wirsen 1981; Cavanaugh *et al.* 1981). Consequently, vent tubeworms rely on dissolved compounds (e.g. HS^-, CO_2, O_2) delivered in the surrounding fluids to fuel their endosymbionts; uptake is through their branchial plume and transported via their vascular system (Figure 2.2) (Fisher et al. 1997; Childress 1988; Arp & Childress 1983).

Ridgeia piscesae is capable of colonizing many different vent habitats and dominates species biomass in most community assemblages (Tsurumi & Tunnicliffe

2003). Habitat differences correspond to phenotypic variation in *Ridgeia piscesae* that has led to studies that confirmed that only one species is present (Southward *et al.* 1995; Black *et al.* 1998; Carney *et al.* 2002). Distance data of allozymes, restriction fragment length polymorphisms (RFLPs) and mitochondrial cytochrome c oxidase subunit I gene revealed no substantial genetic differences among *Ridgeia piscesae* morphotypes (Southward *et al.* 1995; Black *et al.* 1998; Carney *et al.* 2002). Phenotypic plasticity is primarily driven by the flux of dissolved sulphide (Tunnicliffe et al., in review) that is most obvious in tubeworms from habitat extremes. High fluid flux and ephemeral habitats are generally characterized by vigorous high temperature venting around sulphide structures with high sulphide concentrations (~200 µM) and rapid turnover rates (Sarrazin *et al.* 1997; Tunnicliffe *et al.* 1997; Sarrazin & Juniper 1999; Tunnicliffe et al., in review). Low flux habitats are more stable, present on the basalt substrata or at the base and flanks of chimneys, and are characterized by weak fluid flux venting and low temperature and sulphide concentrations (<0.1µM) (Sarrazin *et al.* 1997; Sarrazin & Juniper 1999; Urcuyo *et al.* 2003). Optimal high flux habitat is sparsely distributed, whereas low flux conditions dominate vent field habitats (Sarrazin *et al.* 1997; Sarrazin & Juniper 1999; Tunnicliffe et al., in review).

Differences in morphology, physiology, reproduction and growth in *R. piscesae* reflect the variable hydrothermal vent environments the species inhabits (e.g. Southward *et al.* 1995; MacDonald *et al.* 2002; Urcuyo *et al.* 2003, 2007; Carney *et al.* 2007; St. Germain 2011; Tunnicliffe et al., in review). In high flux habitat, tubeworms defined as the "short-fat" phenotype have fast growth rates of up to 95 cm yr^{-1} and rapid senescence with a longevity of approximately three years (Figure 2.2) (Tunnicliffe *et al.* 1997; Tunnicliffe et al., in review). Low flux habitat support the "long-skinny" phenotype with much slower growth rates, 0 - 25.2 cm yr^{-1} (averaging < 4 cm yr^{-1}) and likely live for decades (Figure 2.2) (Urcuyo *et al.* 2003, 2007). Breeding appears continuous but it is concentrated in few individuals occupying rare high flux habitats (Tunnicliffe *et al.*,in review; MacDonald *et al.* 2002; St. Germain 2011).

Generally, population persistence at hydrothermal vents is sustained by species with rapid growth rates, high reproductive output and effective dispersal and colonization capabilities (Vrijenhoek, 2010). The first two features occur mostly in high flux

tubeworm aggregations. Although little is known about the larval behaviour of this phenotypically plastic tubeworm species, we can draw inferences from other vestimentiferan species. Typically, genetic exchange and colonization initiates through slightly buoyant eggs that develop into non-feeding, pelagic trochophore larvae remaining in the water column for several weeks to a month prior to settlement (Marsh et al. 2001; Young et al. 1996). High estimates of gene flow and connectivity have been reported in *R. piscesae* from several genetic markers at multiple geographic scales (Southward *et al.* 1996; Black *et al.* 1998; Carney *et al.* 2002; Young *et al.* 2008). Phenotypic plasticity may be favoured over local adaptation and eventual speciation (see Cowart *et al.* 2013; Tunnicliffe, in review), as little genetic differentiation and high estimates of gene flow occurs among individuals from each high flux and low flux habitat (Southward *et al.* 1995; Carney *et al.* 2002). However, very small sample sizes and design in these studies may have failed to detect localized genetic structure. Furthermore, tubeworm recruitment occurs in both high flux and low flux habitats (St. Germain 2011).

Mitochondrial DNA (mtDNA) is widely used in population genetic studies (Avise 1998) and, when analyzed with coalescence based methods, can be very useful for characterizing historical patterns of gene flow and fine scaled genetic differentiation (see Swearer *et al.* 2002; e.g Martínez-Solano *et al.* 2006). Mitochondrial DNA has also been useful for identifying demographic instability (Harpending 1994; Alvarado Bremer *et al.* 2005) that may occur in metapopulations (e.g. Hurtado *et al.* 2004; Plouviez *et al.* 2009). Cytochrome c oxidase subunit I (*mtCOI*) encodes a mitochondrial gene that is involved in the electron transport chain of mitochondrial oxidative phosphorylation (Fontanesi *et al.* 2006). Advantages to using the *mtCOI* marker in population genetics include the ease of isolation and data generation of the haploid sequence (Folmer *et al.* 1994) and, more importantly, its rapid mutation rates and lack of recombination due to maternal inheritance (Brown *et al.* 1979; Hartl & Clark 2007). The *mtCOI* gene has previously been isolated in *R. piscesae* and has shown a considerable amount of variation (Black *et al.* 1998; Young *et al.* 2008).

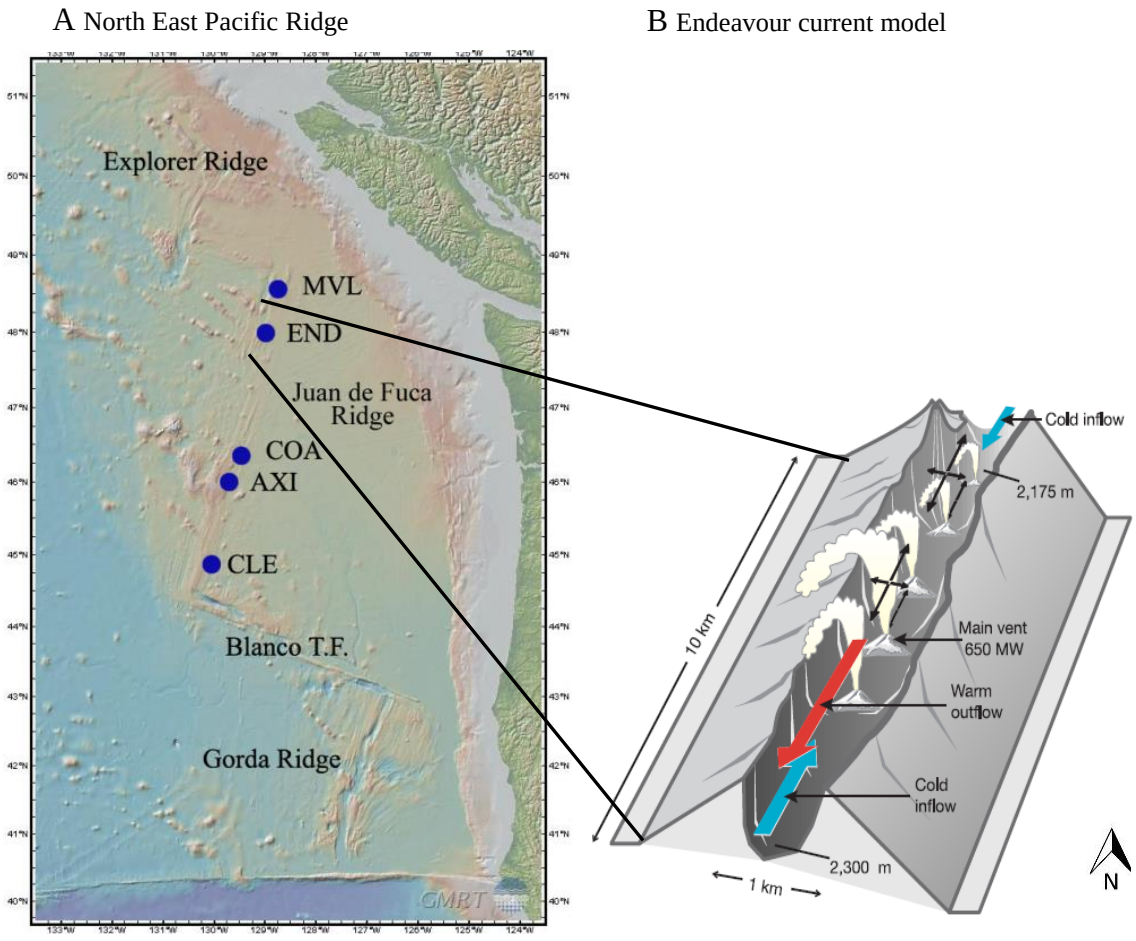

Figure 2-1: Location of sampling sites.

A) The North East Pacific Ridge system highlighting the Endeavour Segment of the Juan de Fuca Ridge. Hydrothermal vent systems sampled in this study include Middle Valley (MVL), Endeavour Segment (END) and Axial Volcano (AXI); additional sites (COA and CLE) were used in the study of Young et al (2008).

B) Diagram of the dominant water flow patterns driven by plume driven circulation, within the axial valley of Endeavour from Thomson et al. (2003). Red arrow shows mean flow at elevations greater than 75 m above the valley floor that is roughly along-axis towards the southwest and often exceeds 5 cm s^{-1}. Blue arrows depict plume induced inflow that is strongest in southern and central sectors of the valley (~5 cm s^{-1}) and weakest at the northern end (~1 cm s^{-1}). Black arrows depict oscillatory currents within the axial valley and above the ridge crest. Plume sizes are roughly proportional to the thermal outputs from the five main vent fields.

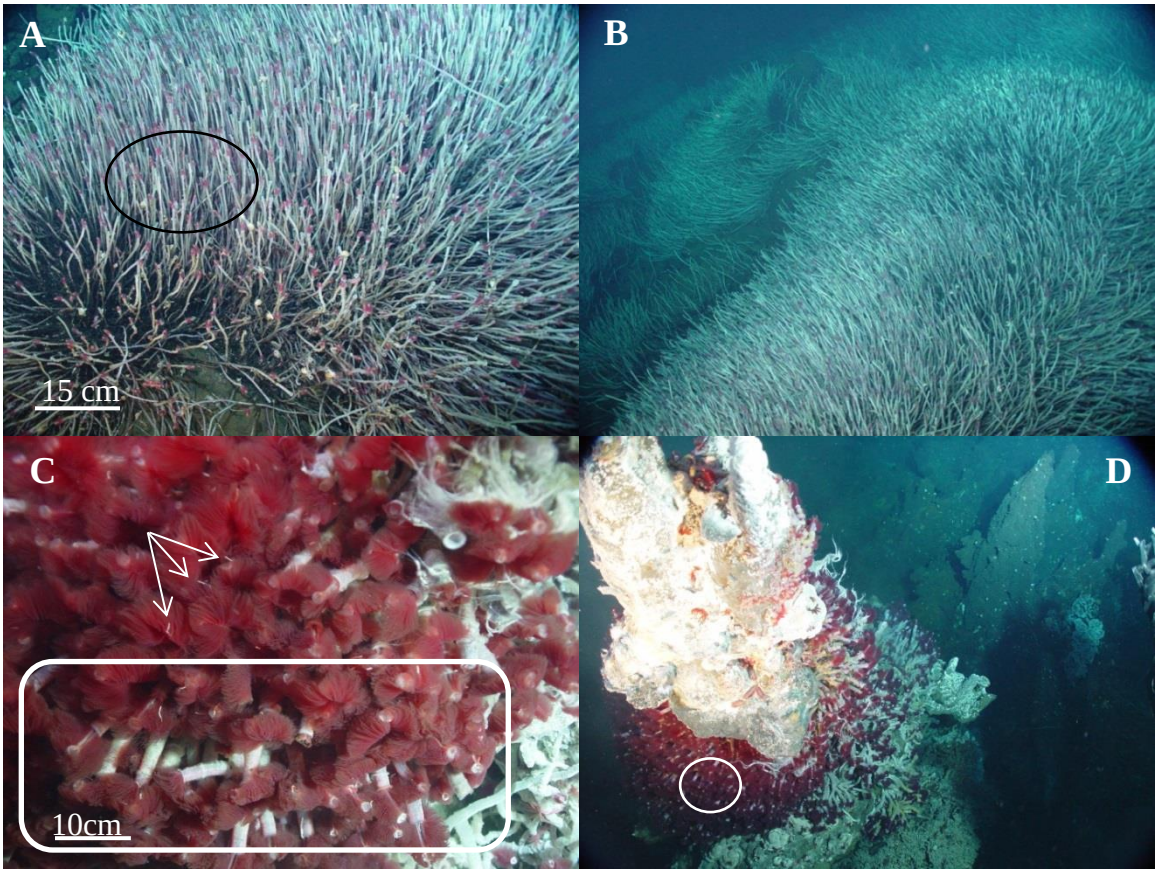

Figure 2-2: Images of "long-skinny" *Ridgeia piscesae* fields on basalt in low flux habitats (A and B) and "short-fat" *Ridgeia piscesae* on sulphide structure in high flux habitats (C and D) at High Rise vent field in the Endeavour Hot Vents MPA. Highlighted areas indicate roughly 50 tubeworms. Arrows in image C are pointing to sperm bundles entangled in branchial filaments. Images from Tunnicliffe/Juniper 2008 cruise.

The Endeavour segment of the Juan de Fuca Ridge is a hydrothermally active intermediate-rate spreading center; the vent site was designated as Canada's first Marine Protected Area (MPA) in 2003 (Figure 2.1; Figure 2.3) (Thomson *et al.* 2003; DFO 2009). The region has five main vent fields, located 2-3 km apart along the roughly linear axial valley that may act as dispersal corridors for vent species (Figure 2.1 B; Figure 2.3 A) (Kelley *et al.* 2001; Thomson *et al.* 2003) over the fragmented habitat (Figure 2.3 B). Valley relief is between 100-150 m and buoyant plumes may rise approximately 50-350 m off the valley floor and spread laterally (Thomson *et al.* 2003, 2005). The buoyant hydrothermal plume drives a circulation at Endeavour that creates a cold, near bottom

inflow at both ends within the axial valley (Figure 2.1 B) (Thomson *et al.* 2003, 2005, 2009). Inflow is strongest and predominantly northward at southern and central sectors (~5-10 cm s^{-1}) where the valley is the deepest (~2300 m) and hydrothermal activity is most intensive. In contrast, the northern sector (~2170 m) is characterized by weaker and predominantly southward inflow (~1 cm s^{-1}) (Thomson *et al.* 2003, 2005; Garcia Berdeal *et al.* 2006). At altitudes greater than 75 m above the seafloor, mean flow in the valley is predominantly southward (Thomson *et al.* 2003, 2005).

The goal of this study is to estimate genetic connectivity in *Ridgeia piscesae* within the Endeavour vent system. Connectivity was estimated by linking patterns of genetic variability and gene flow data to our current understanding of the ecology and biology of *Ridgeia piscesae* and known regional oceanographic circulation. Independent local patch dynamics combined with the clear differences in reproductive success (Tunnicliffe et al., in review) lead to the hypothesis that *Ridgeia piscesae* on the Juan de Fuca Ridge may exist as a metapopulation with a source-sink structure. Using *mtCOI*, I apply several molecular approaches to compare estimators of genetic diversity, differentiation and migration in *R. piscesae* to answer the following questions:

1. Do patterns of genetic variability and gene flow models among vent fields reflect the general oceanographic circulation described at Endeavour?
2. Is there genetic substructure among habitat patches within Endeavour and, if so, do patterns of differentiation and the distribution of genetic diversity reflect metapopulation models?
3. What is the level of gene flow between tubeworm aggregations from high flux and low flux habitat and is it unidirectional?

Materials and Methods

Field collections

Specimens were collected with the remotely operated vehicles (ROV) ROPOS and Jason-2 and with the manned submersible Alvin during research expeditions to hydrothermal vents on the Juan de Fuca Ridge (JDF) (Figure 2.1; Table 2.1). All specimens were collected in the summer of 2008 with the exception of Axial (2007). At

the Endeavour segment (END), *Ridgeia piscesae* was obtained from 14 sites at three vents fields, over 2000 m in depth; Main Endeavour Field (MEF), Clam Bed (CB) and Mothra Ridge (MOT) (Figure 2.3; Table 2.1). Specimens were also collected at one site from Middle Valley (MVL) and at seven sites from Axial Seamount (AXI) (Figure 2.1; Table 2.1). Tubeworms were harvested from high flow and low flow locations by grasping specimens near the base of the aggregation with the submersible hydraulic arm.

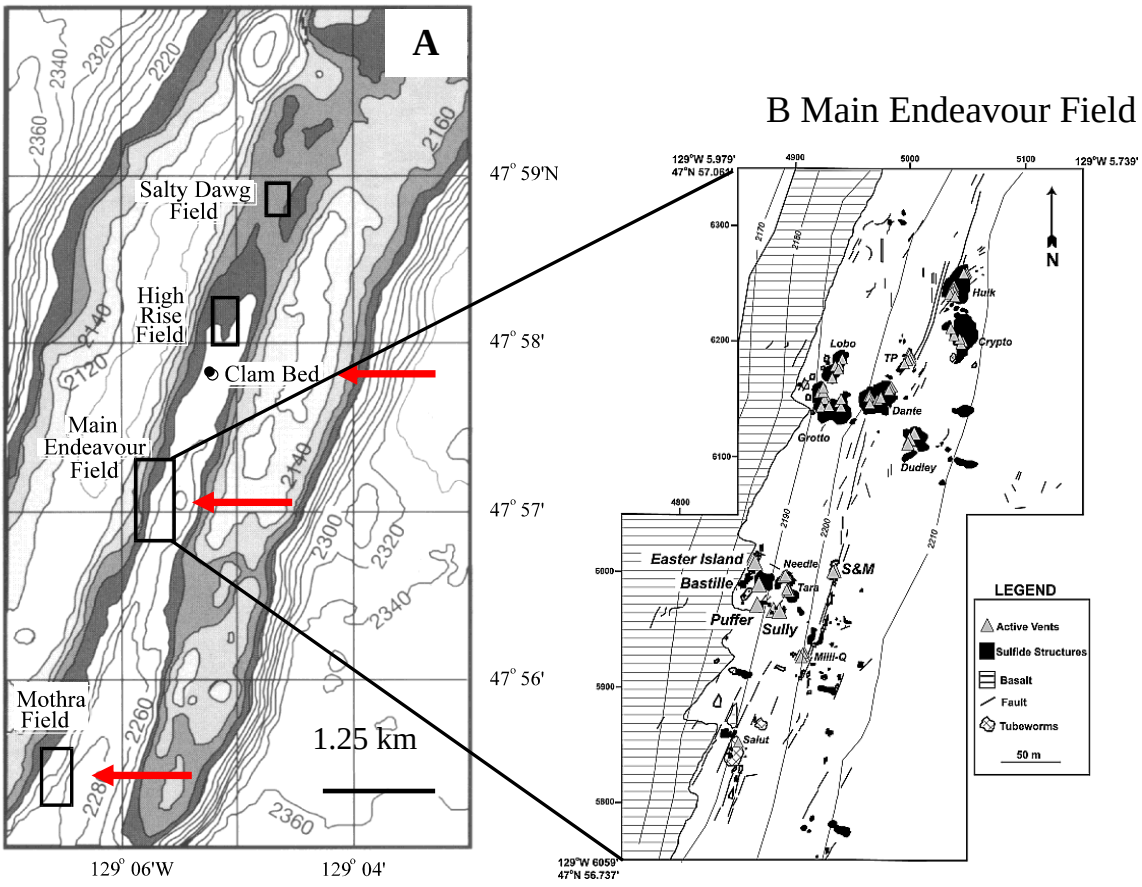

Figure 2-3: Endeavour hydrothermal fields.

A) Bathymetry map of the Endeavour Segment, Juan de Fuca Ridge, showing five main fields within the axial valley. Red arrows indicate hydrothermal vent fields sampled in 2008 (Clam Bed, Main Endeavour and Mothra) (modified from Tunnicliffe 2000).

B) Map depicting the fragmented habitat at Main Endeavour Field (figure modified from Delaney *et al.* 1992).

Before ascent, samples were placed in a "biobox" that was sealed and secured to the submersible. In high flow sites, typically *Ridgeia* was found directly in shimmering hydrothermal fluid flow on sulphide chimneys; low flow sites had little to no shimmering flow on the flanking regions of sulphide chimneys or at seafloor cracks that occurred in close proximity to high flux sites. Once on board, samples were preserved in either 70% ethanol, 95% ethanol or frozen at -80°C.

Molecular techniques: DNA isolation, PCR, sequencing

Genomic DNA was extracted from tubeworm vestimentum tissue, normally devoid of endosymbiotic bacteria, using one of two methods: the QIAGEN DNeasy DNA extraction kit following manufacturer's protocol (QIAGEN Inc., Valencia, CA, USA) or a PrepMan™ Ultra protocol (Applied Biosystems, Foster City, CA). For the PrepMan™ protocol, tissue was added to 100 µL or 120 µL of PrepMan™ Ultra and 40mg of Zirconium/Silica beads (0.5mm) in a 1.5 mL micro centrifuge tube. Samples were pulverized for 45 s in the Minibeadbeater (Biospec, Bartlesville, OK) and centrifuged for 30 s at 13000 rpm and repeated until all tissue was homogenized. The pulverised samples were heated for 10 min at 100°C and subsequently cooled at room temperature for 2 min. The tubes were centrifuged for 3 min at 13000 rpm and an aliquot of 60 µL of the supernatant was removed, purified and stored at -20°C (Appendix A for purification protocol).

A 560 bp fragment of the partial mitochondrial *COI* gene was amplified using a primer set designed in Primer3web (version 4.0.0, Untergrasser *et al*., 2007) from an existing *Ridgeia piscesae* mtDNA *COI* sequence (Genbank accession U74056.1). The primer sequences were RpCOI056-F [5' ATT CGA GCT GAA CTT GGC GA 3'] and RpCOI616-R [5' TGC AGG GTC GAA GAA GGA AG 3']. Polymerase chain reaction (PCR) mixtures included 0.2 mM dNTPs, 0.25 µM of each primer, 1.25 units of GoTaq® DNA polymerase (Promega, Madison, WI), 1x Green GoTaq® Reaction Buffer (supplied by manufacturer and contained 1.5mM $MgCl_2$) and 1 µL of DNA template in a final volume of 15 µL or 20 µL. DNA was amplified using the following PCR program: initial denaturation for 5 min at 95°C followed by 30 cycles of 95°C for 45 s, 60°C for 45 s, 72°C for 45 s, and a final extension at 72°C for 2 min. PCR products were visualized on a

1.6% agarose gel and successful amplicons were purified and sequenced in the reverse direction commercially by Eurofins MGW Operon (Huntsville, AL).

Table 2-1: Summary of sample collections for *Ridgeia piscesae* in this study. Locations are in decimal degrees. MEF refers to Main Endeavour Field, CB refers to Clam Bed, MOT refers to Mothra, HF refers to high flow, LF refers to low flow and N refers to the number of individuals collected. n/a = not available.

Vent field	Flow regime	Abbr	Dive*	N latitude	W longitude	Date	Depth (m)	N
Clam Bed	HF	CB1 H	R1139-08	47.962	129.091	23-06-2008	2188	42
		CB2 H	AD4413-1	47.962	129.091	09-07-2008	2188	25
	LF	CB1 L	R1139-12	47.962	129.091	23-06-2008	2190	22
		CB2 L	AD4412-2	47.962	129.091	08-07-2008	2190	40
		CB3 L	AD4412-1	47.962	129.091	08-07-2008	2190	12
		CB4 L	AD4413-2	47.962	129.091	09-07-2008	2190	20
MEF	HF	MEF1 H	R1138-07	47.949	129.098	22-06-2008	2188	41
		MEF2 H	R1138-27	47.949	129.097	22-06-2008	2201	42
	LF	MEF1 L	R1138-10	47.949	129.098	22-06-2008	2190	40
		MEF2 L	R1138-29	47.949	129.097	22-06-2008	2198	40
Mothra	HF	MOT1 H	AD4417-1	47.933	129.181	13-07-2008	2279	25
		MOT2 H	AD4411-1	47.933	129.181	07-07-2008	2279	42
	LF	MOT1 L	AD4417-2	47.933	129.181	13-07-2008	2279	25
		MOT2 L	AD4417-3	47.933	129.181	13-07-2008	2279	28
Axial	n/a	AXI†	J288-J293	45.933	130.031	09/17-08-2007	1522-1580	28
Middle Valley	n/a	MDV	AD4423-1	48.457	128.709	27-07-2008	2416	26
Total								498

* Dive numbers are labelled R for ROPOS, AD for Alvin and J for Jason.
†Samples were from 7 sites from AXI

Sequence analyses

Sequences were aligned using CLUSTALW (Thompson et al. 1994), trimmed to 503 bp and verified by visual inspection of the chromatograms in BioEdit 7.2.0 (Hall, 1999). Genetic variation within populations (Nei and Tajima, 1981) was measured as the mean number of pairwise differences between pairs of sequences (π), haplotype diversity (H_d) (the number and frequency of each haplotype) and nucleotide diversity (π_n) (the probability that a sample of a particular nucleotide site drawn from two individuals will differ) in Arlequin 3.5.1.2 (Schneider *et al.*, 2000). Population structure and genetic differentiation among sites was estimated with Arlequin by pairwise F_{ST} values (Wright, 1969) assuming Kimura 2-parameter (transitions over transversions are considered separately) distances among haplotypes. A median-joining network of mitochondrial *COI* haplotypes was constructed with NETWORK 4.6 using maximum-parsimony (Bandelt *et al.* 1999). The relationship among haplotypes was further visualized by an unrooted maximum likelihood tree using 500 bootstrap replicates in MEGA 5.2.1 (Tamura *et al*., 2011) and an HKY model of nucleotide evolution. The most likely mutation model for *COI* sequences in *Ridgeia piscesae,* the HKY model, was estimated in PAUP* 4.0a129 (Swofford, 2013).

Demographic history was inferred using two different approaches that test for the null hypothesis of population neutrality (neutral mutation-drift equilibrium) in Arlequin 3.5.1.2: Tajima's D (Tajima, 1989a; Tajima, 1989b) and Fu's F_S (Fu, 1997). Significant values and negative Tajima's D and Fu's F_S values indicate that a population is not in equilibrium ($P<0.05$ for Tajima's D; $P<0.02$ for Fu's Fs) and may have recently undergone rapid population expansion (Tajima, 1989a; Fu, 1997; Ramos-Osnins and Rozas, 2002). Negative D and F_S values occur when mutations arise but have not become common within a population, possibly due to recent demographic expansion. Thus, negative D and F_S values indicate an excess of rare alleles.

Mismatch distributions and haplotype genealogies were also used to infer and visualize demographic history such as the nature of population growth. Star-like genealogies and a Poisson mismatch distribution of pairwise differences between all possible pairs of sequences indicate a recent and rapidly expanding population (Bremer *et al*., 2005; Rogers and Harpending, 1992; Slatkin and Hudson, 1991). Populations that

have been stable over time produce a ragged or erratic mismatch distribution compared to the smooth distributions generated by expanding populations (Rogers & Harpending 1992). The position of the peak in the mismatch distribution reflects the time (mutational time before present) since expansion (Rogers & Harpending 1992; Harpending 1994). Raggedness index (r) calculates the smoothness of the observed mismatch distributions and high and significant r values indicate that the population has been stable over time (Harpending, 1994). Mismatch distributions and raggedness indices were developed in Arlequin. Demographic parameters θ_0, θ_1 and τ were calculated in Arlequin to estimate the magnitude (θ_0=initial population size at equilibrium; θ_1= final population size after growth) and time (τ) since the population expansion ($\tau = 2\ \mu t$ where t measures time in generations and μ is the mutation rate) (Rogers & Harpending 1992).

The best fit models of gene flow among vent fields and habitat types were estimated in MIGRATE-N-MPI 3.6 using the Bayesian framework (Beerli 2006; Beerli and Felsenstein 2001; Beerli and Palczewski, 2010). For vent fields (CB, MEF and MOT), four migration models were compared: (F1) vent fields represent separate subpopulations and individuals move randomly south or north with independent migration rates, (F2) one-way gene flow from north to south, (F3) one-way gene flow from south to north, and (F4) all vent fields form a panmictic population. For habitat types (HF vs. LF), four migration models were estimated: (H1) habitat types represent separate subpopulations and individuals from both habitats move randomly to HF or LF sites with independent migration rates, (H2) one-way gene flow from high flow to low flow habitats, (H3) one-way gene flow from low flow to high flow habitats and, (H4) panmictic model. Convergence was checked by inspecting posterior distributions of the parameters, effective sample sizes (>500) and comparing the results from multiple independent runs. Model comparisons were done using the Bayes factors of the marginal likelihoods for each model (Beerli and Palczewski, 2010) and probabilities for each model were calculated following the guidelines in Kass and Raferty (1995) (see Appendix).

MIGRATE also estimated the mutation scaled population size $\Theta = Ne\mu$, where Ne is the effective population size and μ is the mutation rate per generation per locus, and also the mutation scaled migration rates $M = m/\mu$, where m is the immigration rate per

generation among populations. Parameters were estimated using thermodynamic integration in the Bayesian mode with a Metropolis-coupled heating scheme of 1 cold and 3 heated chains. Chains were run after a burn-in of 100 000 steps using slice sampling (Neal, 2003) of 10 000 states at 100 increments between samples, on a computer cluster in 150 replicates. The HKY mutation model with a transition over transversion rate of 10.11, estimated in PAUP* 4.0a129 (Swofford, 2013), was used in MIGRATE to optimize start parameters. Uniform prior distributions were used with a range of 0.0 to 0.1 for Θ and 0 to 100 000 for M. All estimates of the mutation-scaled effective population size Θ were scaled using an estimate mtDNA mutation rate for hydrothermal vent species of 5×10^{-8} per locus per generation to calculate the average effective population sizes (Audzijonyte & Vrijenhoek, 2010). A generation time of three years was used for HF subpopulations and ten years for LF populations (Tunnicliffe et al., in review).

Results

Genetic variation on the Juan de Fuca Ridge

A 503 bp region of the mtDNA *COI* gene was isolated in 498 *Ridgeia piscesae* specimens from hydrothermal vent sites at Middle Valley (N=26), Endeavour (N=444) and Axial Seamount (N=28) on the Juan de Fuca Ridge. A total of 33 synonymous mutations, 30 transitions and 3 transversions, were identified at 30 segregating sites, all third position, within the mt*COI* coding sequence. No insertions or deletions were identified. We detected 32 unique haplotypes (Table 2.2); 30 of these occur among the Endeavour vestimentiferans, which is 26 more than had been detected previously at this site (Young *et al.* 2008). Haplotypes were generally differentiated by one-step mutations (Figure 2.4). Most individuals (68%) possessed the dominant haplotype (Table 2.2; Figure 2.4). Three other haplotypes were common (4%-7%) and the remainder were rare (<2.2%) with 17 out of the 32 haplotypes found in just one individual (Figure 2.4).

Haplotype diversity estimates from each of the three vent sites on the JDF Ridge were similar and ranged from H_d=0.51 to 0.54, π= 0.0012 to 0.0015 (Table 2.3; Figure 2.5). Pairwise F_{ST} values (Table 2.4) were used to estimate differentiation among the three

vent sites (Middle Valley (N=26), Endeavour (N=444) and Axial Seamount (N=28)). AXI was moderately and significantly differentiation from MVL (F_{ST}=0.082, p=0.00) and END (F_{ST}=0.096, p=0.002), respectively (Table 2.4), mostly because the second most common haplotype at Axial was not present elsewhere (Table 2.2). Furthermore, the second most abundant haplotype (~8%) from END and MVL was not found at AXI, nor were the next three most common END/MVL haplotypes (Figure 2.4; Table 2.2).

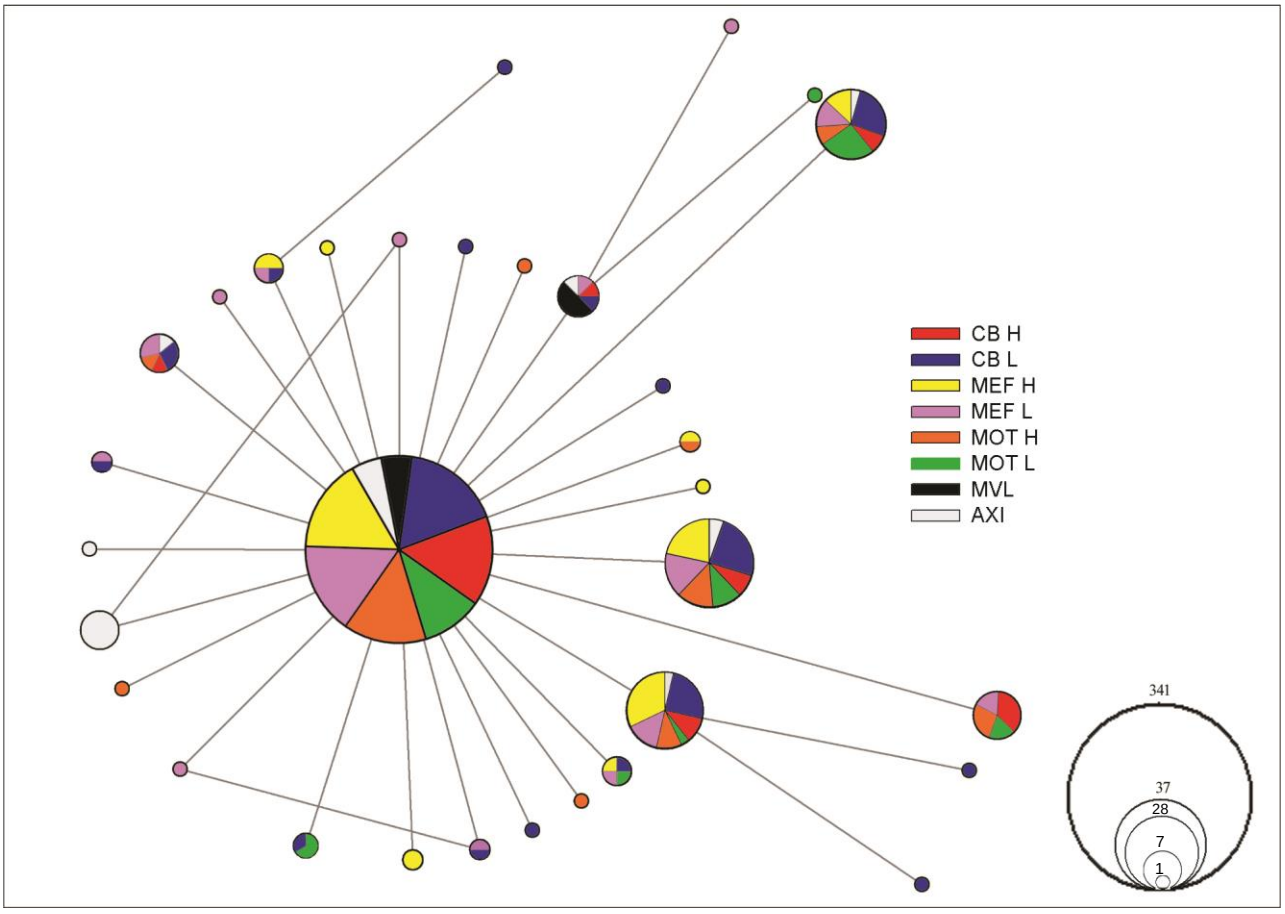

Figure 2-4: Median-joining haplotype network of 32 mtDNA *COI* haplotypes showing the genetic relationship of *Ridgeia piscesae* isolates on the Juan de Fuca Ridge. Branch length is proportional to the number of mutations and circle size is proportional to haplotype frequency. Each circle represents a unique haplotype and colors correspond to the proportion of individuals from each population that share that haplotype.

Table 2-2: Geographic distribution of *COI* haplotypes in *Ridgeia piscesae* from six localities at three vent fields within Endeavour (Mothra (MOT), Main Endeavour Field (MEF) and Clam Bed (CB) and for Endeavour (END) overall, Axial Seamount (AXI) and Middle Valley (MVL) on the Juan de Fuca Ridge.

Hapl.	CB H	CB L	MEF H	MEF L	MOT H	MOT L	END*	MVL	AXI	Total
h1	53	58	55	54	49	36	305	18	18	341
h2	3	9	8	6	5	4	35	2		37
h3	3	7	9	4	3	1	27	1		28
h4	2	6	3	3	2	6	22	1		23
h5	4			2	3	2	11			11
h6	1	2		2	1		6		1	7
h7		1	1	1		1	4			4
h8		1	2	1			4			4
h9		1				2	3			3
h10	1	1		1			3	4	1	8
h11			1		1		2			2
h12		1		1			2			2
h13		1		1			2			2
h14			2				2			2
h15			1				1			1
h16			1				1			1
h17				1			1			1
h18				1			1			1
h19				1			1			1
h20				1			1			1
h21					1		1			1
h22					1		1			1
h23					1		1			1
h24						1	1			1
h25		1					1			1
h26		1					1			1
h27		1					1			1
h28		1					1			1
h29		1					1			1
h30		1					1			1
h31									7	7
h32									1	1
Totals	67	94	83	80	67	53	444	26	28	498

*Haplotype frequencies for all *Ridgeia piscesae* at Endeavour sampled in 2008

Table 2-3: Diversity in *Ridgeia piscesae* mtDNA *COI* gene (503bp) from Endeavour (END) overall, Axial Seamount (AXI) and Middle Valley (MVL) on the Juan de Fuca Ridge and within Endeavour, 6 localities measured separately at 3 vent fields within Endeavour and on groups of localities from vent fields and habitats types. Indices of genetic diversity: n: total number of specimens sampled, h: number of haplotypes (total = 32), S: number of segregating sites, π: mean number of pairwise differences between all pairs of haplotypes within a population, Hd: haplotype diversity, $(\pi)_n$: nucleotide diversity, priv. S: private segregating sites.

Localities	n	h	S	π	Hd	$(\pi)_n$	priv. S
CB H	67	7	8	0.58	0.37	0.0012	0
CB L	94	17	16	0.93	0.61	0.0018	6
MEF H	83	10	10	0.70	0.54	0.0014	3
MEF L	80	15	15	0.78	0.54	0.0016	3
MOT H	67	10	11	0.67	0.46	0.0013	2
MOT L	53	8	10	0.92	0.53	0.0018	1
CB	161	18	18	0.78	0.51	0.0015	6
MEF	163	19	19	0.74	0.54	0.0015	6
MOT	120	13	15	0.78	0.49	0.0016	3
HF	217	16	18	0.68	0.47	0.0014	6
LF	227	23	20	0.84	0.56	0.0017	11
MVL	26	5	5	0.65	0.51	0.0013	0
END	444	30	29	0.76	0.52	0.0015	22
AXI	28	5	4	0.60	0.54	0.0012	1

*Diversity indices for all *Ridgeia piscesae* at Endeavour sampled in 2008

Table 2-4: Pairwise distances of Fst from mtDNA *COI* haplotype frequencies using Kimura 2-parameter method (10000 permutations) for *Ridgeia piscesae* at Middle Valley, Endeavour and Axial (lower diagonal) and associated p-values (above diagonal). Bold values are statistically significant ($P<0.05$).

	MVL	END	AXI
MVL	*	0.124	**0.000**
END	0.012	*	**0.002**
AXI	0.082	0.096	*

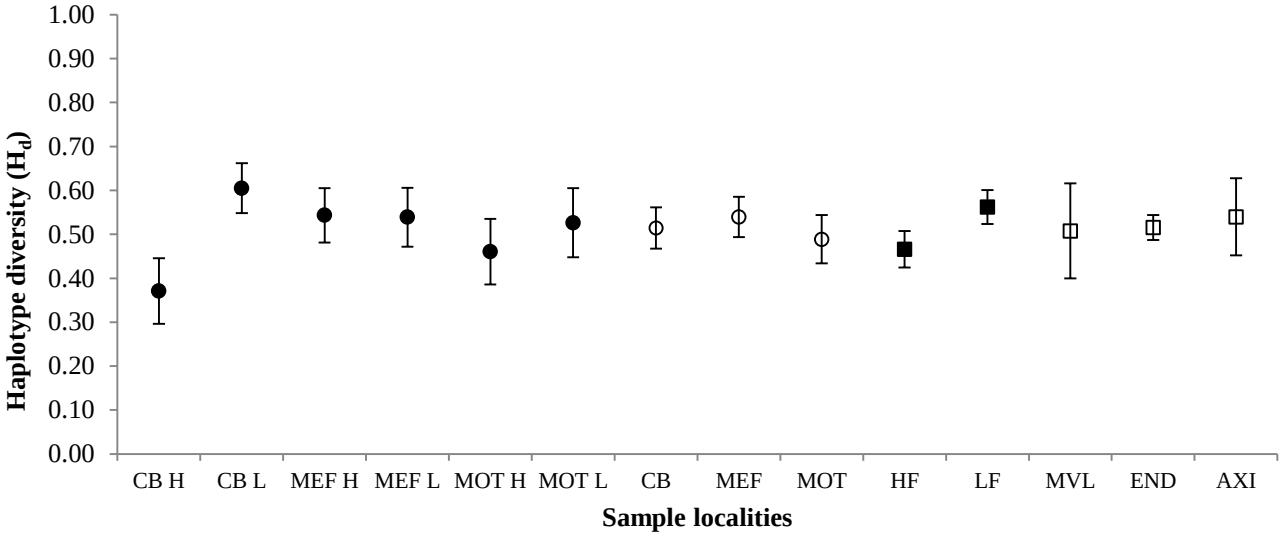

Figure 2-5: Mean haplotype diversity (H_d) in mtDNA *COI* gene in *Ridgeia piscesae* from the Juan de Fuca Ridge ordered from north to south. Error bars represent standard error of the mean. (●) Comparison of high flow and low flow sites at each vent field within Endeavour (CB H/L, MEF H/L, MOT H/L). (○) Comparison of pooled data among vent fields within Endeavour (CB, MEF, MOT). (■) Comparison between pooled high flow and pooled low flow habitats at Endeavour. (□) Comparison among vent fields on the Juan de Fuca Ridge (MVL, END, AXI)

Genetic variation with the Endeavour axial valley

Haplotype diversity for all individuals sampled within Endeavour was 0.52+/-0.027 and nucleotide diversity (π_d) was 0.0015+/-0.0012, however, averages hide within-site variation (Table 2.3). The 444 individuals from Endeavour came from 14 samples (six from CB and four each from MEF and MOT) that were subsequently grouped based on habitat and vent field location (see below). Groupings were validated after assessing genetic differentiation among the 14 samples. F_{ST} values that significantly differed from zero were observed three times: between a high flow and a low flow site within Clam Bed (F_{ST}=0.057, $p<0.05$), between CB1 H and a MOT2 L (F_{ST}=0.045), and between MOT2 L and MEF2 L (F_{ST} = 0.027) (Table 2.5). Pairwise F_{ST} values among the 14 samples revealed little differentiation and validated grouping the data. Individuals were first merged into six separated HF and LF groups from each of the three vent fields (CB H, CB L, MEF H, MEF L, MOT H and MOT L). A separate test ignored HF and LF habitat differences and merged all samples from a single vent field for among vent site

comparisons (CB, MEF and MOT). Finally, all high flow and separately grouped all low individuals were grouped for between habitat comparisons (HF and LF).

Diversity estimates from each of the six groups varied (Table 2.3). At two of the three Endeavour vent fields, rare haplotypes were more common in low flux habitats (Table 2.3). Haplotype diversity for the low flux and high flux sites significantly differed at CB were 0.61±0.06 and 0.37±0.07 respectively, and estimates for MOT were 0.53±0.08 (LF) and 0.46±0.07 (HF) while MEF estimates were the same (0.54) (Table 2.3; Figure 2.5). When HF and LF were combined at each vent field, diversity estimates were similar among vent fields (Table 2.3) ranging from 0.49 to 0.54. When the LF samples from all three vent fields were combined and compared to HF samples from all three vent fields, a significantly larger amount genetic diversity was observed in LF (H_d = 0.56±0.04) compared to HF (H_d = 0.47±0.04) (Figure 2.5).

In the calculation of among-group differentiation, there were 15 pairwise F_{ST} estimates among the six groups and two were significant (CB H-MEF H, MOT H-MOT L) (Table 2.6). F_{ST} estimated among the three paired vent fields (CB-MEF, CB-MOT, and MEF-MOT) were not significantly different from zero as was the case for F_{ST} estimates between habitat comparisons of the HF (merged) and LF (merged). The discovery of a few significant F_{ST} values and the clear difference in haplotype diversity and frequency of rare alleles between LF groupings and their respective HF counterparts, provide some support for the hypothesis of asymmetrical migration and substructure among vent fields and habitat types. Asymmetrical migration violates F_{ST} based methods therefore models of gene flow and genetic structure were subsequently estimated in MIGRATE (Beerli & Felsenstein, 2001; Beerli & Palczewski, 2010).

Table 2-5: Pairwise estimates of Fst from mtDNA *COI* haplotype frequencies using Kimura 2-parameter method (10000 permutations) among 14 *Ridgeia piscesae* 2008 sample sites within Endeavour (lower diagonal) and associated p-values (above diagonal). Bold values are statistically significant (P<0.05).

	MEF1 H	MEF2 H	MEF1 L	**MEF2 L**	MOT1 H	MOT2 H	MOT1 L	**MOT2 L**	**CB1 H**	CB2 H	**CB1 L**	CB2 L	CB3 L	CB4 L
MEF1 H	*	0.810	0.473	0.483	0.533	0.446	0.261	0.216	0.071	0.575	0.455	0.653	0.867	0.702
MEF2 H	-0.012	*	0.293	0.618	0.747	0.278	0.177	0.065	0.139	0.216	0.443	0.603	0.902	0.383
MEF1 L	-0.001	0.004	*	0.147	0.545	0.450	0.589	0.571	0.089	0.807	0.077	0.862	0.882	0.714
MEF2 L	-0.002	-0.005	0.010	*	0.891	0.775	0.211	**0.025**	0.733	0.484	0.130	0.382	0.813	0.640
MOT1 H	-0.005	-0.012	-0.005	-0.016	*	0.558	0.192	0.141	0.479	0.433	0.114	0.638	0.656	0.506
MOT2 H	0.000	0.004	-0.001	-0.009	-0.004	*	0.740	0.253	0.898	0.707	0.085	0.454	0.775	0.687
MOT1 L	0.009	0.014	-0.008	0.011	0.022	-0.014	*	0.447	0.216	0.687	0.225	0.635	0.822	0.325
MOT2 L	0.013	0.027	-0.009	**0.027**	0.030	0.007	-0.004	*	**0.016**	0.456	0.052	0.505	0.651	0.420
CB1 H	0.021	0.014	0.019	-0.011	-0.002	-0.013	0.015	**0.044**	*	0.213	**0.009**	0.087	0.220	0.157
CB2 H	-0.009	0.010	-0.015	-0.002	0.007	-0.013	-0.015	-0.008	0.014	*	0.236	0.469	0.904	0.982
CB1 L	-0.003	-0.002	0.026	0.015	0.027	0.024	0.013	0.042	**0.057**	0.012	*	0.216	0.829	0.149
CB2 L	-0.008	-0.006	-0.013	0.001	-0.008	-0.001	-0.009	-0.005	0.018	-0.004	0.011	*	0.940	0.573
CB3 L	-0.029	-0.031	-0.033	-0.020	-0.016	-0.020	-0.031	-0.020	0.019	-0.039	-0.028	-0.038	*	0.763
CB4 L	-0.013	0.002	-0.015	-0.007	-0.001	-0.009	0.005	-0.009	0.017	-0.027	0.024	-0.008	-0.025	*

Wright's F_{ST} based methods assume that populations are in equilibrium (Slatkin, 1993), all subpopulations are of equal size and that migration rates are all symmetric (Beerli & Felsenstein, 2001). *Ridgeia piscesae* within Endeavour violates one, if not all, of these assumptions, delivering unreliable estimates of differentiation. In addition, one of the goals of this study was to test for asymmetrical migration. The program MIGRATE can compare and rank different population models and estimate migration rates without the assumption of equal population sizes and symmetric migration (Beerli & Felsenstein, 2001; Beerli & Palczewski, 2010).

Table 2-6: Pairwise estimates of F_{st} from mtDNA *COI* haplotype frequencies using Kimura 2-parameter method (10000 permutations) among *Ridgeia piscesae* subpopulations within Endeavour (lower diagonal) and associated p-values (above diagonal). Bold values are statistically significant based on exact tests (P<0.05).

	CB H	CB L	MEF H	MEF L	MOT H	MOT L
CB H	*	0.126	**0.047**	0.837	0.979	0.169
CB L	0.007	*	0.769	0.796	0.375	0.281
MEF H	**0.014**	-0.005	*	0.359	0.190	**0.035**
MEF L	-0.006	-0.005	0.001	*	0.981	0.226
MOT H	-0.011	0.001	0.005	-0.009	*	0.251
MOT L	0.010	0.003	**0.021**	0.005	0.005	*

Gene flow model comparisons using MIGRATE

Analyses of gene flow models among vent fields in MIGRATE were assessed on high flow and low flow samples separately due to the different life history strategies among the tubeworm morphotypes. Vent field models of population structure and gene flow, among HF from CB, MEF, and MOT, and, in a separate analysis, among LF from CB, MEF, and MOT, supported the F1 model: each vent field represents a separate subpopulation in which migrants are free to move north or south with independent migration rates. The estimated extent of north and south migration differed for the HF data compared to the LF data set (see below). The support for distinct subpopulations with independent migration model was strongest in the HF comparisons; model probabilities were 0.95 for HF and 0.66 for LF (Figure 2.6). This was consistent with the observation that one of the between HF group F_{ST} comparisons was significantly different

from zero (Table 2.6). The one-way migration models, F2 and F3, had probabilities near zero and the panmictic model, F4, ranked second for both HF and LF analyses with low probabilities of 0.08 and 0.33 respectively (Figure 2.6).

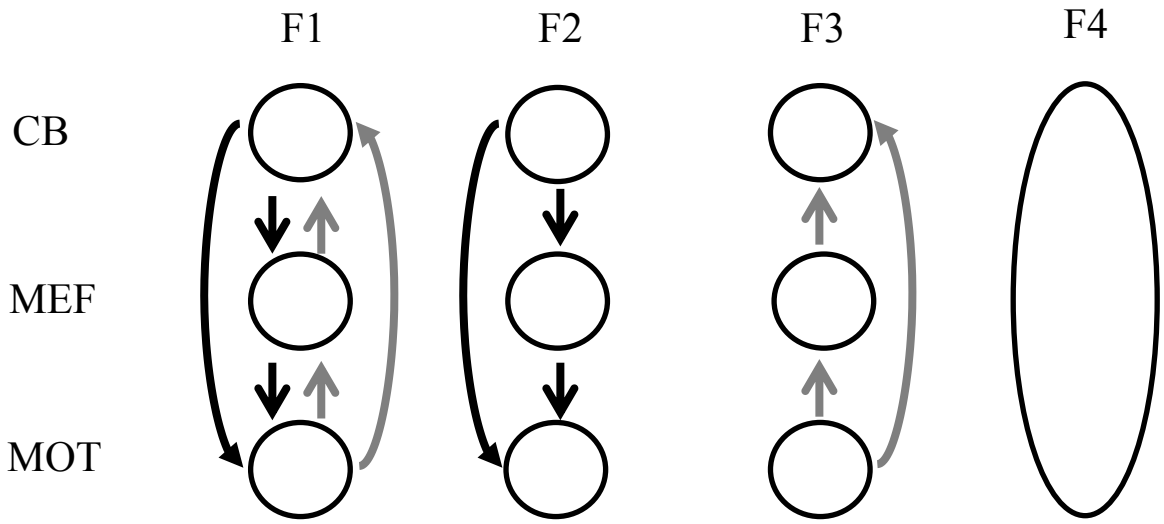

HF	**1** (0.92)	**3** (0)	**4** (0)	**2** (0.08)
LF	**1** (0.66)	**3** (<0.001)	**4** (<0.001)	**2** (0.33)

Figure 2-6: Comparison of gene flow models for mtDNA *COI* gene in *Ridgeia piscesae* among vent fields at Endeavour (CB, MEF, MOT) with high flow and low flow samples analyzed separately. Details of the models are described in Materials and Methods. The bolded numbers in the box represent model ranks based on Bayes factors calculated in MIGRATE for high flow and low flow subpopulations and the numbers in parentheses represent the probability of each model.

MIGRATE was also used to estimate gene flow models among tubeworms from HF and LF habitats. The chain did not converge (*i.e.* consistent results from multiple independent runs) with six subpopulations, so all HF data from each vent field were grouped and all LF data from each vent field were grouped prior to further analysis. Models of population structure and gene flow between habitat types was best supported by the H1 model, where *Ridgeia* habitat types (all LF pooled vs all HF pooled) represented separate subpopulations and migration occurs independently in both directions between habitat types (Figure 2.7). Estimates of migration rate between the

habitat types differed, with HF to LF higher than the alternative (see below). Model H1 probability was 0.54 and, here, the panmictic H4 model had some support 0.29 (Figure 2.7). Model H1 was also the favoured model for gene flow in separate analyses between each pair of HF and LF groups within a vent field: H1 probabilities were CB p=0.88, MEF p=0.73 and MOT p=0.75. Here, panmixia had much less support (highest is MOT at p=0.13). Migration among habitat types within vent fields was also asymmetrical, with higher estimates of migration rates from HF to LF than the alternative in CB and MEF. Unexpectedly, evidence for slightly higher migration from LF to HF in MOT was estimated and it was suspected that this might be an artefact driven by the higher degree of variation in MOT HF as a consequence of dominant north to south migration rates estimated among vent fields in the HF samples (see below). Grouping HF and LF samples from each vent field in our habitat comparisons, despite having been previously identified as separate subpopulations (in the F1 model), decreased the likelihood of excluding important sources from the analyses at the cost of an observed increased probability for the panmictic model. Overall, panmixia was still rejected as the best fit model of gene flow among grouped habitat types demonstrating another example of MIGRATE showing genetic substructure that F_{ST} missed.

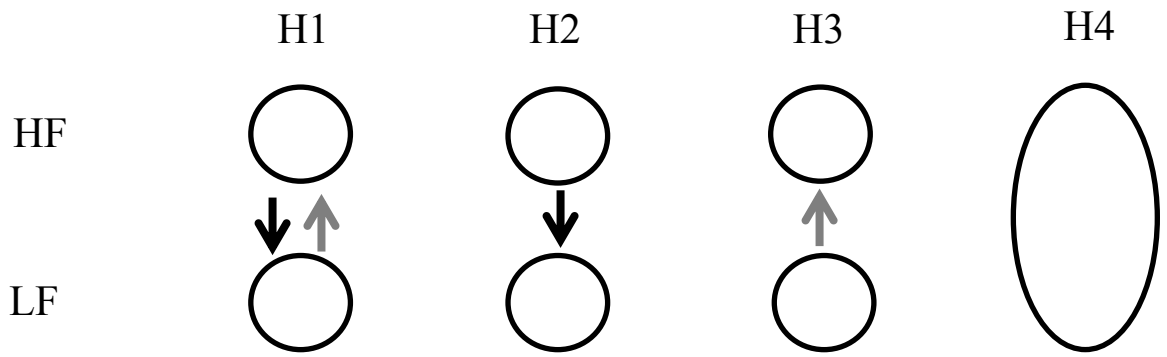

	1 (0.54)	**3** (0.17)	**4** (0)	**2** (0.29)

Figure 2-7: Comparison of gene flow models for mtDNA *COI* gene in *Ridgeia piscesae* between High flow and Low flow habitat types for pooled HF vs. pooled LF data from each vent field. Details of the models are described in Materials and Methods. The bolded numbers in the box represent model ranks based on Bayes factors calculated in MIGRATE for high flow and low flow subpopulations and the numbers in parentheses represent the probability of each model.

Effective population size and migration rates

Estimates of immigration rates per generation among vent fields (CB- MEF-MOT) suggested a higher amount of gene flow in a north to south direction in the HF data, which also had the lowest estimates of effective population size in the north ($N_{e\,(CB)}$ = 11000) and highest in the south ($N_{e\,(MOT)}$ =15000) (Table 2.7). The LF data suggested just the opposite, in which dominant gene flow direction among vent fields was south to north and effective population size increased from southern to northern vent fields ($N_{e\,(MOT)}$ =3000, $N_{e\,(CB)}$ =10000) (Table 2.7). A separate analysis of gene flow between pooled HF and LF habitats revealed asymmetrical gene flow (Table 2.8). Estimates of the number of immigrants per generation moving from HF to LF subpopulations were four times higher than in the reverse direction and effective population size was three times greater in high flow habitat ($N_{e\,(HF)}$=27000, $N_{e\,(LF)}$=17000) (Table 2.8). Estimating effective population sizes with different age estimates for individuals from HF and LF habitat had little effect on the patterns identified above, however, the magnitude of the values changed.

Table 2-7: Summary of the estimates of gene flow based on Bayesian inferences of mutation scaled immigration rates (M=m/μ) and mutation scale effective population sizes (Θ = 4Neμ) using MIGRATE among *Ridgeia piscesae* from three vent fields at Endeavour. High flow and low flow data from each vent field were analyzed separately. Source populations are represented in rows and receiving populations in columns. Mutation scaled effective population sizes are along the diagonals and associated effective population sizes in parentheses (N_e). Values above the diagonal indicate gene flow moving from north to south and values below the diagonal indicate gene flow moving from south to north.

Low Flow Receiving subpopulations				**High Flow** Receiving subpopulations			
Source	CB	MEF	MOT	Source	CB	MEF	MOT
CB	0.0050 (10 000)	10400	6600	CB	0.0016 (11 000)	20233	48367
MEF	12000	0.0045 (9000)	5900	MEF	22833	0.0019 (13 000)	41300
MOT	17500	21500	0.0015 (3000)	MOT	18633	18300	0.0022 (15 000)

Table 2-8: Summary of the estimates of gene flow based on Bayesian inferences of mutation scaled immigration rates (M=m/μ) and mutation scale effective population sizes (Θ = 4Neμ) using MIGRATE. Gene flow was estimated between *Ridgeia piscesae* from habitat extremes using pooled high flow and pooled low flow *COI* data. Source populations are represented in rows and receiving populations in columns. Mutation scaled effective population sizes are along the diagonals and associated effective population sizes in parentheses (N_e). Values above the diagonal indicate gene flow moving from high flow to low flow habitat and values below the diagonal indicate gene flow moving from low flow to high flow habitat.

	Receiving subpopulation	
Source	HF	LF
HF	0.0040 (27000)	25000
LF	6400	0.0086 (17000)

Demographic history

Demographic tests were conducted for each vent site on the Juan de Fuca Ridge and within Endeavour for the six groups separately and on groups from vent fields and habitats types. Departures from neutrality were not significant for Middle Valley or Axial Volcano however, this may be due to the small sample size collected from each of these sites and mismatch distributions and test statistics suggest recent expansion (Figure 2.8; Table 2.9). Test results suggest that the overall population of *R. piscesae* from Endeavour has recently undergone a demographic expansion with highly significant and negative Tajima's D (-2.17, P=0.00) and Fu's F_s (-29.07, P=0.00) values (Table 2.9). Significant and negative Tajima's D and Fu's F_s were also obtained for all groupings within Endeavour and reflect the observation that groupings had low diversity, but a high number of polymorphic sites (*i.e.*, a high abundance of rare alleles) (Table 2.3). Mismatch statistics support demographic tests and suggest that all sample sites are in a population expansion phase (Figure 2.8). The star-like genealogy of haplotypes (Figure 2.4) and the Poisson distribution of pairwise differences among sequences indicate a recent and rapidly expanding population (Figure 2.8; Figure 2.9). Further evidence of

population expansion within Endeavour is present in mismatch distributions and raggedness indices (r) that were all non-significant (P>0.05) and mismatch statistics indicated that the initial population size (θ_0) was less than the final population size (θ_1) after expansion (Table 2.9; Figure 2.8). The null hypothesis of recent demographic expansion for all subpopulations within Endeavour could not be rejected.

Figure 2-8: Mismatch distributions and τ values for *Ridgeia piscesae* specimens from six populations, one high flow and one low flow population at three vent fields (Mothra (MOT), Main Endeavour Field (MEF) and Clam Bed (CB); top two rows) and from Middle Valley, Endeavour and Axial seamount on the Juan de Fuca Ridge (bottom row). X-axis represents the number Bars on the histogram represent the frequency of observed number of pairwise differences between pairs of individuals. The solid line represents the expected distribution under the rapid population expansion model and the P value corresponds to the test between observed and expected differences (i.e. null hypothesis: population undergoing recent demographic expansion). The $\tau = 2ut$ estimates the mutational time since the occurrence of the population expansion.

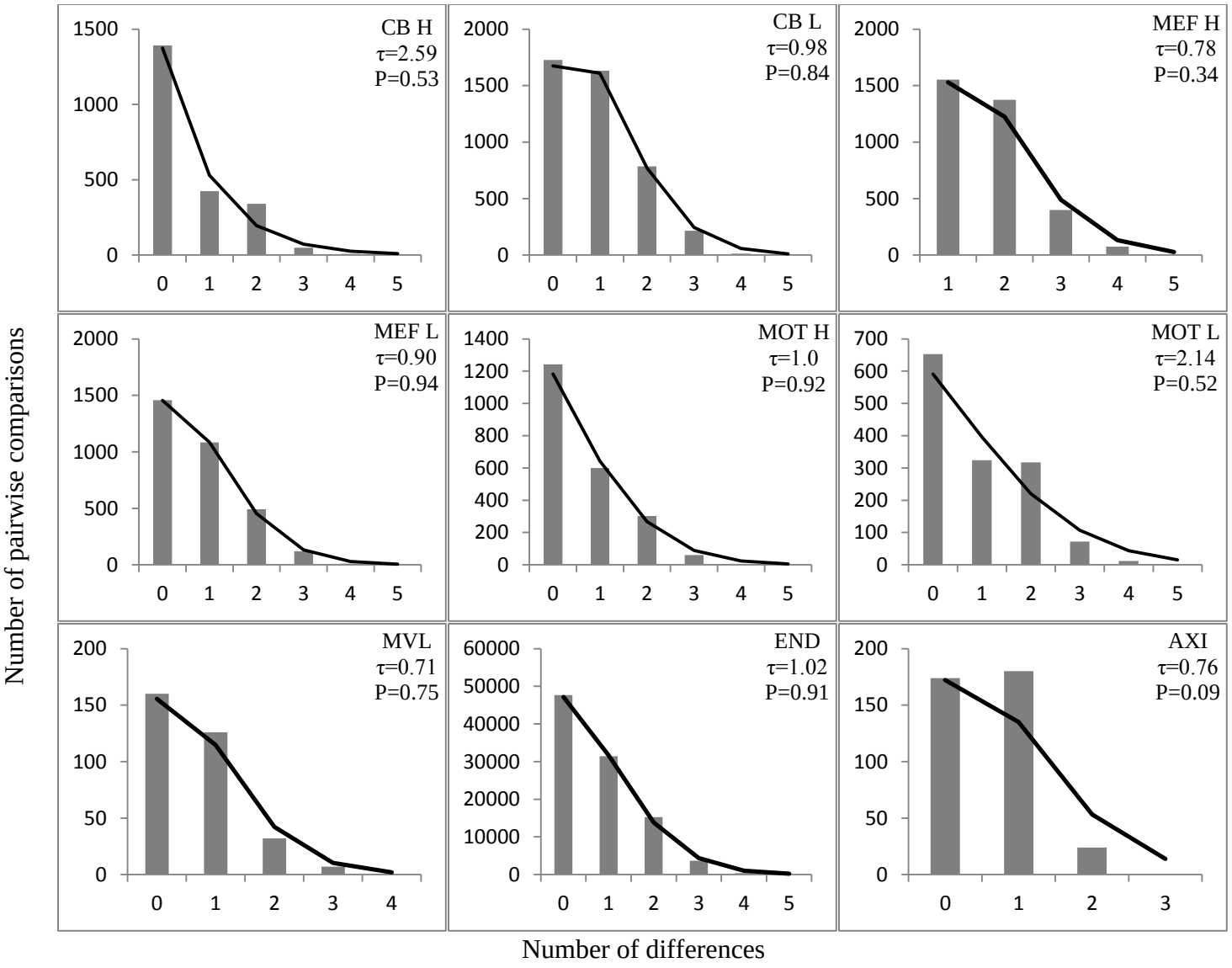
CB H
τ=2.59
P=0.53
CB L
τ=0.98
P=0.84
MEF H
τ=0.78
P=0.34
MEF L
τ=0.90
P=0.94
MOT H
τ=1.0
P=0.92
MOT L
τ=2.14
P=0.52
MVL
τ=0.71
P=0.75
END
τ=1.02
P=0.91
AXI
τ=0.76
P=0.09
Number of pairwise comparisons
Number of differences

Table 2-9: Tests of neutrality and population expansion for the mtDNA *COI* gene sequence data in *Ridgeia piscesae* from the Juan de Fuca Ridge. D= Tajima's D-test; F_S= Fu's FS test; r=Raggedness index. Bold values denote significant D (P<0.05) or Fs value (P<0.02). θ_0=initial population size at equilibrium; $\theta_{1=}$ final population size after growth

Population	D	P_D	Fs	P_{Fs}	θ_0	θ_1	r	P_r
CB H	-1.69	**0.018**	-3.66	**0.016**	0.00	0.61	0.21	0.57
CB L	-2.00	**0.003**	-15.49	**0.000**	0.00	17.45	0.05	0.79
MEF H	-1.70	**0.018**	-6.40	**0.002**	0.00	99999	0.09	0.28
MEF L	-2.12	**0.002**	-14.17	**0.000**	0.00	4.02	0.06	0.85
MOT H	-1.97	**0.004**	-7.22	**0.000**	0.06	1.18	0.10	0.82
MOT L	-1.64	**0.029**	-3.24	0.031	0.00	1.27	0.11	0.66
CB	-2.04	**0.002**	-17.05	**0.000**	0.02	0.16	0.07	0.84
MEF	-2.11	**0.001**	-19.59	**0.000**	0.00	99999	0.08	0.47
MOT	-1.95	**0.004**	-9.25	**0.001**	0.00	1.07	0.10	0.77
HF	-2.02	**0.001**	-13.93	**0.000**	0.07	1.21	0.09	0.80
LF	-2.11	**0.001**	-23.96	**0.000**	0.11	3.32	0.05	0.86
MVL	-1.43	0.066	-1.93	0.058	0.00	99999	0.10	0.55
END	-2.17	**0.000**	-29.07	**0.000**	0.05	1.78	0.07	0.84
AXI	-1.08	0.163	-2.05	0.031	0.00	99999	0.17	0.11

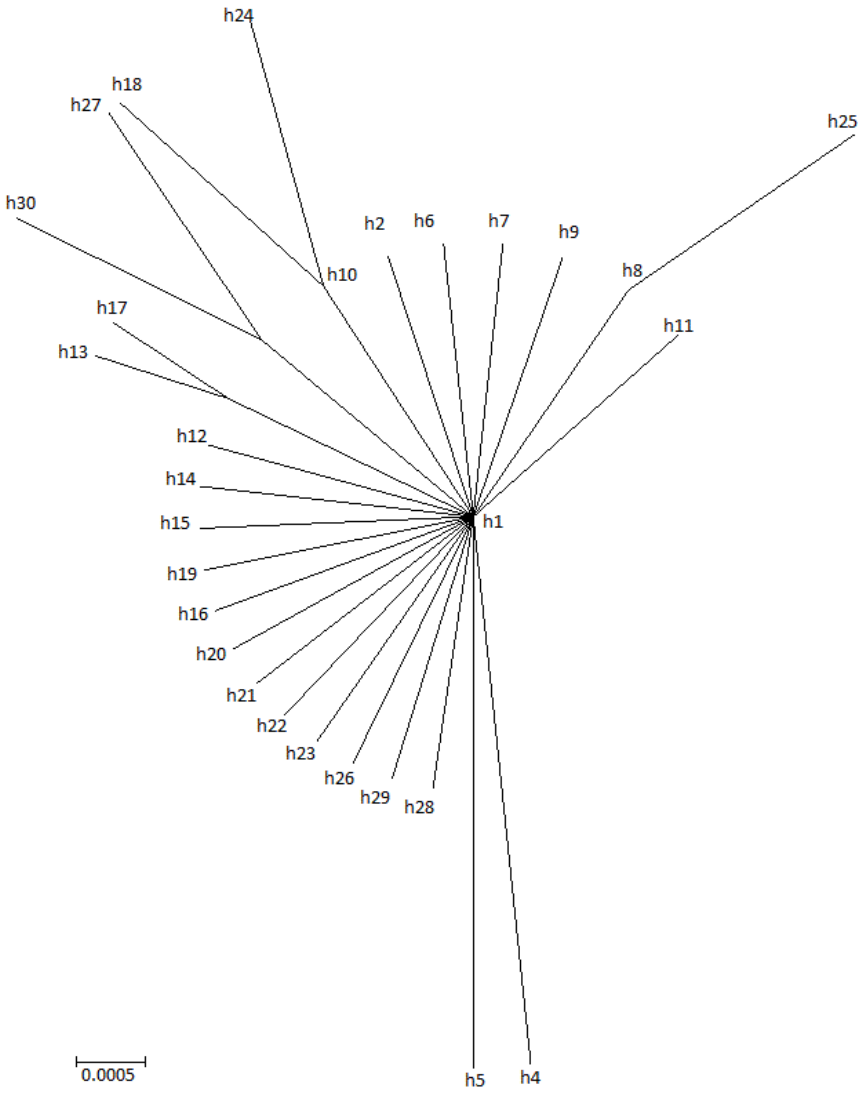

Figure 2-9: Un-rooted maximum likelihood tree among mtDNA COI haplotypes in *Ridgeia piscesae* from Endeavour using 500 bootstrap replicates in MEGA 5.2.1 (Tamura *et al*., 2011) and an HKY model of nucleotide evolution.

Discussion

The low to intermediate levels of genetic diversity in *Ridgeia piscesae*, surveyed over one year on the Juan de Fuca Ridge, were within the range of values generally found for *COI* in this species and other hydrothermal vent organisms (Young *et al.* 2008; Vrijenhoek 2010). This study identified eleven *COI* haplotypes identical to previously published *COI* sequence data for *Ridgeia piscesae* along the northeast Pacific ridge

system (Young *et al.* 2008). Only four haplotypes were known to occur within Endeavour (Young *et al.* 2008), which correspond to the four most frequent *Ridgeia COI* haplotypes in this study. An additional six of the eleven haplotypes were also identified within Endeavour, likely due to the extensive regional sampling done here. Twenty-one novel *COI* haplotypes were discovered along the Juan de Fuca Ridge, nineteen of which were exclusively found within Endeavour. The large number of individuals sequenced in this study increased the genetic resolution within Endeavour and demonstrated that average *mtCOI* genetic diversity hid within site variation, which is not uncommon for mitochondrial DNA (Hedgecock 1994). The number of haplotypes was well correlated (r^2 = 0.83) with sample size but other measures of genetic diversity were not, likely due the frequency of rare alleles and one-step mutations among haplotypes in the overall sample set.

At the ridge scale, patterns of genetic differentiation were similar to those previously identified among *Ridgeia piscesae*; AXI was the most divergent population on the Juan de Fuca Ridge (Young *et al.* 2008). High estimates of gene flow and connectivity are known in *Ridgeia piscesae* from several genetic markers at multiple geographic scales (Southward *et al.* 1996; Black *et al.* 1998; Carney *et al.* 2002). At the larger regional scale, including three northeast Pacific ridges, *R. piscesae* gene flow is unidirectional and biased in a southward direction across the Blanco Transform Fault, consistent with the dominant southeasterly currents that move across the region (Young *et al.* 2008). The Blanco Transform Fault is thought to dampen dispersal between the Gorda Ridge and Juan de Fuca/Explorer ridge system for species with high dispersal capabilities (e.g. *Ridgeia*) and act as a barrier to exchange for other vent species, such as the vent limpets *Lepetodrilus spp.* (Johnson *et al.* 2006; Young *et al.* 2008). However, depth may also act as a barrier to gene flow. Axial Seamount (~1500 m) is the shallowest hydrothermal vent system on the Juan de Fuca Ridge and hosts the only population significantly differentiated from deeper (by over 500 m) hydrothermal vent locations to the north and south of the volcano on the Juan de Fuca Ridge. Furthermore, this study identified that *Ridgeia piscesae* from Endeavour shared more haplotypes with those previously identified in individuals from the Cleft Segment of the Juan de Fuca Ridge which is located further south than Axial but at similar depths to Endeavour (both ~ 2200 m).

Genetic variability in Endeavour

Mitochondrial *COI* data provided adequate variation to identify fine-scale substructure and genetic connectivity in *Ridgeia piscesae* from Endeavour. Results from this study identified genetic sub-structuring of *Ridgeia piscesae* among samples < 10 km apart on the Endeavour Segment of the Juan de Fuca Ridge, despite being locally abundant and probably having relatively long-lived larvae with dispersal potential (Marsh *et al.* 2001). Significant genetic differentiation over such geographical distances is not unique to *Ridgeia piscesae* and occurs in riparian flowering plants, insects and reptiles that experience metapopulation processes (e.g., Tero et al. 2003; Manier & Arnold 2005; Darvill et al. 2006). Coalescent based approaches using *Ridgeia* mtDNA data did not favour panmixia as the best fit model of gene flow among vent fields and habitat types that were consistent with several F_{ST}-values. Genetic sub-structure among samples identified that vent fields and habitat types should be treated as separate subpopulations (demes) experiencing independent local dynamics (Hotz et al., 2013; reviewed in Lowe & Allendorf, 2010). Although F_{ST} based methods detected some sub-structuring among *Ridgeia* demes within Endeavour, MIGRATE was more consistent at rejecting panmixia and identifying distinct geographical- and habitat-defined groups. Despite departures from panmixia, estimates of migration rates suggest that successful colonists are drawn from a small proportion of individuals that represent a well-mixed migrant pool with the capacity to access many, if not all subpopulations, within the axial valley. Genetic structure of *Ridgeia piscesae* within the Endeavour axial valley is likely a signature of differences in reproductive success and metapopulation processes rather than physical barriers to gene flow, further discussed below.

Consistency with oceanographic circulation model within Endeavour

One of the goals of this study was to use genetic data to test the consistency between gene flow and oceanographic circulation models within the Endeavour axial valley to estimate connectivity of *Ridgeia piscesae* among vent fields within the region. Though estimates of migration rates and effective population sizes are likely not absolute values, because the *COI* mutation rate and generation times are not definitively known for *R. piscesae* (Audzijonyte & Vrijenhoek 2010; Tunnicliffe et al., in review), they are

useful indicators of the general patterns of gene flow identified in our data. Asymmetry in gene flow among tubeworms sampled from Clam Bed, Main Endeavour Field and Mothra were evident for both HF and LF data, but surprisingly, the directions for each data set differed. For low flux tubeworms, effective population size increased from south to north among vent fields and estimates of migration rates were up to three times greater in the northward direction. Gene flow in low flux worms is northward biased and consistent with the hypothesis of near-bottom larval transport among vent fields, where mean residual flow is in a northward direction (Thomson *et al.* 2003, 2009; Garcia Berdeal *et al.* 2006). At a larger scale, northward flow is near steady and strong (~5-10 cm s^{-1}) within 75 m above bottom around CB, MEF and MOT (Thomson *et al.* 2003, 2009). Mean northward flow was also observed at MEF, being strongest (~4 cm s^{-1}) at 7 m above bottom and decreasing upward to 20 m where direction starts shifting across axis (Garcia Berdeal *et al.* 2006).

In contrast, *COI* data from high flux samples indicated southward biased gene flow among vent fields, consistent with larvae being transported in currents at elevations greater than 75 m above the axial valley, where mean flow (~5 cm s^{-1}) is predominantly southward (Thomson *et al.* 2003, 2005). Adult position on or near chimneys may influence larval dispersal trajectories at the time of their release which depends on the local topography and hydrodynamics (Bailly-Bechet *et al.* 2008). High flux worms live on chimney walls and occupy hot sulphidic waters near direct fluid flux sources (Sarrazin *et al.* 1997; Sarrazin & Juniper 1999); the location may increase the likelihood of their larvae being entrained in the buoyant plume (Kim *et al.* 1994; Bailly-Bechet *et al.* 2008) or self-recruiting back onto the same chimney wall (Bailly-Bechet *et al.* 2008). Hydrothermal fluids are discharged from chimneys at high velocities, up to meters per second (Ginster & Mottl 1994), and ascend to heights approximately 50-350 m above the seafloor where they become neutrally buoyant (Thomson *et al.* 2003; Rona *et al.* 2006; Iorio *et al.* 2012). As the plume rises, it entrains ambient seawater (see Rona *et al.* 2006; Iorio *et al.* 2012) and, in the process, may also advect larvae upwards (Kim *et al.* 1994) depending on the topography of the chimney and the local near-bottom current velocity (Bailly-Bechet *et al.* 2008). Modeling data suggest that most larvae survive plume entrainment because they enter the plume at a distance away from the point source

effluents, where temperatures have already dropped (Bailly-Bechet *et al.* 2008). Furthermore, temperature and pressure tolerances in two hydrothermal vent polychaetes suggest that entrainment in the plume is viable (Pradillon & Gaille 2007; Brooke & Young 2009).

Entrainment in the plume may provide a mechanism for larvae to access currents higher above the seafloor for southward transport among vent fields at Endeavour prior to sinking and colonizing new vent habitat. Low flux worms occur in diffuse venting at the base or flanks of chimneys and on surrounding basalts (Sarrazin *et al.* 1997; Sarrazin & Juniper 1999; Tsurumi & Tunnicliffe). Contrary to the situation for high flux worms, where larvae may have no choice but be entrained in the plume, larvae from low flux habitat are at greater distances away from fluid flux sources and may remain near-bottom for dispersal. Evidence of back migration suggests that larvae from low flux sources may occasionally become entrained in the plume or use tidal reversals to move southward. Similarly, high flux larvae can access near-bottom currents (*i.e.* remain near bottom or, if entrained in the plume, sink down to vertical levels where currents switch directions prior to colonizing new habitat). Our findings are consistent with the hypothesis that dispersal occurs not only at the level of the neutrally buoyant plume but also in near-bottom currents (Kim *et al.* 1994; Mullineaux *et al.* 1995). Adult source location is important in the vertical displacement of larvae in the water column (Bailly-Bechet *et al.* 2008) and consequently the dominant direction of movement among vent fields within Endeavour.

Larvae of several other vent species have been found in high abundance in both the buoyant hydrothermal plumes at Endeavour and >100 m away from vent sources ~15-20 m off the seafloor (Kim *et al.* 1994; Mullineaux *et al.* 1995; Metaxas 2004). Larval abundance at different heights in the water column both above and at various horizontal distances from venting sources combined with our gene flow data among vent fields support the hypothetical model of dispersal presented above. Cross-axis currents above the ridge crest may transport larvae that are entrained in the plume away from the ridge axis (Vrijenhoek, 1997; Thomson *et al.*, 2003; Marsh *et al*., 2001; Hurtado *et al.*, 2004). However, downward movement by sinking or active swimming is thought to occur in hydrothermal vent larvae from the East Pacific Rise, and acts to reduce off-axis transport into inhospitable habitat (Mullineaux *et al.* 2013). Sinking of larvae combined with

plume driven circulation within the axial valley of Endeavour may effectively enhance larval retention within the region (Thomson *et al.* 2003; Metaxas 2004; Mullineaux *et al.* 2013) while providing individuals with the capacity to colonize many if not all vent fields along the axial valley. Effective larval dispersal and retention are fundamentally important in maintaining high levels of connectivity and thus the overall viability of a metapopulation (Hanski & Gilpin 1997).

Metapopulations, source-sink dynamics and demographic history

Metapopulation processes affect demes differentially, establishing age structure among non-identical subpopulations that are connected through gene-flow (Pannell & Charlesworth 2000). Genetic properties of metapopulations depend on how extinction and re-colonization processes change the genetic composition of younger subpopulations relative to older ones (Pannell & Charlesworth 2000; Hanski & Gaggiotti 2004). Under the assumption of one panmictic population, we would expect every deme or habitat patch to have similar genetic diversities and effective population sizes. Differentiation, however, does occur in this study. The distribution of coalescence times should vary among subpopulations within a metapopulation (Pannell & Charlesworth 2000; Hanski & Gaggiotti 2004), which MIGRATE identified and rejected panmixia as the best fit model of gene flow using the *Ridgeia* mtDNA *COI* sequence data. Alternatively, MIGRATE identified grouped sites as separate subpopulations, each with various levels of genetic variation and different effective population sizes, consistent with metapopulation models (Hanski & Gilpin 1991; Pannell & Charlesworth 2000). In some cases, habitat turnover within a metapopulation can cause patterns of genetic differentiation to decrease with subpopulation age (Pannell & Charlesworth 2000). When significant F_{ST} –values were detected in our data, they only occurred between comparisons that included a pooled, younger and more ephemeral, high flux subpopulation. Differentiation was never detected between any two pooled low flux demes that generally occupy more stable habitat supporting older tubeworm aggregations. Furthermore, population turnover may substantially reduce genetic variation within subpopulations experiencing frequent local extinction events, which was identified in two of the grouped high flux sites containing the lowest levels of genetic diversity.

This study used a coalescent based approach to identify if directionality in gene flow occurred among *Ridgeia* demes in two habitats within Endeavour. Asymmetrical estimates of gene flow were evident and variation in effective population sizes supports the source-sink hypothesis. Total net immigration into low flux, putative sink demes, far exceeded net emigration, opposite to their high flux counterparts, and meets Pulliam's criteria for sources and sinks (Pulliam 1988). Higher levels of genetic diversity in low flux subpopulations support these findings, where asymmetrical net gene flow from high flux sources can cause an accumulation of genetic diversity (number of haplotypes, mean number of alleles and private alleles) in sinks (Kawecki 1995; Pannell & Charlesworth 2000; Hänfling & Weetman 2006). When immigration is high, sink subpopulations can sustain larger effective sizes than sources (Hänfling & Weetman 2006; Pulliam 1988). Scaled effective sizes would be larger for low flux worms if generation times are equal. However, when I accounted for differences in tubeworm longevity from high flow and low flow habitats (Tunnicliffe et al., in review), high flux worms had a higher overall effective population size.

Rapid coalescence has been observed in populations that experience high rates of habitat turnover (Coykendall *et al.* 2011). High flux demes display similar behaviour, thus explaining the smaller mutation scaled effective population sizes ($\Theta = N_e\mu$) compared to their low flux counterparts. However, when generation time is considered, high flux demes are effectively contributing much more to the overall metapopulation. This is consistent with known reproductive output differences between the two phenotypes (Tunnicliffe *et al.*in review; St. Germain 2011). Furthermore, although low flux subpopulations have longer generation times (Urcuyo *et al.* 2007) and would accumulate mutations at a slower evolutionary rate (Hartl & Clark 2007), we saw just the opposite, which provides further evidence of asymmetrical migration and source-sink dynamics. Observed genetic variability, combined with known biological features, indicate that most recruits originate from high flux habitat. High rates of local extinction coupled with dispersal of successful colonists from a limited number of sources lead to a very small overall effective size and, consequently, reduced genetic diversity within the metapopulation (Pannell & Charlesworth 2000; Turner *et al.* 2002).

Mitochondrial *COI* data analysis within the Endeavour axial valley identified one shared common haplotype, several occasional, and many rare haplotypes consisting of mostly one-step mutations. Such signatures of genetic variation can arise in populations that i) are undergoing recent expansion (e.g. Alvarado Bremer et al. 2005), ii) have differences in individual reproductive success (e.g. Li & Hedgecock 1998), and/or iii) are driven by asymmetrical gene flow among subpopulations (Reynolds & Fitzpatrick 2013; Paz-Vinas *et al.* 2013). One of the draw backs in using sequence data to estimate evolutionary connectivity is that different demographic processes can generate similar patterns of genetic variation, despite the very different mechanisms generating that signal (Reynolds & Fitzpatrick 2013). Based on our current biological understanding of *Ridgeia piscesae*, combined with the genetic data presented here, the following discussion will focus on the possibility that *Ridgeia piscesae*, as a metapopulation at Endeavour, is likely experiencing all three demographic processes.

Different demographic analyses consistently supported recent expansion in *Ridgeia piscesae* at the level of geographical- and habitat-defined groups as well as in the metapopulation as a whole. Demographic instability due to regional extinction and recolonization events frequently create patterns of population growth and expansion in hydrothermal vent species (Hurtado *et al.* 2004; Plouviez *et al.* 2009; Vrijenhoek 2010; Coykendall *et al.* 2011; Teixeira *et al.* 2012; Beedessee *et al.* 2013). Rapidly expanding populations feature a star-like genealogy of haplotypes and an excess of rare alleles, where mutations arise but have not yet become common within a population (Pannell 2003; Alvarado Bremer *et al.* 2005; Reynolds & Fitzpatrick 2013). Asymmetrical gene flow can also generate a signal of an excess of rare alleles and, in turn, generate false signals of recent population growth (Reynolds & Fitzpatrick 2013; Paz-Vinas *et al.* 2013). Both processes are likely occurring *R. piscesae*. If asymmetrical gene flow were the only process affecting patterns of genetic variation, we would expect to see an accumulation of rare alleles in sinks only and, therefore, only detect false positives for rapid expansion in the low flux subpopulations. However, high flux, putative source demes identified recent demographic expansion which would be expected from the rapid turnover and ephemeral nature of this habitat type: high rates of extinction followed by re-colonization remove much of the genetic variation and feature an excess of low

frequency segregating sites (Pannell 2003). I therefore suggest that high flux subpopulations are undergoing rapid expansion and that asymmetrical migration is, likely, exaggerating the number of rare alleles in low flux sinks due to an accumulation of alleles from multiple and rapidly expanding high flux sources. In addition, if low flux sinks were evolutionary "satellites" of sources, then low flux subpopulations would never appear to reach equilibrium, despite supporting long-lived tubeworms in a more stable habitat, due to the consistent net immigration from rapidly expanding sub-populations.

It is not uncommon in marine systems for a small proportion of adults to contribute to the majority of the recruitment (see Hedgecock et al., 2007). Differences in reproductive success occur among phenotypes of *Ridgeia piscesae* (Tunnicliffe *et al., in review*; St. Germain 2011). Habitat differences correspond to variation in reproductive output of *R. piscesae*, whereby tubeworms from high flux optimal habitat can mature within months and have high fecundity with continuous gamete output compared to tubeworms from other habitats that rarely showed reproductive readiness (Tunnicliffe et al., in review). Because high flux habitat is very limited at hydrothermal vents (Tunnicliffe et al., in review; Sarrazin & Juniper 1999; Sarrazin et al. 1997), many individuals likely fail to contribute to the overall population. When a small proportion of adults account for most of the recruitment, a large number of closely related haplotypes, that may differ by as little as a single nucleotide substitution, are observed within the population and are thought to be recently derived from one common ancestral sequence (Li & Hedgecock 1998). Because effective size for the overall population is small, the observed haplotype frequencies, with one common haplotype and many rare haplotypes in the population, arise from genetic drift (Li & Hedgecock 1998). In addition, due to the extreme variance in reproductive success, "chaotic" heterogeneity on small spatial scales is likely the result of temporal variation in the genetic composition of new recruits (Hedgecock 1994; Li & Hedgecock 1998; Planes & Lenfant 2002); however, this pattern is also a signature of metapopulation processes (Pannell & Charlesworth 2000; Hanski & Gaggiotti 2004).

Alternative demographic hypotheses

Low flux habitats are far more abundant and stable within Endeavour and support longer-lived tubeworms than those found in high flux habitats (Sarrazin *et al.* 1997; Sarrazin & Juniper 1999; Urcuyo *et al.* 2003, 2007; Tunnicliffe et al., in review). High flux ephemeral habitat is sparsely distributed and tubeworms located at HF sites experience high rates of habitat turnover (Sarrazin *et al.* 1997; Sarrazin & Juniper 1999; Tunnicliffe et al., in review). When local extinction is followed by a propagule-pool colonization event, where colonists of the newly vacant habitat originate from a single source subpopulation, genetic variation is expected to be low and coalescence times is expected to be rapid (e.g. Pannell & Charlesworth 2000; Pannell 2003) which is what we observed in HF samples. It is possible that HF habitats are colonized by larvae that originate from LF habitats, despite asymmetrical estimates of migration in the opposite direction, and that genetic variability and coalescence times is reduce in HF sites due to colonists originating from a single LF deme. It is important to consider the differences in habitat longevity and associated tubeworm longevity and how such factors may be confounding the patterns of genetic variability and gene flow identified among habitat types. Furthermore, oceanographic currents and gene flow data observed among vent fields within Endeavour, suggest that larvae have the capacity to colonize many if not all vent fields along the axial valley which may also extend to all habitat types. Thus, it is viable that larvae originating in LF habitats can reach HF sites.

Environmental conditions are more extreme in high flux habitat, thus selection on mtDNA haplotypes may be more stringent on *Ridgeia piscesae* from HF compared LF environments. For example, evidence of habitat-specific selection in pocket mice (*Chaetodipus intermedius*) across a habitat gradient has been documented (Hoekstra *et al.* 2004). Selection was stronger against one phenotype to habitat type than the other, despite high levels of gene flow among both populations (Hoekstra *et al.* 2004). If variation in the mitochondrial genome in *Ridgeia piscesae* is not strictly neutral, but weakly deleterious (Ballard & Kreitman 1994; Nachman *et al.* 1996; Rand & Kann 1998; Nielsen & Weinreich 1999; Rand 2001; Ballard & Rand 2005) then the variation in gene frequencies, including mtDNA *COI,* among habitats might be a consequence of different

strengths of selection in the different environments (e.g., Hoekstra *et al.* 2004). When natural selection is strong, variation in local gene frequencies can occur across heterogeneous environments, despite high levels of gene flow among habitats (e.g., Nagylaki 1975; Sandoval 1994; Chevillon *et al.* 1995; Ross & Keller 1995). Thus, stronger habitat-based selection may potentially explain the lower genetic diversity and coalescence times identified in tubeworms from HF habitats. If selection rather than source-sink dynamics explains the observed variation in gene frequencies among HF and LF worms, then gene flow may be symmetric between habitat types or possibly asymmetrical in the reverse direction from LF to HF worms. Asymmetrical gene flow from LF to HF samples was identified at Mothra when habitat types from each vent field were analysed separately in MIGRATE. Furthermore, LF-specific alleles (n=14) and HF-specific alleles (n=6) were identified in the mtDNA *COI* sequence data.

Limitations of this study

Vent fields in the northern sectors of the Endeavour axial valley were not sampled in this study however, they may act as important source subpopulations to the overall metapopulation. Consequently, the values of effective population size may have been overestimated due to the upward bias in this parameter (Θ) estimation in MIGRATE when gene flow from the unknown population(s) is large (Beerli 2004). However, because estimates of migration (M) in MIGRATE are robust to unsampled populations, modifications of the patterns of gene flow among vent fields identified in this study should be minimal (Beerli 2004). Also, tubeworm aggregations were only sampled from habitats thought to be of most significance in the study area, therefore, some subpopulations were excluded. Intermediate forms of *Ridgeia piscesae* are considered non-reproductive (Tunnicliffe et al., in review); excluding these tubeworms from the sampling design likely had minimal impact on the results from this study.

While mitochondrial *COI* data provided adequate variation to identify fine-scale substructure and genetic connectivity in *Ridgeia piscesae* from Endeavour, there are limitations to only using one molecular marker in population genetic analyses (reviewed in Zhang & Hewitt 2003). Mitochondrial *COI* is still a widely used marker in population genetic studies; however, population parameters estimated in this study were based on

data from a single non-recombining region of the genome which can be associated with a large variance in the estimates. Furthermore, patterns of genetic diversity and relationships among populations vary widely among loci therefore, an accurate estimation of the demographic history requires multiple unlinked loci (reviewed in Zhang & Hewitt 2003). Mitochondrial DNA used in combination with nuclear markers, such as single nucleotide polymorphisms (SNPs) or microsatellites, has great potential for unravelling complex evolutionary and ecological processes (e.g. Pabijan & Babik 2006; Martínez-Solano & González 2008). Genotypic data could be used to compare present-day patterns of migration to the patterns of average genetic connectivity that were estimated over multiple generations in this study and should be considered in for future population genetic analysis in *Ridgeia piscesae*. Nonetheless, ecological, biological and oceanographic data are consistent with the patterns of genetic connectivity identified using mtDNA *COI*. Furthermore, the uncertainties that arise when using one molecular marker to estimate genetic connectivity decrease with an increasing sample size and provide robust estimates of population parameters when using coalescent based models (Beerli & Felsenstein 2001; Beerli 2004). Sequencing nearly 500 *Ridgeia piscesae* individuals increased the genetic resolution needed to identify fine-scale substructure and provided reliable estimates of gene flow at Endeavour and adjacent vent sites.

Conclusions

Models of gene flow in *Ridgeia piscesae* reflect the general oceanographic circulation described at Endeavour (Thomson *et al.* 2003). Genetic data suggest that dispersing larvae have the capacity to exploit the bi-directional currents created through plume driven circulation within the Endeavour axial valley. Adult position on or near chimneys may influence larval dispersal trajectories at the time of their release (Bailly-Bechet *et al.* 2008). Colonization of high flux habitat occurs through dispersal in southward biased currents further above the seafloor, whereas colonization of low flux habitat is achieved through near-bottom larval transport. Together, these data suggest that local conditions within meters around the venting chimneys influence the dispersal and colonization processes of *Ridgeia piscesae* (Bailly-Bechet *et al.* 2008).

Patterns of genetic variation and substructure in *Ridgeia piscesae* at Endeavour are likely due to differences in metapopulation processes and reproductive success rather than a genetic basis for local adaptation to different habitats. Demographic instability is due to metapopulation processes (Hurtado *et al.* 2004; Vrijenhoek 2010), whereby high flux subpopulations are frequently subjected to local extinction and recolonization events on independent time scales, causing greater genetic sub-structure than in their low flux counterparts (Reynolds & Fitzpatrick 2013). Asymmetrical gene flow identified source-sink dynamics and confirmed that successful recruits originate from highly productive tubeworms in limited high flux habitat. Although tubeworms from high flow and low flow habitat were identified as separated subpopulations that experience independent local dynamics, high estimates of asymmetrical gene flow suggest that phenotypic plasticity is favoured over local specialization, as proposed by Tunnicliffe et al. (in review).

Chapter 3 - Cross-species amplification of microsatellite loci in *Ridgeia piscesae*: assessment and application

Introduction

By determining the relationships among species, populations and individuals, we can learn a lot about adaptation and the speciation process, about animal migration (past and present), and about who is or is not reproducing within a population. These relationships, which are often difficult to delimit using morphological data or field observations, can often be characterized using molecular tools. Although cameras have very recently turned some of the focus back to the whole organism (e.g. whales from satellites, grizzly bears in highway tunnels, hydrothermal vent colonization) (e.g. Sawaya *et al.* 2014; Fretwell *et al.* 2014), the distribution of alleles at polymorphic markers is usually the only way to infer historical events (e.g., patterns of cladogenesis, population expansions or bottlenecks) or to quantify contemporary events hidden from view.

The choice of suitable genetic markers is largely based on the biological question of interest (Avise 2004; Selkoe & Toonen 2006) and markers are often used in combination to estimate parameters such as recent and past migration rates and population size, demographic expansion and species divergence (e.g. Pabijan & Babik 2006; Martínez-Solano & González 2008; Barson *et al.* 2009; Andreasen *et al.* 2012; Cowart *et al.* 2013; Teixeira *et al.* 2013). Differences in the effective population sizes, inheritance profiles and mutation rates between different molecular markers (e.g. mitochondrial DNA and nuclear microsatellite loci) provide the potential to separate and reveal complex evolutionary and ecological processes within a population (Hellberg *et al.* 2002; Avise 2004; Selkoe & Toonen 2006).

Nuclear microsatellites are currently the most popular and frequently used markers in fine-scale population genetic studies due to their rapid mutation rates, which generate a large number of alleles (Schlötterer 2000; Estoup *et al.* 2002; Balloux & Lugon-Moulin 2002; Avise 2004; Ellegren 2004; Selkoe & Toonen 2006; Barbará *et al.* 2007). Microsatellites are tandemly repeated, short (2-6 bp) nucleotide motifs. They are abundant throughout the genome of most taxa (Estoup *et al.* 2002; Avise 2004). For

example, microsatellites comprise approximately 3% of the human genome, which equates to one motif per every two kilobase of DNA (Lander *et al.* 2001). Microsatellites are used to measure naturally occurring genetic diversity over small spatial scales, population substructure and present-day directional migration or gene flow among weakly differentiated populations (e.g. Sunnucks *et al.* 1997; Saccheri *et al.* 1998; Marshall & Ritland 2002; Barson *et al.* 2009; Andreasen *et al.* 2012). Microsatellites are particularly useful in genetic studies estimating demographic processes acting on ecological time scales (e.g. years), because such studies require molecular markers with high levels of allelic diversity (Avise 2004; Selkoe & Toonen 2006; Hedgecock *et al.* 2007a; Lowe & Allendorf 2010). Source-sink dynamics have been identified in wild populations using assignment tests, that calculate the probability that a given individual originated from a particular source population based on its multilocus genotype (Paetkau *et al.* 1995; Manel *et al.* 2005; Hänfling & Weetman 2006; Martínez-Solano & González 2008; Andreasen *et al.* 2012; Brüniche-Olsen *et al.* 2013; Thomas & Bell 2013). Applying direct genetic methods, such as assignment tests, is conceptually similar to non-genetic approaches for estimating contemporary connectivity, an important component in developing effective conservation strategies (Hedgecock *et al.* 2007; Lowe & Allendorf 2010).

Although the development of microsatellite markers for individual species can be difficult and time consuming, cross-species amplification of microsatellites developed for closely related taxa is a simple and cost efficient alternative. Microsatellites are not generally considered as "universal" genetic markers that can easily be transferred between a wide range of species, such as mitochondrial cytochrome c oxidase subunit I (*mtCOI*) (Folmer *et al.* 1994), however, primers are known to bind to the conserved flanking regions of microsatellite motifs in closely related species (e.g. Primmer *et al.* 2005). Successful marker amplification in a target species is most often assessed by the comparison of amplified product to the expected fragment size in the source species and/or less frequently through direct sequencing of the amplified fragments (see Barbará *et al.* 2007). Cross-species utility of microsatellite loci has been reported in animals, fungi and plants at varying levels of success and depend mainly on the phylogenetic

distance between the source and focal species, though this varies across taxa (e.g. Primmer *et al.* 2005; Barbará *et al.* 2007; Hendrix *et al.* 2010; Jan *et al.* 2012).

Despite their increased use over the past decades, the application of microsatellites to infer genetic structure and population connectivity is limited in hydrothermal vent species (e.g. Thaler *et al.* 2011; Teixeira *et al.* 2012a, 2013). Vestimentiferan tubeworms belong to the family Siboglinidae and include the hydrothermal vent tubeworms and the cold seep "escarpids" and "lamellibrachids" (Figure 3.1) (McMullin *et al.* 2003; Rouse *et al.* 2004; Pleijel *et al.* 2009; Hilário *et al.* 2011). Microsatellites have been developed for three vestimentiferan species closely related to the hydrothermal vent tubeworm *Ridgeia piscesae* (Figure 3.1) (McMullin *et al.* 2004; Fusaro *et al.* 2008). McMullin et al. (2004) developed twelve microsatellite loci for two cold seep tubeworm species, *Lamellibrachia luymesi* and *Seepiophila jonesi,* and identified a decrease in cross-species amplification success across deeper evolutionary distances. The same study reported successful cross-amplification of polymerase chain reaction (PCR) products in *Ridgeia piscesae* using primer pairs designed for the *Escarpia* sibling species *Seepiophila jonesi*. Additionally, twelve microsatellite loci have recently been developed for the hydrothermal vent species *Riftia pachyptila* (Fusaro *et al.* 2008). Although cross-species amplification success was not tested across other vestimentiferan species, *Riftia pachyptila* microsatellite loci may also cross-amplify PCR product in *Ridgeia piscesae* as they are more closely related than the seep species (Figure 3.1) (McMullin *et al.* 2003; Rouse *et al.* 2004; Pleijel *et al.* 2009; Hilário *et al.* 2011).

The goal of this study was to amplify multiple microsatellite loci in *Ridgeia piscesae* through cross-amplification of loci previously developed in three closely related taxa; *Lamellibrachia luymesi*, *Seepiophila jonesi* and *Riftia pachyptila* (McMullin *et al.* 2004; Fusaro *et al.* 2008). Microsatellite markers would be used to augment the results obtained from *Ridgeia piscesae mtCOI* data (see Chapter 2 of this thesis) and to assess demographic connectivity using direct genetic methods (e.g. assignment tests). Highly polymorphic nuclear markers, combined with direct genetic measures of population connectivity would increase the resolving power to distinguish source-sink metapopulation dynamics identified in *Ridgeia piscesae* from Endeavour using *mtCOI* data.

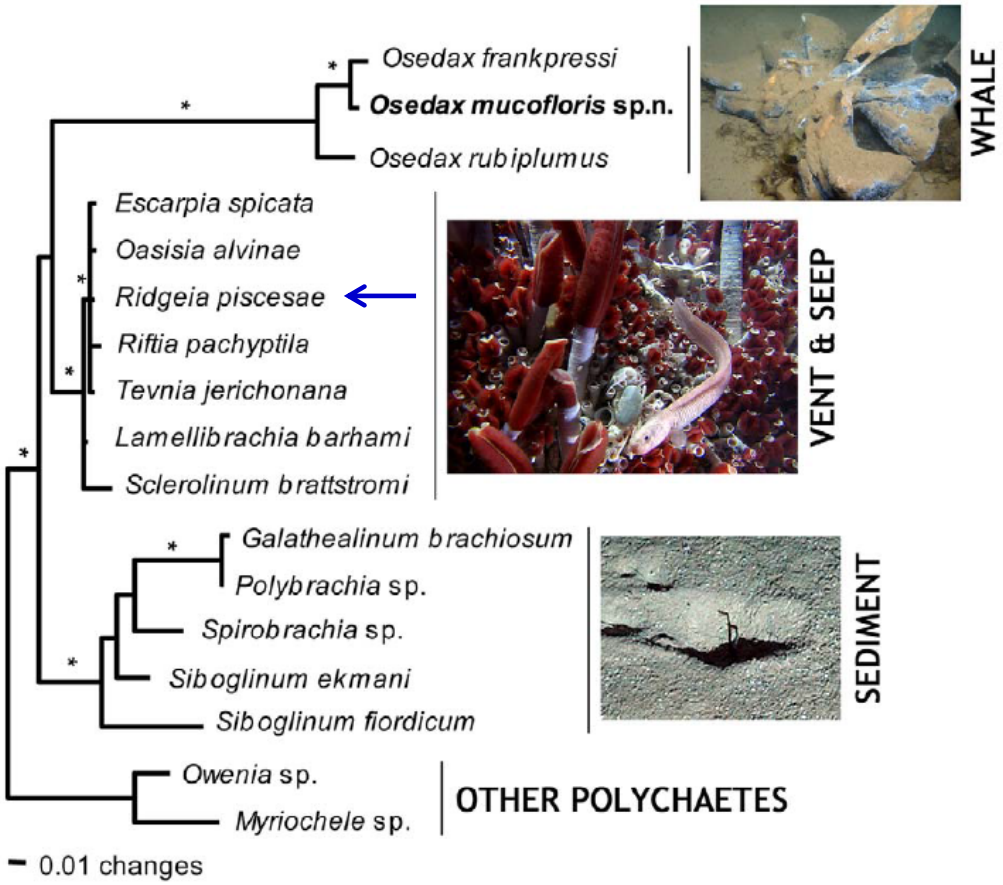

Figure 3-1: Phylogenetic relationships among Siboglinidae from a Bayesian analysis of 18S ribosomal RNA sequences. Branch length reflects numbers of nucleotide changes between species. Blue arrow indicates the target species, *Ridgeia piscesae*, for cross amplification of microsatellite loci and red arrows indicate vestimentiferan source taxa (not necessarily the same species) of microsatellites loci. (Figure from (Hilário *et al.* 2011)).

Materials and Methods

To study the use of vestimentiferan microsatellite markers for cross-species amplification in *Ridgeia piscesae*, twelve primer pairs from three source species were tested in PCR reactions with *R. piscesae* genomic DNA (Table 3.1). Genomic DNA was previously extracted from tubeworm vestimentum tissue that is normally devoid of endosymbiotic bacteria (see Young *et al.* 2008). Cross-species amplification was tested in

at least four individuals, two from high flux and two from low flux habitat, and randomly chosen from the three vent fields sampled within Endeavour (CB, MEF, MOT) (see Material and Methods from Chapter 2 for DNA extraction protocols and sample site descriptions).

Polymerase chain reactions (PCRs) were optimized for the expected size fragment of amplified DNA, as specified in the literature, for microsatellite loci listed in Table 3.1. Reactions were prepared in 12.5 µl volumes containing 10x *Taq* Buffer (Fermentas), variable concentrations of $MgCl_2$ (Table 3.1), 0.2 mM dNTPs, 0.4 µM each primer, 1 unit *Taq* DNA polymerase (Fermentas), 1.0 µl genomic DNA of varying concentrations, and the appropriate volume of ddH_2O. The amplification profile typically consisted of an initial denaturing step of 2 minutes at 95°C followed by 39 cycles of denaturation at 94°C for 30 seconds, primer annealing at X°C (Table 3.1) for 45 seconds, extension at 72°C for 1 minute, and a final extension at 72°C for 5 minutes. For the locus ECL2-12C the amplification profile consisted of an initial denaturing step of 2 minutes at 95°C followed by 5 cycles of denaturation at 94°C for 30 seconds, primer annealing at 53°C for 45 seconds, extension at 72°C for 1 minute, and 34 cycles of denaturation at 94°C for 30 seconds, primer annealing at 58°C for 45 seconds, extension at 72°C for 1 minute. The final extension was at 72°C for 5 minutes.

PCR products were electrophoresed on a 1.6% agarose gel pre-stained with SYBR® Safe (Invitrogen) and visualized on the AlphaImager® Imaging System (Alpha Innotech). Amplification success of microsatellite loci was classified into the five following criteria prior to further analysis: (++) loci showing clear signals of amplification success with potential heterozygous alleles, (+) loci showing clear signals of amplification success with monomophic products, (w) markers that showed weak signals of amplification success, (-) loci without amplification success and, (mb) loci showing multiple banding patterns and considered as negative cross-amplification success.

To confirm the presence of microsatellite repeats, the PCR product of one individual was direct sequenced at the nine loci that showed weak to strong amplification success (Table 3.1). Successful amplicons were purified using Qiagen's QIAquick® Gel Extraction Kit. Purified PCR products were sequenced in the forward or reverse direction

commercially by Eurofins MGW Operon (Huntsville, AL). Sequences were edited in BioEdit 7.2.0 (Hall, 1999) and manually verified by eye to confirm the presence or absence of microsatellite repeats prior to being used as query sequences in a BLASTn (default parameter) search implemented on the NCBI nucleotide database.

Results

Seven out of the twelve primer pairs from source microsatellite loci showed consistent and clear signals of amplification in all *Ridgeia piscesae* specimens, four of which had diagnostically different allele size ranges than those found in the respective source species (Table 3.1; Figure 3.2). Four loci showed positive signals for polymorphic products; R2E142, ECL3-8D, E3-10A and Rpa10CA07[3] (Figure 3.2). Weak amplification signals were identified in several *R. piscesae* specimens from the R3D3[3] and ECL2-12C loci (Figure 3.2). The E3-2D locus generated products with identifiable but weak and inconsistent signals of amplification that sometimes showed multiple banding patterns of three of more alleles that were difficult to score according to size or intensity and were therefore considered as negative results of cross amplification (Figure 3.2, Table 3.1). Two loci failed to amplify PCR products in *R. piscesae*, the E3-10A#2 and L2-D2 *inner* loci (Table 3.1). Microsatellite repeats motifs were absent in all sequences from all loci that originally suggested successful cross-amplification of monomorphic or bi-allelic PCR products. The BLASTn search returned no sequences with significant similarity to the DNA fragments isolated in *Ridgeia piscesae* in the NCBI database. All primer pairs from source species microsatellite loci failed to amplify interpretable products in *Ridgeia piscesae*.

Table 3-1: Details of the 12 microsatellite markers tested for cross-species amplification success in *Ridgeia piscesae* developed for closely related vestimentiferan species. Amplification success based on agarose gel electrophoresis indicated by: (++) loci showing clear signals of amplification success with potential heterozygous alleles, (+) loci showing clear signals of amplification success with monomophic products, (w) markers that showed weak signals of amplification success, (-) loci without amplification success and (mb) loci showing multiple banding patterns and considered as negative cross-amplification success. (*): different allele size ranges than those found in the respective source species (Ta): annealing temperature

Locus (GenBank Accession No.)	Locus source species	Repeat motif in source	Primer sequence (5'-3')	Allele size range in source	Approximate allele size in *Ridgeia piscesae*	Amplification success	Ta (°C)	[$MgCl_2$] (mM)	Reference
R2D12[1] (EF586194)	*Riftia pachyptila*	$(TG)_{27}$	F: GCAGCAGAATTGAAGGTCGT R: GCCTAGCATCTGTCTCTTATTGA	213–278	200-300	+	58	2	Fusaro *et al.* (2008)
Rpa10CA06[5] (EF586201)	*Riftia pachyptila*	$(AC)_{15}$	F: GGCAAGGAATGCAGTGAGAT R: GAGTGCGTGAAGATGAGTGC	225–254	100-200*	+	44	2	Fusaro *et al.* (2008)
Rpa10CA07[3] (EF586202)	*Riftia pachyptila*	$(AC)_{38}$	F: GATCGAACCACCTGTTAGATGTT R: GTCCTCAAAGTCGCAAACAGA	147–231	~200	++	49	2	Fusaro *et al.* (2008)
R3D3[3] (EF586197)	*Riftia pachyptila*	$(GT)_{15}(GCGT)_{15}$	F: CATACAAGGGCAACAACGTTTA R: ATACCGCGTAATTTGGCTAAGA	215–269	300-400*	w	45	2	Fusaro *et al.* (2008)
R2E14[2] (EF586195)	*Riftia pachyptila*	$(AC)_{26}GC(AC)_3$	F: AATACCATGCTGGGTGGAAC R: GCTGAAATTGGTCTCTTCGTG	187–232	200-300	++	45	1.25	Fusaro *et al.* (2008)
L2-2D inner AY263755	*Lamellibrachia luymesi*	$(CA)_{13}(CACG)_3$	F: ATAAGATGCGACTTCGATGC R: CTCTACATGAACAAGTTTGC	245–287	N/A	-	43	2	McMullin *et al.* (2004)
E3-2D AY263777	*Seepiophila jonesi*	$(CGTG)_9$	F: GATCTCTTCTGGCAGGCGTT R: CTCCATTGCATCTACGGGTC	128–195	100-500	mb	53	2	McMullin *et al.* (2004)
ECL3-8D AY263763	*Seepiophila jonesi*	$(TGCG)_9$	F: GCGTTGCTAACTGCCAAGTG R: ATCTTGACCAGTCGCTGACC	323–563	300-400	++	46	2	McMullin *et al.* (2004)
ECL2-12C AY265354	*Seepiophila jonesi*	$(CTGT)_7$	F: GGAGCCTCCTTGACTTTACA R: CAAAGCTCATCGCACACTTG	194–224	100-200	w	53, 58	2	McMullin *et al.* (2004)
E3-10A AY263780	*Seepiophila jonesi*	$(TGTC)_8$	F: AGGTCAGAGGCATTGCCATA R: ACAACGGACAGGTCTGCATT	305–329	400-500*	++	46	2	McMullin *et al.* (2004)
E4-7G AY263779	*Seepiophila jonesi*	$(GT)_{19}$	F: TCATTGCTCTCCTGGTTTAG R: GCCTGGTTTCTGATGACTTA	271–316	100-200*	+	45	1.75	McMullin *et al.* (2004)
E1-10A#2 AY263764	*Seepiophila jonesi*	$(CACG)_9(CA)_{13}$	F: GTCTTCTGATGTCATGGTCC R: CGAACACCTCGACAATCAAC	128–234	N/A	-	43	2	McMullin *et al.* (2004)

Discussion

The attempt to amplify microsatellite markers in *Ridgeia piscesae*, from loci developed for closely related genera, likely failed due to genetic distances that were too large to maintain conserved priming regions across taxa. Low annealing temperatures, such as those used in this study, decreased the specificity of the primer pairs to template DNA and likely amplified imperfect matches throughout the *Ridgeia piscesae* genome. This may also explain the lack of sequence hits with significant similarity to the amplified *Ridgeia piscesae* sequences.

Cross-species amplification is only successful if the flanking regions of the microsatellite markers are conserved between species. The level of sequence conservation in the priming regions varies among loci and is possibly due to their location in the genome (Peakall *et al.* 1998; Primmer *et al.* 2005; Küpper *et al.* 2008; Jan *et al.* 2012). Although the majority of microsatellite loci are located in the intergenic regions of the genome (Tóth *et al.* 2000), microsatellites associated with coding regions are more likely to have conserved priming regions and cross amplify among more distantly related species (e.g. Peakall *et al.* 1998). Extreme conservation of microsatellite flanking regions has been reported across several taxa, including fish, turtles, whales and coniferous trees (Schlötterer *et al.* 1991; FitzSimmons *et al.* 1995; Rico *et al.* 1996; Scott *et al.* 2003), however, the proportion of loci that amplify and show polymorphisms typically decreases with phylogenetic distance (e.g. Moore *et al.* 1991; Peakall *et al.* 1998; Primmer *et al.* 2005; Barbará *et al.* 2007; Hendrix *et al.* 2010; Jan *et al.* 2012). As genetic distance between the source and target species increases, mutations are more likely to evolve in the flanking regions of the microsatellite loci, where primers bind, thereby decreasing cross-amplification success (e.g. Hendrix *et al.* 2010).

Cross-species transferability of microsatellite loci is unevenly distributed across taxa (Barbará *et al.* 2007). Invertebrates, birds, reptiles and mammals generally cross-amplify a high percent of microsatellites markers between species within the same genera. Reptiles and mammals generally cross-amplify successfully at the next taxonomic level however, transfer success drastically drops for invertebrates among closely related genera within the same family (e.g. Barbará *et al.* 2007). The abundance

of microsatellites is highly variable in the genomes of some marine invertebrate species which can negatively impact cross-species amplification (Cruz *et al.* 2005). Microsatellite sequences mutate frequently due to slipped-strand mispairing during DNA replication or repair, resulting in changes to the number of repeats and thus the length of the locus (reviewed in Chistiakov *et al.* 2006). Species-specific properties of the mutation/repair mechanism of replication slippage may affect the birth and death of microsatellites and these differences may explain the variation in locus density among marine invertebrate genomes (Cruz *et al.* 2005). Similarly, if differences in the mutation/repair mechanisms of replication slippage occurred among vestimentiferan species, variation in the abundance, and thus presence or absence, of microsatellite loci among species may also be expected and thus contribute to the lack of cross-amplification success in *Ridgeia piscesae*.

Cross-amplification success is higher in species with long generation times as they typically accumulate mutation at a slower evolutionary rate (Hartl & Clark 2007) and thus priming regions are more likely to be conserved (Barbará *et al.* 2007). Generation times within and among vestimentiferan species are highly variable and can range from years to possibly centuries (e.g. Bergquist *et al.* 2000; Tunnicliffe et al., in review). Unlike cold seep species, that are characterized by generation times of approximately 200 years (Bergquist *et al.* 2000), hydrothermal vent tubeworms have much shorter generation times, for example two to ten years for *Ridgeia piscesae* (Tunnicliffe *et al*., in review), which may contribute to the unsuccessful cross-amplification among these taxa.

Larger genome sizes may negatively affect cross-amplification success (e.g. Garner 2002; Barbará *et al.* 2007b), however, this relationship is not universal (Cruz *et al.* 2005; Hendrix *et al.* 2010). Although unknown in *Ridgeia piscesae*, genome size has been identified in three vestimentiferans vent species. C-values - the quantity of haploid DNA in picograms- ranged from 0.76-1.06 in vent tubeworms, which is small compared to other invertebrate taxa (Bonnivard *et al.* 2009). If the genome size of *Ridgeia piscesae* is similar to other vent tubeworms, it is considerably smaller than the genome of animals that successfully cross-amplified microsatellite loci among closely related taxa (e.g.

Hendrix *et al.* 2010). These results are therefore inconsistent with the above pattern and not likely the cause for failed amplification success in this study.

Numerous studies infer cross-species transfer success of microsatellite loci in target species using results from agarose gel electrophoresis (e.g. Reading *et al.* 2003; Cruz *et al.* 2007; Hardesty *et al.* 2008; Zelnio *et al.* 2010). Though gel electrophoresis is simple, it fails to provide sufficient resolution to assess amplification success. This study demonstrated that, despite similar fragment size ranges to source species and identifiable polymorphisms in amplified products, without direct sequencing, it is impossible to confirm transfer success of microsatellite markers across taxa. The potential for cross-species amplification of microsatellite markers among vestimentiferan taxa appears to be much more limited than previously anticipated (McMullin *et al.* 2004).

Although this study failed to cross-amplify microsatellite loci in *Ridgeia piscesae*, there has recently been an increasing effort to develop microsatellite markers for hydrothermal vent species (e.g. Teixeira *et al.* 2011; Schultz *et al.* 2011; Boyle *et al.* 2013; Roterman *et al.* 2013; Jacobson *et al.* 2013). It is increasingly more viable for researchers to obtain de-novo molecular markers in non-model organisms due to the development of high-throughput sequencing and the increase in accessible resources (e.g. statistical software) (Seeb *et al.* 2011; Peterson *et al.* 2012; Poland *et al.* 2012; Somme *et al.* 2012; Dobeš & Scheffknecht 2012; Reid *et al.* 2012). In future studies, the isolation and characterization of new microsatellite loci in *Ridgeia piscesae* may be quite simple to develop using next generation sequencing. However, until more highly polymorphic genetic markers are developed for this species, patterns of recent migration and contemporary connectivity remain difficult to assess.

As more nuclear microsatellites are developed for new species, the possibility of mining for highly conserved microsatellite loci among more distantly related taxa may increase the potential for finding "universal" microsatellite markers (e.g. Küpper *et al.* 2008). Mining sequence databases for conserved microsatellite markers has enhanced the cross-species utility in birds and bats, with the intention of reducing the dependence of transfer success on genetic distance from the source species (Küpper *et al.* 2008; Dawson *et al.* 2010; Jan *et al.* 2012). The availability of a larger number of population genetic markers would be of considerable benefit to research in conservation biology, especially

for endemic species such as hydrothermal vent organisms, in which sufficiently polymorphic markers have not been widely available for estimating demographic processes acting on ecological time scales.

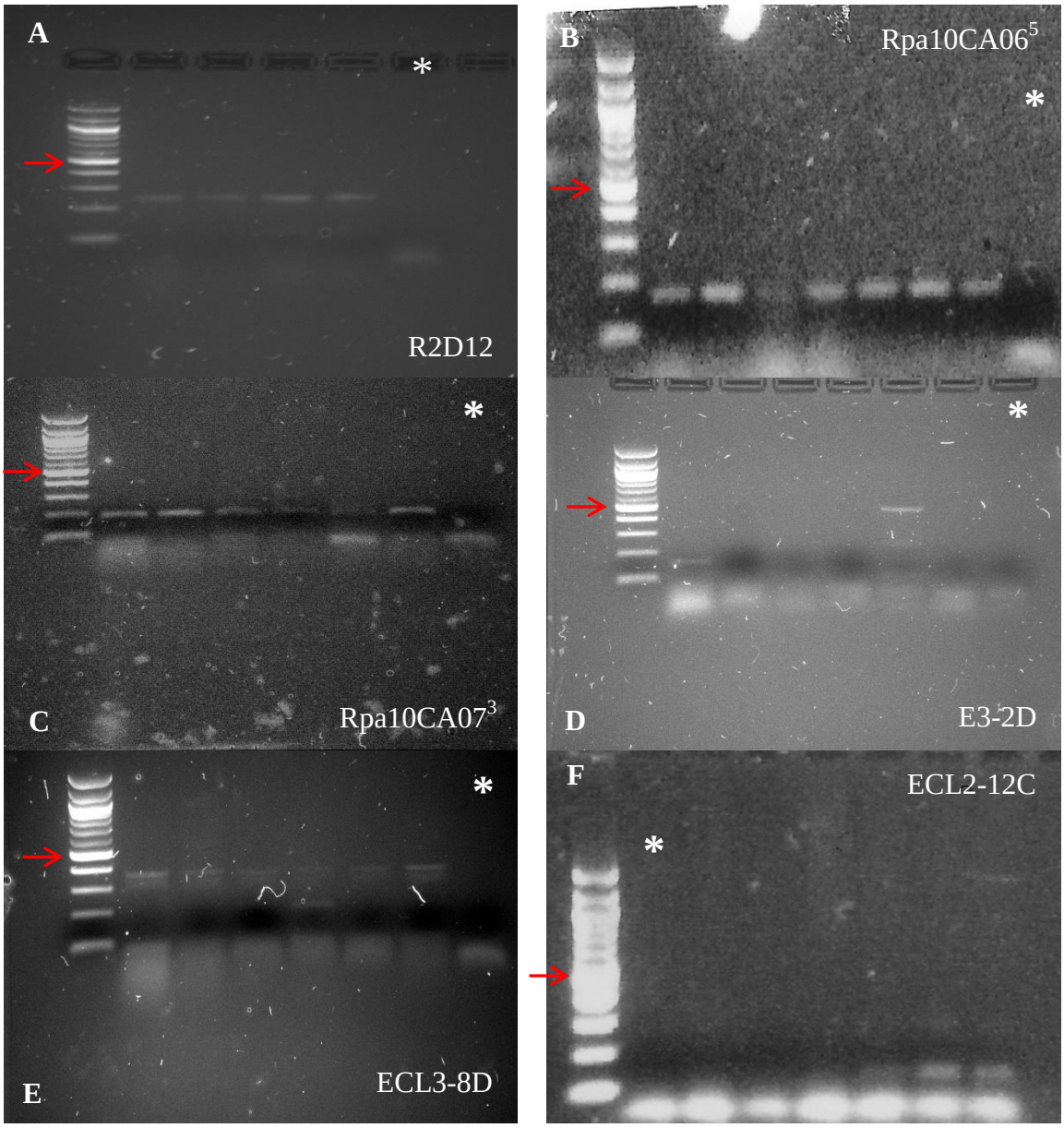

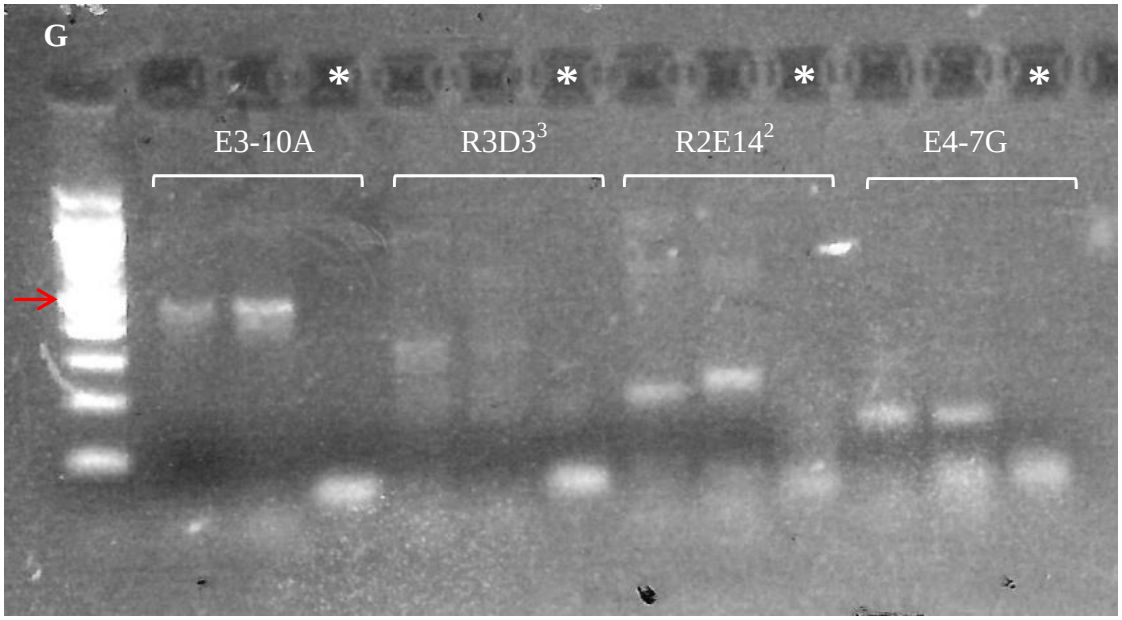

Figure 3-2: Visualization of the cross-species amplification success of 10 microsatellite markers in the target species, *Ridgeia piscesae*, electrophoresed on a 1.6% agarose gel electrophoresis stained with SYBR safe. Microsatellite markers were designed for three vestimentiferan vent species *Lamellibrachia luymesi*, *Seepiophila jonesi* and *Riftia pachyptila* (McMullin *et al.* 2004; Fusaro *et al.* 2008). Lane 1 in figures A-G represents a 100 base pair ladder and red arrows indicate 500 base pairs. * indicate lanes in which no template DNA was added to the PCR reaction. Cross-species amplification was tested in two to seven individuals from high flux and low flux habitat, and randomly chosen from the three vent fields sampled within Endeavour (CB, MEF, MOT)(see Material and Methods from Chapter 2 for DNA sample descriptions).

Chapter 4 -
Applications of genetic connectivity in the conservation of deep-sea hydrothermal vent ecosystems: Why should we care?

4.1 The era of deep sea industrialisation

Since the discovery of hydrothermal vents over 30 years ago, the greatest anthropogenic threat to vent communities has been scientific exploration (Van Dover 2012). In response, the scientific community adopted a set of guidelines for responsible marine research, the InterRidge code of conduct, to minimise their impacts on hydrothermal vent communities and set the stage for exemplary behaviour for deep-sea exploration (Devey *et al.* 2007; Van Dover 2012). Though scientific research still has the potential to adversely impact hydrothermal ecosystems (Voight *et al.* 2012), these impacts are minimal compared to the potential disturbance created by industrial deep sea mining activities (Devey *et al.* 2007; Van Dover 2011, 2012). Advances in technology and recent economic incentives from the metals markets have renewed interest in hydrothermal vent mining and moved the prospect of deep sea mineral exploitation closer to reality (Halfar & Fujita 2007; Hoagland *et al.* 2010; Van Dover 2011). To date, no commercial mining has occurred anywhere in the world but deep sea mineral extraction is likely to commence within the next decade (Van Dover 2012; Boschen *et al.* 2013). In the last decade, the number of known active hydrothermal vent systems has almost doubled, from 277 to 521, due to the developments and access to technology and the increased interest in hydrothermal vent mining (Beaulieu *et al.* 2013). At least 18.5% of all known hydrothermal vents fields are under consideration for mineral prospecting and exploration (Beaulieu *et al.* 2013). The most likely candidate for the first hydrothermal vent mining activities are the Manus Basin in the Exclusive Economic Zone (EEZ) of Papua New Guinea, where a mining lease was granted (to a Canadian company) in 2011; a site within the EEZ of New Zealand has been licensed for prospecting (Halfar & Fujita 2007; Boschen *et al.* 2013).

Seafloor massive sulphides (SMS) are metal rich geological deposits associated with hydrothermal vent activity (Hoagland *et al.* 2010). They are economically attractive

because SMS contain commercially viable quantities of high grade ores that are dense in copper and zinc but may also contain substantial quantities of silver and gold (Hoagland *et al.* 2010; Van Dover 2011; Collins *et al.* 2013a). The mineral extraction process (Figure 4.1) is expected to severely impact communities of vent endemic species but also background communities of fauna that colonize inactive sulphide deposits (Boschen *et al.* 2013). Negative impacts may include degradation or loss of sulphide habitat, modification of fluid regimes, a decrease in genetic and species diversity, a decrease in primary production and modifications of trophic structure (Van Dover 2011). Many hydrothermal vent species cannot persist away from vents and are therefore extremely susceptible to habitat loss or degradation during mining events (Collins *et al.* 2013a). Invertebrate hosts, for example, rely on chemosynthetic symbionts and consequently the venting fluids that support their symbionts (Corliss *et al.* 1979; Karl *et al.* 1980; Jannasch & Wirsen 1981; Cavanaugh *et al.* 1981). Furthermore, removing a significant portion of vent habitat may decrease population connectivity and potentially prevent recolonization of mined sites and/or tectonically disturbed habitat (Van Dover 2011; Boschen *et al.* 2013).

Although industrial mining appears to be the most imminent and destructive human threat to hydrothermal vent ecosystems, other anthropogenic activities, such as tourism, interests in biotechnology and pharmaceuticals, and indirect factors (e.g. ocean acidification and climate change) have the potential to adversely affect vent communities (Halfar & Fujita 2007; Arrieta *et al.* 2010; Van Dover 2012; Van Dover *et al.* 2014). Consequently, there is a need and opportunity to establish environment baseline studies for hydrothermal vent systems and develop conservation strategies prior to industrial exploitation (Van Dover *et al.* 2012; Boschen *et al.* 2013; Collins *et al.* 2013a; b).

4.2 Marine Protected Areas

Establishing effective Marine Protected Areas (MPA) or maintaining a network of marine reserves is an essential first step in preserving hydrothermal vent communities in regions of intense mineral exploitation (Van Dover *et al.* 2012). MPAs generally have varying levels of protection within their boundaries whereas marine reserves are a type of marine protected area (or areas within an MPA) that ensures the highest levels of

protection (*i.e.* no-take zones). Overall, MPAs are designed to enhance the conservation of marine species and their biophysical environments, with the goal of maintaining natural biodiversity and the structure, function and resilience of the ecosystem (Lubchenco *et al.* 2003; Van Dover *et al.* 2012). A detailed understanding of the ecological and physical characteristics of the ecosystem is therefore essential to identifying representative habitats requiring the highest protection within a hydrothermal vent site (Gaines *et al.* 2010; Boschen *et al.* 2013). Replicate reserves of similar habitat types also need to be considered because it promotes overall persistence when the frequency, size and intensity of disturbance are high (Gaines *et al.* 2010; Boschen *et al.* 2013). Currently, only 8% of hydrothermal vent sites fall within a Marine Protected Area (Beaulieu et al., 2013).

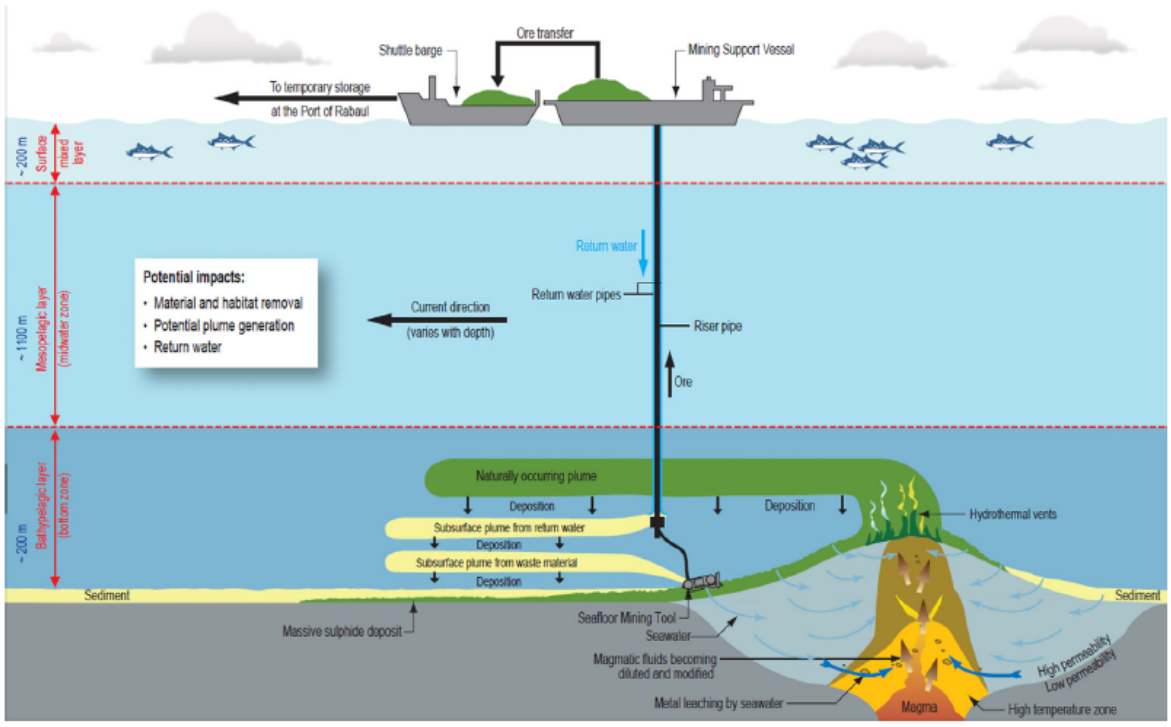

Figure 4-1: Schematic showing one possible model of the mining process to extract seafloor massive sulphides from deep sea hydrothermal vents. The process with likely involve a Remotely Operated Vehicle (ROV) that macerates the SMS deposit into a slurry followed by the ore being de-watered and transferred to a barge for transport to shore. (Figure taken from (Collins *et al.* 2013a)).

Environmental baseline studies have the potential to identify critical habitat, the distribution and abundance of species and genetic diversity, connectivity among hydrothermal vents (local and regional), and ecologically and biologically significant areas (EBSA) to be set aside for protection (Van Dover *et al.* 2012; Boschen *et al.* 2013; Collins *et al.* 2013a; b). Well-connected habitats and/or vent fields that contain high levels of genetic and species diversity are essential to the recolonization of exploited and naturally disturbed habitats that should be targeted as conservation priorities that are immune to the effects of mining (Collins *et al.* 2013b). Candidate sites should also include populations that are inherently persistent, have high local carrying capacity and act as sources populations that also receive sufficient larvae from other source habitats (Gaines *et al.* 2010). No MPA design can provide benefits for every species however, including spatial heterogeneity in the selection of habitats and patterns of connectivity will buffer against uncertainties (Gaines *et al.* 2010).

4.3 Estimating connectivity

Understanding population connectivity is an important component of establishing effective conservation areas and will influence the optimal reserve configuration and/or the levels of protection for hydrothermal vent habitats within an MPA (e.g. Palumbi 2003; Gaines *et al.* 2010; Hughes *et al.* 2013; Magris *et al.* 2014). Estimating connectivity requires an understanding of the biophysical interactions within an ecosystem that include the physical attributes of the landscape, oceanographic processes and the organismal response to both (Cowen & Sponaugle 2009). Oceanographic data, physical modelling and behavioural data (e.g. pelagic larval duration, active vertical positioning) can be used together to estimate the trajectory and dispersal potential of an organism reaching new habitat (Cowen & Sponaugle 2009). Successful colonization and recruitment into a new habitat is more difficult to quantify.

Several studies have used capture-mark-recapture models to identify the demographic exchange of individuals in a population (reviewed in Cowen & Sponaugle 2009; Lowe & Allendorf 2010), however, such a method is not feasible for benthic invertebrate larvae and difficult to study in other hydrothermal vent organisms. Currently,

the most promising and powerful technique for estimating connectivity in hydrothermal vent species is using genetic markers to estimate gene flow among (sub)populations (e.g. Johnson *et al.* 2006; Shank & Halanych 2007; Young *et al.* 2008; Coykendall *et al.* 2011; Thaler *et al.* 2011; Van Dover 2011; this thesis). Genetic data combined with network theory and modelling have been useful for identifying important source subpopulations and patterns of connectivity in metapopulations (Rozenfeld *et al.* 2008). A similar approach may prove to be valuable for estimating connectivity of hydrothermal vent species.

4.4 The Endeavour Hydrothermal Vents Marine Protected Area (EHV-MPA)

The unique habitat and high productivity found at the Endeavour Hydrothermal Vents are two of many reasons why it was established as Canada's first marine protected area in 2003 and one of the world's first deep sea MPAs (Tunnicliffe 2000; Devey *et al.* 2007; DFO 2009). It is a remarkable and dynamic setting hosting abundant microbial life and numerous unique species of animals, some of which are rare and only occur at Endeavour (Tunnicliffe 2000). The EHV- MPA is approximately 100 km^2 and has four management areas that correspond to four principal vent fields within its boundaries (SaltyDawg, High Rise, Main Endeavour and Mothra) (Figure 4.2) (DFO 2009). The Salty Dawg and High Rise vent fields are no-take areas. Salty Dawg is reserved for observation-based research that is minimally intrusive, whereas High Rise is reserved for projects focusing on education and public outreach. Mothra and Main Endeavour are the most intensively studied vent fields within the MPA and research activities remain focused within these areas. Research includes observational to moderate sampling operations (DFO 2009). This overall design places a north to south gradient of impact onto the MPA.

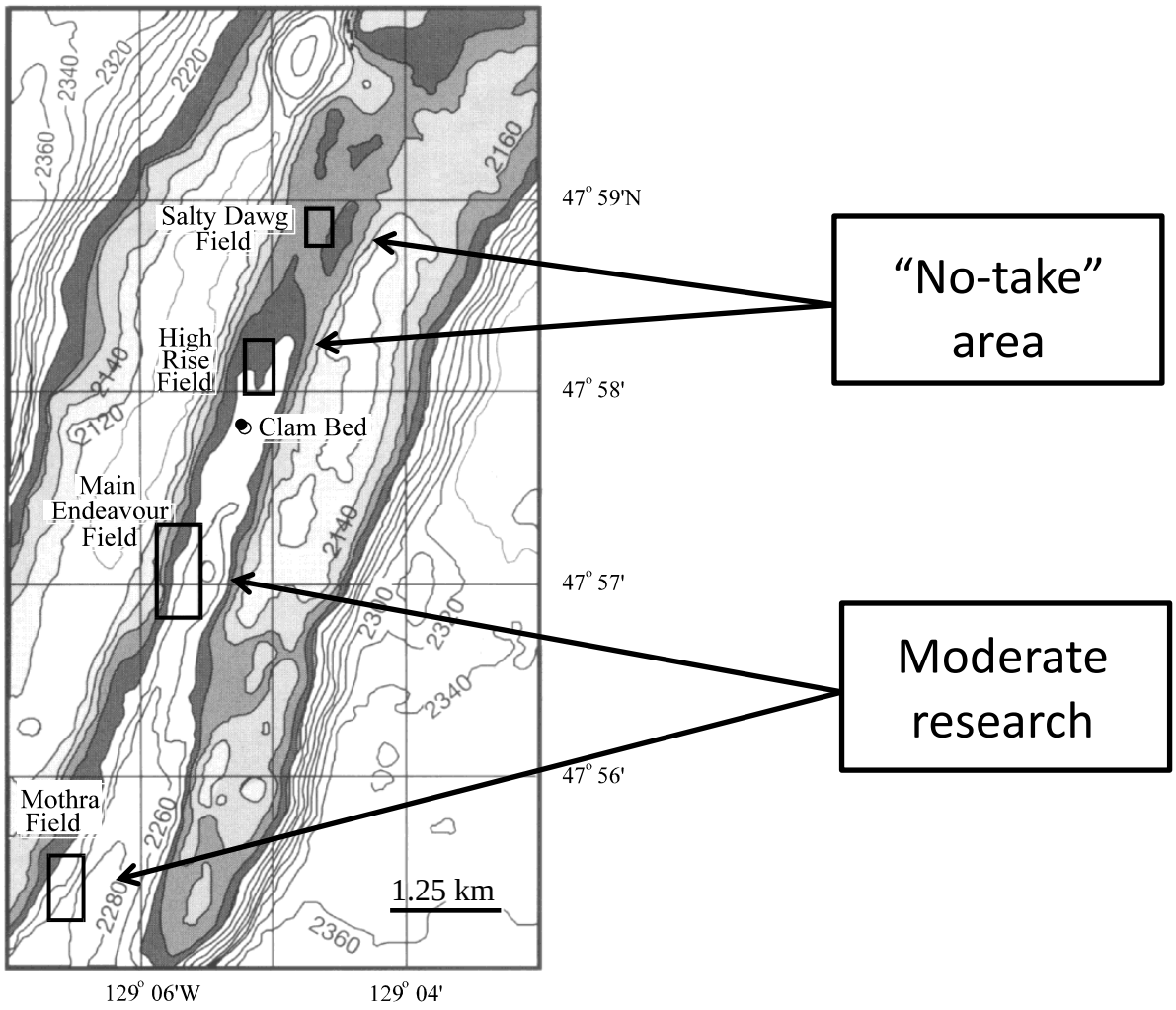

Figure 4-2: Bathymetry and boundary map of the Endeavour Hydrothermal Vents Marine Protected Area (EHV-MPA) showing the four management areas that correspond for the four principal vent fields within its boundaries. Salty Dawg and High Rise vent fields are no-take areas. Moderate sampling and research activities are focused in Mothra and Main Endeavour vent fields (modified from Tunnicliffe, 2000).

Designing effective conservation boundaries, through either a network of marine reserves or larger MPAs, is not a simple task and many MPAs fail to achieve their desired conservation goals (Edgar *et al.* 2014). Spatial design and clear management strategies are important MPA components that must be carefully identified prior to implementation (Van Dover *et al.* 2012). A global assessment of MPAs identified five key planning and management features that determined their ecological potential and success: no-take regulations, efficient enforcement, large area (>100 km^2), old age (>10 years) and the isolation of habitat allowing for unconstrained movement of species (NEOLI) (Edgar *et al.* 2014). MPAs that scored highest had multiple NEOLI features however, only four out of the 87 MPAs that were investigated in the study possessed all five features. Although Endeavour Hydrothermal Vents MPA was not included in this report, it has the potential to rank highly for all NEOLI features.

The following section will address several recommendations that should be considered in future management plans for the EHV-MPA to reach its full potential. Recommendations are based on the patterns of genetic connectivity that were identified in *Ridgeia piscesae* from Endeavour and described in Chapter 2 in this thesis.

4.5 Implications of the current study

Models of gene flow in *Ridgeia piscesae* reflected the general oceanographic circulation described at Endeavour (Thomson *et al.* 2003). Genetic data suggest that dispersing larvae have the capacity to exploit the bi-directional currents created through plume driven circulation within the Endeavour axial valley, however, adult position on or near chimneys may influence larval dispersal trajectories at the time of their release. Colonization into high flux habitat occurs through dispersal in southward biased currents further above the seafloor, whereas colonization into low flux habitat is achieved through near-bottom larval transport. These findings have important implications on the varying levels of protection currently enforced at each of the four management areas within Endeavour.

Larvae of the vent species that live on chimney walls, near direct fluid flux sources, may have a higher likelihood of becoming entrained in the buoyant plume (Kim *et al.* 1994) and would therefore disperse predominantly in currents moving in a

southward direction at Endeavour (Thomson *et al.* 2003, 2005). Consequently, source population for high flux habitat would be located at vent fields in the north, and should receive higher protection than sink populations in the south. However, species that occur in diffuse venting at the base or flanks of chimneys and on surrounding basalts are at greater distances away from fluid flux sources and may remain near-bottom for larval dispersal. Near bottom currents at Endeavour are predominantly northward (Thomson *et al.* 2003, 2009; Garcia Berdeal *et al.* 2006) therefor source populations for diffuse vent habitat would be located in the southern vents fields and receive higher protection than the sinks in the north. It would be useful to test gene flow models in species that are predominantly found in high flux habitats (usually at smoker tops) on chimneys (e.g. *Paralvinella sulfincola*) and in species that only occur in low flux habitats lower on chimneys and on the basalts (e.g. *Buccinum thermophilum*). These two studies may reflect the high- and low-flux *Ridgeia piscesae* gene flow models, respectively. Provided that there was enough genetic variation identified in the two species that represented each habitat, it would be possible to confirm the hypothesis that adult position at hydrothermal vents may predict larval dispersal trajectories and colonization patterns (Bailly-Bechet *et al.* 2008).

By linking ecological and biological data from past studies with genetic variability over small spatial scales, this study identified that *Ridgeia piscesae* from limited and ephemeral high flux habitat act as critical sources to the overall metapopulation and, asymmetrical migration and habitat stability sustain high genetic diversity in low flux sinks. The overall metapopulation at Endeavour experiences frequent extinction and recolonization events, differences in individual reproductive success and source-sink dynamics that decrease the overall effective size and genetic diversity within the population (e.g. Pannell & Charlesworth 2000; Turner *et al.* 2002; Hedgecock *et al.* 2007) all of which have important implications for conservation biology. Conservation strategies focusing on the long-term persistence of metapopulations might target protection of multiple habitat patches over the seascape whereas differences in reproductive success and source-sink dynamics would concentrate on significant sources of successful recruits (see Franzén & Nilsson 2013).

Design and implementation of management strategies in the EHV-MPA should consider appropriate protection of both high flux and low flux habitat types at all major vents fields within Endeavour. Protection of high flux habitats, for *Ridgeia piscesae*, will ensure the prosperity of the overall metapopulation, because tubeworms from this habitat output the largest of number of new recruits into the population. Low flux habitats also require protection as they maintain genetic diversity and, due to the inherent stability of the habitat, tubeworms from these habitats may rescue the overall metapopulation during high regional instability (Tunnicliffe *et al.*, in review). Currently, the highest levels of protection are only implemented in two vent fields in the northern sectors of Endeavour, Salty Dawg and High Rise, however, southern vent fields also need to be considered for protection because important source populations likely occur in both the northern and southern vent fields. Establishing multiple reserves and replicates of each habitat type at all major vent fields within Endeavour may prove to be an effective management strategy for the EHV-MPA and buffer against any uncertainties.

Although Endeavour is an unlikely candidate for SMS mining activities (Devey *et al.* 2007), it is a simple system that may serve as an example of how to draw conservation boundaries and define use in an MPA for similar vulnerable marine ecosystems. This study used coalescent based models to estimate gene flow and, combined with previous biological, ecological and oceanographic data, identified vulnerable habitat locations and sources of genetic variation in an ecologically significant species within an MPA. Furthermore, genetic data identified fine-scale population substructure, source-sink dynamics and the role of each habitat type in the maintenance of the overall metapopulation. To my knowledge, there is only one other study of hydrothermal vent species that identified genetic subdivision at similar spatial scales to *Ridgeia piscesae* and it was in populations of the vestimentiferan tubeworm *Riftia pachyptila*, however, sample sizes were small (Shank & Halanych 2007). The results from this present study and that of Shank & Halanych (2007) suggest that there is greater population structure than previously thought in hydrothermal vent organisms. This may change the general assumption of high connectivity among populations of hydrothermal vent species and consequently its implications on conservation strategies.

Bibliography

Adams DK, Arellano SM, Govenar B (2012) Larval dispersal: Vent life in the water column. *Oceanography*, **25**, 256–268.

Alvarado Bremer JR, Viñas J, Mejuto J, Ely B, Pla C (2005) Comparative phylogeography of Atlantic bluefin tuna and swordfish: the combined effects of vicariance, secondary contact, introgression, and population expansion on the regional phylogenies of two highly migratory pelagic fishes. *Molecular Phylogenetics and Evolution*, **36**, 169–87.

Andreasen AM, Stewart KM, Longland WS, Beckmann JP, Forister ML (2012) Identification of source-sink dynamics in mountain lions of the Great Basin. *Molecular Ecology*, **21**, 5689–701.

Arp AJ, Childress JJ (1983) Sulfide Binding by the Blood of the Hydrothermal Vent Tube Worm Riftia pachyptila. *Science*, **219**, 295–297.

Arrieta JM, Arnaud-Haond S, Duarte CM (2010) What lies underneath: conserving the oceans' genetic resources. *Proceedings of the National Academy of Sciences USA*, **107**, 18318–24.

Audzijonyte A, Vrijenhoek RC (2010) When gaps really are gaps: statistical phylogeography of hydrothermal vent invertebrates. *Evolution; International Journal of Organic Evolution*, **64**, 2369–84.

Avise JC (1998) The history and purview of phylogeography: a personal reflection. *Molecular Ecology*, **7**, 371–379.

Avise JC (2004) *Molecular markers, natural history and evolution*. Sinauer Associates, Sunderland, MA.

Bailly-Bechet M, Kerszberg M, Gaill F, Pradillon F (2008) A modeling approach of the influence of local hydrodynamic conditions on larval dispersal at hydrothermal vents. *Journal of Theoretical Biology*, **255**, 320–31.

Ballard JW, Kreitman M (1994) Unraveling selection in the mitochondrial genome of Drosophila. *Genetics*, **138**, 757–72.

Ballard JWO, Rand DM (2005) The population biology of mitochondrial Dna and its phylogenetic implications. *Annual Review of Ecology, Evolution, and Systematics*, **36**, 621–642.

Balloux F, Lugon-Moulin N (2002) The estimation of population differentiation with microsatellite markers. *Molecular Ecology*, **11**, 155–65.

Bandelt HJ, Forster P, Röhl A (1999) Median-joining networks for inferring intraspecific phylogenies. *Molecular Biology and Evolution*, **16**, 37–48.

Barbará T, Palma-Silva C, Paggi GM *et al.* (2007) Cross-species transfer of nuclear microsatellite markers: potential and limitations. *Molecular Ecology*, **16**, 3759–67.

Barson NJ, Cable J, Van Oosterhout C (2009) Population genetic analysis of microsatellite variation of guppies (Poecilia reticulata) in Trinidad and Tobago: evidence for a dynamic source-sink metapopulation structure, founder events and population bottlenecks. *Journal of Evolutionary Biology*, **22**, 485–97.

Beaulieu SE, Baker ET, German CR, Maffei A (2013) An authoritative global database for active submarine hydrothermal vent fields. *Geochemistry, Geophysics, Geosystems*, **14**, 4892–4905.

Beedessee G, Watanabe H, Ogura T *et al.* (2013) High connectivity of animal populations in deep-sea hydrothermal vent fields in the central Indian ridge relevant to its geological setting. *PloS one*, **8**, e81570.

Beerli P (2004) Effect of unsampled populations on the estimation of population sizes and migration rates between sampled populations. *Molecular Ecology*, **13**, 827–836.

Beerli P, Felsenstein J (2001) Maximum likelihood estimation of a migration matrix and effective population sizes in n subpopulations by using a coalescent approach. *Proceedings of the National Academy of Sciences USA*, **98**, 4563–8.

Beerli P, Palczewski M (2010) Unified framework to evaluate panmixia and migration direction among multiple sampling locations. *Genetics*, **185**, 313–26.

Beier P (1993) Determining habitat areas and habitat corridors for cougars. *Conservation Biology*, **7**, 94–108.

Bergquist DC, Williams FM, Fisher CR (2000) Longevity record for deep-sea invertebrate. *Nature*, **403**, 499–500.

Black MB, Lutz RA, Vrijenhoek RC (1994) Gene flow among vestimentiferan tube worm (Riftia pachyptila) populations from hydrothermal vents of the eastern Pacific. *Marine Biology*, **120**, 33–39.

Black MB, Trivedi A, Maas PA Y, Lutz RA, Vrijenhoek RC (1998) Population genetics and biogeography of vestimentiferan tube worms. *Deep Sea Research Part II: Topical Studies in Oceanography*, **45**, 365–382.

Bonnivard E, Catrice O, Ravaux J, Brown SC, Higuet D (2009) Survey of genome size in 28 hydrothermal vent species covering 10 families. *Genome*, **536**, 524–536.

Boschen RE, Rowden A, Clark MR, Gardner JP (2013) Mining of deep-sea seafloor massive sulfides: A review of the deposits, their benthic communities, impacts from mining, regulatory frameworks and management strategies. *Ocean & Coastal Management*, **84**, 54–67.

Botsford LW, Micheli F, Hastings A (2003) Principles for the design of marine reserves. *Ecological Applications*, **13**, 25–31.

Boyle EA, Thaler AD, Jacobson A, Plouviez S, Dover CL (2013) Characterization of 10 polymorphic microsatellite loci in Munidopsis lauensis, a squat-lobster from the southwestern Pacific. *Conservation Genetics Resources*, **5**, 647–649.

Bright M, Lallier FH (2010) The biology of vestimentiferan tubeworms. *Oceanography and Marine Biology: An Annual Review*, **48**, 213–266.

Brooke SD, Young CM (2009) Where do the embryos of Riftia pachyptila develop? Pressure tolerances, temperature tolerances, and buoyancy during prolonged embryonic dispersal. *Deep Sea Research Part II: Topical Studies in Oceanography*, **56**, 1599–1606.

Brown WM, George M, Wilson AC (1979) Rapid evolution of animal mitochondrial DNA. *Proceedings of the National Academy of Sciences of the United States of America*, **76**, 1967–71.

Brüniche-Olsen A, Burridge CP, Austin JJ, Jones ME (2013) Disease induced changes in gene flow patterns among Tasmanian devil populations. *Biological Conservation*, **165**, 69–78.

Carney SL, Flores JF, Orobona KM *et al.* (2007) Environmental differences in hemoglobin gene expression in the hydrothermal vent tubeworm, Ridgeia piscesae. *Comparative biochemistry and physiology. Part B, Biochemistry & molecular biology*, **146**, 326–37.

Carney SL, Peoples JR, Fisher CR, Schaeffer SW (2002) AFLP analyses of genomic DNA reveal no differentiation between two phenotypes of the vestimentiferan tubeworm Ridgeia piscesae. *Cahiers de Biologie Marine*, **43**, 363–366.

Cavanaugh CM, Gardiner SL, Jones ML, Jannasch HW, Waterbury JB (1981) Prokaryotic cells in the hydrothermal vent tube worm Riftia pachyptila Jones: Possible chemoautotrophic symbionts. *Science*, **213**, 340–2.

Chevillon C, Pasteur N, Marquine M, Heyse D, Raymond M (1995) Population structure and dynamics of selected genes in the mosquito Culex pipiens. *Evolution*, **49**, 997–1007.

Childress JJ (1988) Biology and chemistry of a deep . sea hydrothermai vent on the Galapagos Rift ; the Rose Garden in 1985 . Introduction. *Deep Sea Research Part I: Oceanographic Research Papers*, **35**, 1677–1680.

Chistiakov DA, Hellemans B, Volckaert FAM (2006) Microsatellites and their genomic distribution, evolution, function and applications: A review with special reference to fish genetics. *Aquaculture*, **255**, 1–29.

Collins PC, Croot P, Carlsson J *et al.* (2013a) A primer for the Environmental Impact Assessment of mining at seafloor massive sulfide deposits. *Marine Policy*, **42**, 198–209.

Collins PC, Kennedy B, Copley J *et al.* (2013b) VentBase: Developing a consensus among stakeholders in the deep-sea regarding environmental impact assessment for deep-sea mining–A workshop report. *Marine Policy*, **42**, 334–336.

Corliss JB, Dymond J, Gordon LI *et al.* (1979) Submarine thermal springs on the Galápagos Rift. *Science*, **203**, 1073–1083.

Corliss J, RD B (1977) Oasis of life in the cold abyss. *National Geographic Magazine*, **152**, 441–453.

Cowart DA, Huang C, Arnaud-Haond S *et al.* (2013) Restriction to large-scale gene flow vs. regional panmixia among cold seep Escarpia spp. (Polychaeta, Siboglinidae). *Molecular Ecology*, **22**, 4147–62.

Cowen RK (2000) Connectivity of Marine Populations: Open or Closed? *Science*, **287**, 857–859.

Cowen RK, Gawarkiewicz G, Pineda J, Thorrold SR, Werner FE (2007) Population Connectivity in Marine Systems: An Overview. *Oceanography*, **20**, 14–21.

Cowen RK, Sponaugle S (2009) Larval Dispersal and Marine Population Connectivity. *Annual Review of Marine Science*, **1**, 443–466.

Coykendall DK, Johnson SB, Karl SA, Lutz RA, Vrijenhoek RC (2011) Genetic diversity and demographic instability in Riftia pachyptila tubeworms from eastern Pacific hydrothermal vents. *BMC Evolutionary Biology*, **11**, 96.

Cruz F, Pérez M, Presa P (2005) Distribution and abundance of microsatellites in the genome of bivalves. *Gene*, **346**, 241–7.

Cruz P, Yáñez-Jacome B, Ibarra A M, Rangel-Becerril J (2007) Isolation and characterization of microsatellite loci in the Pacific pleasure oyster, Crassostrea corteziensis, and their cross-species amplification in four other oyster species. *Molecular Ecology Notes*, **7**, 448–450.

Darvill B, Ellis JS, Lye GC, Goulson D (2006) Population structure and inbreeding in a rare and declining bumblebee, Bombus muscorum (Hymenoptera: Apidae). *Molecular Ecology*, **15**, 601–11.

Davis EE, Wang K, Thomson RE, Becker K, Cassidy JF (2001) An episode of seafloor spreading and associated plate deformation inferred from crustal fluid pressure transients site. *Journal of Geophysical Research. B, Solid Earth*, **106**, 21953 – 21963.

Dawson DA, Horsburgh GJ, Küpper C *et al.* (2010) New methods to identify conserved microsatellite loci and develop primer sets of high cross-species utility - as demonstrated for birds. *Molecular Ecology Resources*, **10**, 475–94.

Delaney JR, Robigou V, McDuff RE, Tivey MK (1992) Geology of a vigorous hydrothermal system on the Endeavour Segment, Juan de Fuca Ridge. *Journal of Geophysical Research: B Solid Earth*, **97**, 19663–19682.

Denver DR, Morris K, Lynch M, Vassilieva LL, Kelley W (2000) High Direct Estimate of the Mutation Rate in the Mitochondrial Genome of Caenorhabditis elegans. *Science*, **289**, 2342–2344.

Devey CW, Fisher CR, Scott S (2007) Responsible Scient at Hydrothermal Vents. *Oceanography*, **20**, 162–171.

DFO (2009) Endeavour Hydrothermal Vents Marine Protected Area-Marine Protected Area Management Plan.

Dias PC (1996) Sources and sinks in population biology. *Trends in Ecology & Evolution*, **11**, 326–330.

Dittel AI, Perovich G, Epifanio CE (2008) Biology of the Vent Crab Bythograea thermydron: A Brief Review. *Journal of Shellfish Research*, **27**, 63–77.

Dixon DR, Lowe DM, Miller PI *et al.* (2006) Evidence of seasonal reproduction in the Atlantic vent mussel Bathymodiolus azoricus, and an apparent link with the timing of photosynthetic primary production. *Journal of the Marine Biological Association of the UK*, **86**, 1363.

Dobeš C, Scheffknecht S (2012) Isolation and characterization of microsatellite loci for the Potentilla core group (Rosaceae) using 454 sequencing. *Molecular Ecology Resources*, **12**, 726–39.

Van Dover CL (2000) *The ecology of deep sea hydrothermal vents*. Princeton University Press, New Jersey.

Van Dover CL (2011) Mining seafloor massive sulphides and biodiversity: what is at risk? *ICES Journal of Marine Science*, **68**, 341–348.

Van Dover CL (2012) Ocean policy: Hydrothermal vent ecosystems and conservation. *Oceanography*, **25**, 313–316.

Van Dover CL, Aronson J, Pendleton L *et al.* (2014) Ecological restoration in the deep sea: Desiderata. *Marine Policy*, **44**, 98–106.

Van Dover CL, Smith CR, Ardron J *et al.* (2012) Designating networks of chemosynthetic ecosystem reserves in the deep sea. *Marine Policy*, **36**, 378–381.

Dubilier N, Bergin C, Lott C (2008) Symbiotic diversity in marine animals: the art of harnessing chemosynthesis. *Nature reviews. Microbiology*, **6**, 725–40.

Edgar GJ, Stuart-Smith RD, Willis TJ *et al.* (2014) Global conservation outcomes depend on marine protected areas with five key features. *Nature*, **506**, 216–220.

Ellegren H (2004) Microsatellites: simple sequences with complex evolution. *Nature Reviews. Genetics*, **5**, 435–45.

Estoup A, Jarnne P, Cornuet J-M (2002) Homoplasy and mutation model at microsatellite loci and their consequences for population genetics analysis. *Molecular Ecology*, **11**, 1591–1604.

Felbeck H, Somero GN (1982) Primary production in deep-sea hydrothermal vent organisms: roles of sulfide-oxidizing bacteria. *Trends in Biochemical Sciences*, **7**, 201–204.

Fisher AT, Harris RN (2010) Using seafloor heat flow as a tracer to map subseafloor fluid flow in the ocean crust. *Geofluids*, **10**, 142–160.

Fisher C, Urcuyo I, Simpkins M, Nix E (1997) Life in the slow lane: growth and longevity of cold-seep vestimentiferans. *Marine Ecology*, **18**, 83–94.

FitzSimmons NN, Moritz C, Moore SS (1995) Conservation and dynamics of microsatellite loci over 300 million years of marine turtle evolution. *Molecular Biology and Evolution*, **12**, 432–40.

Folmer O, Black M, Hoeh W, Lutz R, Vrijenhoek R (1994) DNA primers for amplification of mitochondrial cytochrome c oxidase subunit I from diverse metazoan invertebrates. *Molecular Marine Biology and Biotechnology*, **3**, 294–9.

Fontanesi F, Soto IC, Horn D, Barrientos A (2006) Assembly of mitochondrial cytochrome c-oxidase, a complicated and highly regulated cellular process. *American Journal of Physiology. Cell Physiology*, **291**, C1129–47.

Franzén M, Nilsson SG (2013) High population variability and source-sink dynamics in a solitary bee species. *Ecology*, **94**, 1400–8.

Fretwell PT, Staniland IJ, Forcada J (2014) Whales from space: counting southern right whales by satellite. *PloS one*, **9**, e88655.

Fusaro AJ, Baco A R, Gerlach G, Shank TM (2008) Development and characterization of 12 microsatellite markers from the deep-sea hydrothermal vent siboglinid Riftia pachyptila. *Molecular Ecology Resources*, **8**, 132–4.

Gaines SD, White C, Carr MH, Palumbi SR (2010) Designing marine reserve networks for both conservation and fisheries management. *Proceedings of the National Academy of Sciences of the USA*, **107**, 18286–93.

Garcia Berdeal I, Hautala SL, Thomas LN, Paul Johnson H (2006) Vertical structure of time-dependent currents in a mid-ocean ridge axial valley. *Deep Sea Research Part I: Oceanographic Research Papers*, **53**, 367–386.

Garner TWJ (2002) Genome size and microsatellites : the effect of nuclear size on amplification potential. *Genome*, **45**, 212–215.

St. Germain C (2011) Reproductive and physiological condition and juvenile recruitment in the hydrothermal vent tubeworm Ridgeia piscesae Jones (Polychaeta: Siboglinidae) in the context of a highly variable habitat on Juan de Fuca Ridge. Masters Thesis.

Ginster U, Mottl MJ (1994) Heat flux from black smokers on the Endeavour and Cleft segments, Juan de Fuca Ridge. *Journal of Geophysical Research. B, Solid Earth*, **99**, 4937–4950.

Halfar J, Fujita RM (2007) Danger of Deep-Sea Mining. *Science*, **316**, 987.

Hänfling B, Weetman D (2006) Concordant genetic estimators of migration reveal anthropogenically enhanced source-sink population structure in the river sculpin, Cottus gobio. *Genetics*, **173**, 1487–501.

Hanski I (1991) Single-species metapopulation dynamics: concepts, models and observations. *Biological Journal of the Linnean Society*, **42**, 17–38.

Hanski I (1999) *Metapopulation ecology*. Oxford University Press, New York.

Hanski I, Gaggiotti OE (2004) *Ecology, genetics, and evolution of metapopulations* (I Hanski, OE Gaggiotti, Eds,). Elsevier, Burlington, MA.

Hanski I, Gilpin M (1991) Metapopulation dynamics: brief history and conceptual domain. *Biological Journal of the Linnean Society*, **42**, 3–16.

Hanski I, Gilpin ME (1997) *Metapopulation biology: Ecology, genetics and evolution*. Academic Press, San Diego.

Hanski I, Thomas CD (1994) Metapopulation dynamics and conservation: A spatially explicit model applied to butterflies. *Biological Conservation*, **68**, 167–180.

Hardesty BD, Hughes SL, Rodriguez VM, Hawkins J (2008) Characterization of microsatellite loci for the endangered cactus Echinocactus grusonii, and their cross-species utilization. *Molecular Ecology Resources*, **8**, 164–7.

Harpending HC (1994) Signature of ancient population growth in a low-resolution mitochondrial DNA mismatch distribution. *Human Biology*, **66**, 591–600.

Hartl DL, Clark AG (2007) *Principles of population genetics*. Sinauer Associates, Sunderland, MA.

Hedgecock D (1994) Temporal and spatial genetic structure of marine animal populations in the California Current. *California Cooperative Oceanic Fisheries Investigations, Progress Report*, **35**, 73–81.

Hedgecock D, Barber PH, Edmands S (2007a) Genetic approaches to measuring connectivity. *Oceanography*, **20**, 70–79.

Hedgecock D, Launey S, Pudovkin a. I *et al.* (2007b) Small effective number of parents (N b) inferred for a naturally spawned cohort of juvenile European flat oysters Ostrea edulis. *Marine Biology*, **150**, 1173–1182.

Hellberg ME, Burton RS, Neigel JE, Palumbi SR (2002) Genetic assessment of connectivity among marine populations. *Bulletin of Marine Science*, **70**, 273–290.

Hendrix R, Susanne Hauswaldt J, Veith M, Steinfartz S (2010) Strong correlation between cross-amplification success and genetic distance across all members of "True Salamanders" (Amphibia: Salamandridae) revealed by Salamandra salamandra-specific microsatellite loci. *Molecular Ecology Resources*, **10**, 1038–47.

Hilário A, Capa M, Dahlgren TG *et al.* (2011) New perspectives on the ecology and evolution of siboglinid tubeworms. *PloS one*, **6**, e16309.

Hilário A, Young CM, Tyler P A (2005) Sperm storage, internal fertilization, and embryonic dispersal in vent and seep tubeworms (Polychaeta: Siboglinidae: Vestimentifera). *The Biological Bulletin*, **208**, 20–8.

Hoagland P, Beaulieu S, Tivey M A *et al.* (2010) Deep-sea mining of seafloor massive sulfides. *Marine Policy*, **34**, 728–732.

Hoekstra HE, Drumm KE, Nachman MW (2004) Ecological genetics of adaptive color polymorphism in pocket mice: geographic variation in neutral and selected genes. *Evolution*, **58**, 1329–1341.

Hotz H, Beerli P, Uzzell T *et al.* (2013) Balancing a cline by influx of migrants: a genetic transition in water frogs of eastern Greece. *The Journal of Heredity*, **104**, 57–71.

Hughes JM, Huey JA, Schmidt DJ (2013) Is realised connectivity among populations of aquatic fauna predictable from potential connectivity? *Freshwater Biology*, **58**, 951–966.

Humphris SE, Zierenberg RA, Mullineaux LS, Thomson RE (1995) *Seafloor Hydrothermal Systems: Physical, Chemical, Biological, and Geological Interactions, Geophysical Monograph Series*. AGU, Washington, D. C.

Hurtado L A, Lutz R A, Vrijenhoek RC (2004) Distinct patterns of genetic differentiation among annelids of eastern Pacific hydrothermal vents. *Molecular Ecology*, **13**, 2603–15.

Iorio D, Lavelle JW, Rona PA *et al.* (2012) Measurements and models of heat flux and plumes from hydrothermal discharges near the deep seafloor. *Oceanography*, **25**, 168–179.

Jacobson A, Plouviez S, Thaler AD, Dover CL (2013) Characterization of 13 polymorphic microsatellite loci in Rimicaris hybisae, a shrimp from deep-sea hydrothermal vents. *Conservation Genetics Resources*, **5**, 449–451.

Jan C, Dawson D, Altringham JD, Burke T, Butlin RK (2012) Development of conserved microsatellite markers of high cross-species utility in bat species (Vespertilionidae, Chiroptera, Mammalia). *Molecular Ecology Resources*, **12**, 532–48.

Jannasch HW, Wirsen CO (1981) Morphological survey of microbial mats near deep-sea thermal vents. *Applied and Environmental Microbiology*, **41**, 528–538.

Johnson H, Hutnak M, Dziak R *et al.* (2000) Earthquake-induced changes in a hydrothermal system on the Juan de Fuca mid-ocean ridge. *Nature*, **407**, 174–7.

Johnson SB, Young CR, Jones WJ, Warén A, Vrijenhoek RC (2006) Migration, isolation, and speciation of hydrothermal vent limpets (Gastropoda; Lepetodrilidae) across the Blanco Transform Fault. *The Biological Bulletin*, **210**, 140–57.

Jollivet D (1996) Specific and genetic diversity at deep-sea hydrothermal vents : an overview. *Biodiversity and Conservation*, **1653**, 1619–1653.

Jollivet D, Chevaldonne P, Planque B (1999) Hydrothermal-Vent Alvinellid Polychaete Dispersal in the Eastern Pacific. 2. A Metapopulation Model Based on Habitat Shifts. *Evolution*, **53**, 1128–1142.

Juniper KS, Tunnicliffe V (1997) Crustal accretion and the hot vent ecosystem. *Philosophical Transactions: Mathematical, Physical and Engineering Sciences,*, **355**, 459–474.

Karl DM, Wirsen CO, Jannasch HW (1980) Deep-sea primary production at the Galápagos hydrothermal vents. *Science*, **207**, 1345–1347.

Kawecki TJ (1995) Demography of source-sink populations and the evolution of ecological niches. *Evolutionary Ecology*, **9**, 38–44.

Kelley DS, Carbotte SM, Caress DW *et al.* (2012) Endeavour Segment of the Juan de Fuca Ridge: One of the most remarkable places on Earth. *Oceanography*, **25**, 44–61.

Kelley DS, Delaney JR, Lilley MD, Butterfield DA (2001) Vent field distribution and evolution along the Endeavour segment, Juan de Fuca Ridge. *Eos Trans. AGU (Fall Mtg Suppl. Abstr)*, **82**, OS21B–0439.

Kim SL, Mullineaux LS (1998) Distribution and near-bottom transport of larvae and other plankton at hydrothermal vents. *Deep Sea Research Part II: Topical Studies in Oceanography*, **45**, 423–440.

Kim SL, Mullineaux LS, Helfrich KR (1994) Larval dispersal via entrainment into hydrothermal vent plumes. *Journal of Geophysical Research*, **99**, 12655–12665.

Kinlan BP, Gaines SD (2003) Propagule dispersal in marine and terrestrial environments: a community perspective. *Ecology*, **84**, 2007–2020.

Küpper C, Burke T, Székely T, Dawson D a (2008) Enhanced cross-species utility of conserved microsatellite markers in shorebirds. *BMC Genomics*, **9**, 502.

Lander ES, Linton LM, Birren B *et al.* (2001) Initial sequencing and analysis of the human genome. *Nature*, **409**, 860–921.

Li G, Hedgecock D (1998) Genetic heterogeneity, detected by PCR-SSCP, among samples of larval Pacific oysters (Crassostrea gigas) supports the hypothesis of large

variance in reproductive success. *Canadian Journal of Fisheries and Aquatic Sciences*, **55**, 1025–1033.

Loreau M, Daufresne T, Gonzalez A *et al.* (2013) Unifying sources and sinks in ecology and Earth sciences. *Biological reviews of the Cambridge Philosophical Society*, **88**, 365–79.

Lowe WH, Allendorf FW (2010) What can genetics tell us about population connectivity? *Molecular Ecology*, **19**, 3038–51.

Lubchenco J, Palumbi SR, Gaines SD, Andelman S (2003) Plugging a hole in the ocean: the emerging science of marine reserves. *Ecological Applications*, **13**, 3–7.

MacDonald IR, Tunnicliffe V, Southward EC (2002) Detection of sperm transfer and synchronous fertilization in Ridgeia piscesae Jones at Endeavour Segment , Juan de Fuca Ridge *. *Cahiers de Biologie Marine*, **43**, 395–398.

Magris R A, Pressey RL, Weeks R, Ban NC (2014) Integrating connectivity and climate change into marine conservation planning. *Biological Conservation*, **170**, 207–221.

Manel S, Gaggiotti OE, Waples RS (2005) Assignment methods: matching biological questions with appropriate techniques. *Trends in Ecology & Evolution*, **20**, 136–42.

Manier MK, Arnold SJ (2005) Population genetic analysis identifies source-sink dynamics for two sympatric garter snake species (Thamnophis elegans and Thamnophis sirtalis). *Molecular Ecology*, **14**, 3965–76.

Marcus J, Tunnicliffe V, Butterfield D a. (2009) Post-eruption succession of macrofaunal communities at diffuse flow hydrothermal vents on Axial Volcano, Juan de Fuca Ridge, Northeast Pacific. *Deep Sea Research Part II: Topical Studies in Oceanography*, **56**, 1586–1598.

Marsh AG, Mullineaux LS, Young CM, Manahan DT (2001) Larval dispersal potential of the tubeworm Riftia pachyptila at deep-sea hydrothermal vents. *Nature*, **411**, 77–80.

Marshall HD, Ritland K (2002) Genetic diversity and differentiation of Kermode bear populations. *Molecular Ecology*, **11**, 685–97.

Martínez-Solano I, González EG (2008) Patterns of gene flow and source-sink dynamics in high altitude populations of the common toad Bufo bufo (Anura: Bufonidae). *Biological Journal of the Linnean Society*, **95**, 824–839.

Martínez-Solano I, Teixeira J, Buckley D, García-París M (2006) Mitochondrial DNA phylogeography of Lissotriton boscai (Caudata, Salamandridae): evidence for old, multiple refugia in an Iberian endemic. *Molecular Ecology*, **15**, 3375–88.

Mathias A, Kisdi E, Olivieri I, Url S (2001) Divergent evolution of dispersal in a heterogeneous landscape. *Evolution*, **55**, 246–259.

McMullin ER, Hourdez S, Schaeffer SW, Fisher CR (2003) Phylogeny and Biogeography of Deep Sea Vestimentiferan Tubeworms and Their Bacterial Symbionts. *Symbiosis*, **34**, 1–41.

McMullin ER, Wood J, Hamm S (2004) Twelve microsatellites for two deep sea polychaete tubeworm species, Lamellibrachia luymesi and Seepiophila jonesi, from the Gulf of Mexico. *Molecular Ecology Notes*, **4**, 1–4.

Metaxas A (2004) Spatial and temporal patterns in larval supply at hydrothermal vents in the northeast Pacific Ocean. *American Society of Limnology and Oceanography*, **49**, 1949–1956.

Moore SS, Sargeant LL, King TJ *et al.* (1991) The conservation of dinucleotide microsatellites among mammalian genomes allows the use of heterologous PCR primer pairs in closely related species. *Genomics*, **10**, 654–60.

Mullineaux LS, McGillicuddy DJ, Mills SW *et al.* (2013) Active positioning of vent larvae at a mid-ocean ridge. *Deep Sea Research Part II: Topical Studies in Oceanography*, **92**, 46–57.

Mullineaux L, Mills S, Sweetman A *et al.* (2005) Vertical, lateral and temporal structure in larval distributions at hydrothermal vents. *Marine Ecology Progress Series*, **293**, 1–16.

Mullineaux LS, Wiebe PH, Baker ET (1995) Larvae of benthic invertebrates in hydrothermal vent plumes over Juan de Fuca Ridge. *Marine Biology*, **122**, 585–596.

Nachman MW, Brown WM, Stoneking M, Aquadro CF (1996) Nonneutral mitochondrial DNA variation in humans and chimpanzees. *Genetics*, **142**, 953–963.

Nagylaki T (1975) Conditions for the existence of clines. *Genetics*, **80**, 595–615.

Neubert MG, Mullineaux LS, Hill MF (2006) A metapopulation approach to interpreting diversity at deep-sea hydrothermal vents. In: *Marine Metapopulations* , pp. 321–350.

Nielsen R, Weinreich DM (1999) The age of nonsynonymous and synonymous mutations in animal mtDNA and implications for the mildly deleterious theory. *Genetics*, **153**, 497–506.

Pabijan M, Babik W (2006) Genetic structure in northeastern populations of the Alpine newt (Triturus alpestris): evidence for post-Pleistocene differentiation. *Molecular Ecology*, **15**, 2397–407.

Paetkau D, Calvert W, Stirling I, Strobeck C (1995) Microsatellite analysis of population structure in Canadian polar bears. *Molecular Ecology*, **4**, 347–54.

Palumbi SR (2003) Population genetics , demographic connectivity , and the design of marine reserves. *Ecological Applications*, **13**, 146–158.

Pannell JR (2003) Coalescence in a metapopulation with recurrent local extinction and recolonization. *Evolution; International Journal of Organic Evolution*, **57**, 949–61.

Pannell JR, Charlesworth B (2000) Effects of metapopulation processes on measures of genetic diversity. *Philosophical Transactions of the Royal Society of London. Series B, Biological Sciences*, **355**, 1851–64.

Parvinen K (2002) Evolutionary branching of dispersal strategies in structured metapopulations. *Journal of Mathematical Biology*, **45**, 106–124.

Paz-Vinas I, Quéméré E, Chikhi L, Loot G, Blanchet S (2013) The demographic history of populations experiencing asymmetric gene flow: combining simulated and empirical data. *Molecular Ecology*, **22**, 3279–91.

Peakall R, Gilmore S, Keys W, Morgante M, Rafalski A (1998) Cross-species amplification of soybean (Glycine max) simple sequence repeats (SSRs) within the genus and other legume genera: implications for the transferability of SSRs in plants. *Molecular Biology and Evolution*, **15**, 1275–87.

Peterson BK, Weber JN, Kay EH, Fisher HS, Hoekstra HE (2012) Double digest RADseq: an inexpensive method for de novo SNP discovery and genotyping in model and non-model species. *PloS one*, **7**, e37135.

Planes S, Lenfant P (2002) Blackwell Science, Ltd Temporal change in the genetic structure between and within cohorts of a marine fish, Diplodus sargus, induced by a large variance in individual reproductive success. *Molecular Ecology*, **11**, 1515–1524.

Pleijel F, Dahlgren TG, Rouse GW (2009) Progress in systematics: from Siboglinidae to Pogonophora and Vestimentifera and back to Siboglinidae. *Comptes Rendus Biologies*, **332**, 140–8.

Plouviez S, Shank TM, Faure B *et al.* (2009) Comparative phylogeography among hydrothermal vent species along the East Pacific Rise reveals vicariant processes and population expansion in the South. *Molecular Ecology*, **18**, 3903–17.

Poland J, Brown PJ, Sorrells ME, Jannink J (2012) Development of high-density genetic maps for barley and wheat using a novel two-enzyme genotyping-by-sequencing approach. *PloS one*, **7**, e32253.

Pradillon F, Gaille F (2007) Adaptation to deep-sea hydrothermal vents: Some molecular and developmental aspects. *Journal of Marine Science Technology*, **SI**, 37–53.

Pradillon F, Shillito B, Young C, Gaill F (2001) Developmental arrest in vent worm embryos. *Nature*, **413**, 698–699.

Primmer CR, Painter JN, Koskinen MT, Palo JU, Merilä J (2005) Factors affecting avian cross-species microsatellite amplification. *Journal of Avian Biology*, **36**, 348–360.

Pulliam HR (1988) Sources, Sinks, and Population Regulation. *The American Naturalist*, **132**, 652–661.

Purcell KL, Verner J (1998) Density and reproductive success of California towhees. *Conservation Biology: the Journal of the Society for Conservation Biology*, **12**, 442–450.

Rand DM (2001) The units of selection on mitochondrial DNA. *Annual Review of Ecology, Evolution, and Systematics*, **32**, 415–448.

Rand DM, Kann LM (1998) Mutation and selection at silent and replacement sites in the evolution of animal mitochondrial DNA. *Genetica*, **102-103**, 393–407.

Reading BJ, Wills PS, Heidinger RC, Heist EJ (2003) Development of microsatellite markers for muskellunge (Esox masquinongy) and cross-species amplification in two other esocids. *Molecular Ecology Notes*, **3**, 447–449.

Reid K, Hoareau TB, Bloomer P (2012) High-throughput microsatellite marker development in two sparid species and verification of their transferability in the family Sparidae. *Molecular Ecology Resources*, **12**, 740–52.

Reynolds RG, Fitzpatrick BM (2013) Tests of two methods for identifying founder effects in metapopulations reveal substantial type II error. *Genetica*, **141**, 119–31.

Rico C, Rico I, Hewitt G (1996) 470 Million Years of Conservation of Microsatellite Loci Among Fish Species. *Proceedings of the Royal Society B*, **263**, 549–57.

Rogers AR, Harpending H (1992) Population growth makes waves in the distribution of pairwise genetic differences. *Molecular Biology and Evolution*, **9**, 552–69.

Rona P A., Bemis KG, Jones CD *et al.* (2006) Entrainment and bending in a major hydrothermal plume, Main Endeavour Field, Juan de Fuca Ridge. *Geophysical Research Letters*, **33**, L19313.

Ross KG, Keller L (1995) Joint influence of gene flow and selection on a reproductively important genetic polymorphism in the fire ant Solenopsis invicta. *The American Naturalist*, **146**, 325–348.

Roterman CN, Copley JT, Linse KT, Tyler PA, Rogers AD (2013) Development of polymorphic microsatellite loci for three species of vent-endemic megafauna from deep-sea hydrothermal vents in the Scotia Sea, Southern Ocean. *Conservation Genetics Resources*, **5**, 835–839.

Rouse GW, Goffredi SK, Vrijenhoek RC (2004) Osedax: bone-eating marine worms with dwarf males. *Science (New York, N.Y.)*, **305**, 668–71.

Rozenfeld AF, Arnaud-Haond S, Hernández-García E *et al.* (2008) Network analysis identifies weak and strong links in a metapopulation system. *Proceedings of the National Academy of Sciences of the USA*, **105**, 18824–9.

Saccheri I, Kuussaari M, Kankare M, Vikman P, Hanski I (1998) Inbreeding and extinction in a butterfly metapopulation. *Nature*, **392**, 491–494.

Sandoval CP (1994) The effects of the relative geographic scales of gene flow and selection on morph frequencies in the walking-stick Timema cristinae. *Evolution*, **48**, 1866–1879.

Sarrazin J, Juniper S (1999) Biological characteristics of a hydrothermal edifice mosaic community. *Marine Ecology Progress Series*, **185**, 1–19.

Sarrazin J, Robigou V, Juniper K, Delaney J (1997) Biological and geological dynamics over four years on a high-temperature sulfide structure at the Juan de Fuca Ridge hydrothermal observatory. *Marine Ecology Progress Series*, **153**, 5–24.

Sawaya MA, Kalinowski ST, Clevenger AP (2014) Genetic connectivity for two bear species at wildlife crossing structures in Banff National Park. *Proceedings of the Royal Society B*, **281**, 20131705.

Schlötterer C (2000) Evolutionary dynamics of microsatellite DNA. *Chromosoma*, **109**, 365–371.

Schlötterer C, Amos B, Tautz D (1991) Conservation of polymorphic simple sequence loci in cetacean species. *Nature*, **354**, 63–65.

Schultz TF, Hsing P-Y, Eng A *et al.* (2011) Characterization of 18 polymorphic microsatellite loci from Bathymodiolus manusensis (Bivalvia, Mytilidae) from deep-sea hydrothermal vents. *Conservation Genetics Resources*, **3**, 25–27.

Scott LJ, Shepherd M, Henry RJ (2003) Characterization of highly conserved microsatellite loci in Araucaria cunninghamii and related species. *Plant Systematics and Evolution*, **236**, 115–123.

Seeb JE, Carvalho G, Hauser L *et al.* (2011) Single-nucleotide polymorphism (SNP) discovery and applications of SNP genotyping in nonmodel organisms. *Molecular Ecology Resources*, **11 Suppl 1**, 1–8.

Selkoe K A, Toonen RJ (2006) Microsatellites for ecologists: a practical guide to using and evaluating microsatellite markers. *Ecology Letters*, **9**, 615–29.

Shank TM, Halanych KM (2007) Toward a mechanistic understanding of larval dispersal : insights from genomic fingerprinting of the deep-sea hydrothermal vent tubeworm Riftia pachyptila. *Marine Ecology*, **28**, 25–35.

Shanks AL, Grantham BA, Carr MH (2003) Propagule Dispersal Distance and the Size and Spacing of Marine Reserves. *Ecological Applications*, **13**, 159–169.

Slatkin M (1993) Isolation by Distance in Equilibrium and Non-Equilibrium Populations. *Evolution*, **47**, 264–279.

Somme L, Raabová J, Jacquemart A L, Raspé O (2012) Development and multiplexing of microsatellite markers using pyrosequencing in the clonal plant Comarum palustre (Rosaceae). *Molecular Ecology Resources*, **12**, 91–7.

Southward EC (1988) Development of the gut and segmentation of newly settled stages of Ridgeia (Vestimentifera): implications for relationship between Vestimentifera and Pogonophora. *Journal of the Marine Biological Association of the United Kingdom*, **68**, 465–487.

Southward EC, Tunnicliffe V, Black M (1995) Revision of the species of Ridgeia from northeast Pacific hydrothermal vents, with a redescription of Ridgeia piscesae Jones (Pogonophora: Obturata = Vestimentifera). *Canadian Journal of Zoology*, **295**, 282–295.

Southward E, Tunnicliffe V, Black MB, Dixon D, Dixon LR. (1996) Ocean-ridge segmentation and vent tubeworms (Vestimentifera) in the NE Pacific. In: *Tectonic, Magmatic, Hydrothermal and Biology Segmentation of Mid-Ocean Ridges* (eds MacLeod C, Tyler P, Walker C), pp. 211–224. The Geological Society, London, UK.

Stacey PB, Taper M (1992) Environmental Variation and the Persistence of Small Populations. *Ecological Applications*, **2**, 18–29.

Stewart FJ, Newton ILG, Cavanaugh CM (2005) Chemosynthetic endosymbioses: adaptations to oxic-anoxic interfaces. *Trends in Microbiology*, **13**, 439–48.

Sunnucks P, De Barro PJ, Lushai G, Maclean N, Hales D (1997) Genetic structure of an aphid studied using microsatellites: cyclic parthenogenesis, differentiated lineages and host specialization. *Molecular Ecology*, **6**, 1059–73.

Swearer SE, Shima JS, Hellberg ME *et al.* (2002) Evidence of self-recruitment in demersal marine populations. *Bulletin of Marine Science*, **70**, 251–271.

Teixeira S, Olu K, Decker C *et al.* (2013) High connectivity across the fragmented chemosynthetic ecosystems of the deep Atlantic Equatorial Belt: efficient dispersal mechanisms or questionable endemism? *Molecular Ecology*, **22**, 4663–80.

Teixeira S, Serrão E a., Arnaud-Haond S (2011) Characterization of 15 polymorphic microsatellite loci in Rimicaris exoculata, and cross-amplification in other hydrothermal-vent shrimp. *Conservation Genetics Resources*, **4**, 81–84.

Teixeira S, Serrão E a, Arnaud-Haond S (2012) Panmixia in a fragmented and unstable environment: the hydrothermal shrimp Rimicaris exoculata disperses extensively along the Mid-Atlantic Ridge. *PloS one*, **7**, e38521.

Tero N, Aspi J, Siikamaki P, Jakalaniemi A, Tuomi J (2003) Genetic structure and gene flow in a metapopulation of an endangered plant species, Silene tatarica. *Molecular Ecology*, **12**, 2073–2085.

Thaler AD, Zelnio K, Jones R *et al.* (2010) Characterization of 12 polymorphic microsatellite loci in Ifremeria nautilei, a chemoautotrophic gastropod from deep-sea hydrothermal vents. *Conservation Genetics Resources*, **2**, 101–103.

Thaler AD, Zelnio K, Saleu W *et al.* (2011) The spatial scale of genetic subdivision in populations of Ifremeria nautilei, a hydrothermal-vent gastropod from the southwest Pacific. *BMC Evolutionary Biology*, **11**, 372.

Thomas L, Bell JJ (2013) Testing the consistency of connectivity patterns for a widely dispersing marine species. *Heredity*, **111**, 345–54.

Thomas CD, Kunin WE (1999) The spatial structure of populations. *Journal of Animal Ecology*, **68**, 647–657.

Thomson RE, Mihaly SF, Rabinovich AB *et al.* (2003) Constrained circulation at Endeavour ridge facilitates colonization by vent larvae. *Nature*, **424**, 545–549.

Thomson RE, Subbotina MM, Anisimov M V. (2005) Numerical simulation of hydrothermal vent-induced circulation at Endeavour Ridge. *Journal of Geophysical Research*, **110**, C01004 1–14.

Thomson RE, Subbotina MM, Anisimov M V. (2009) Numerical simulation of mean currents and water property anomalies at Endeavour Ridge: Hydrothermal versus topographic forcing. *Journal of Geophysical Research*, **114**, C09020 1–12.

Tóth G, Gáspári Z, Jurka J (2000) Microsatellites in different eukaryotic genomes: survey and analysis. *Genome research*, **10**, 967–81.

Tsurumi M, de Graaf RC, Verena T (2003) Distributional and Biological Aspects of Copepods at Hydrothermal Vents on the Juan de Fuca Ridge, north-east Pacific ocean. *Journal of the Marine Biological Association of the United Kingdom*, **83**, 469–477.

Tsurumi M, Tunnicliffe V (2001) Characteristics of a hydrothermal vent assemblage on a volcanically active segment of Juan de Fuca Ridge, northeast Pacific. *Canadian Journal of Fisheries and Aquatic Sciences*, **58**, 530–542.

Tsurumi M, Tunnicliffe V (2003) Tubeworm-associated communities at hydrothermal vents on the Juan de Fuca Ridge , northeast Pacific. *Deep Sea Research Part I: Oceanographic Research Papers*, **50**, 611–629.

Tunnicliffe V (2000) A documentation of biodiversity characteristics of the hydrothermal vent assemblages at High Rise ventfield, Endeavour Segment, Juan de Fuca Ridge. *Contract Report to Department of Fisheries and Oceans*.

Tunnicliffe V, Embley RW, Holden JF *et al.* (1997) Biological colonization of new hydrothermal vents following an eruption on Juan de Fuca Ridge. *Deep Sea Research Part I: Oceanographic Research Papers*, **44**, 1627–1644.

Tunnicliffe V, Garrett JF, Johnson HP (1990) Physical and biological factors affecting the behaviour and mortality of hydrothermal vent tubeworms (vestimentiferans). *Deep-Sea Research*, **37**, 103–125.

Tunnicliffe V, Germain CS, Hilario A Phenotypic plasticity and fitness in a tubeworm occupying a broad habitat range at hydrothermal vents. *Axios Review*.

Tunnicliffe V, Juniper SK, Sibuet M (2003) Reducing environments of the deep- sea floor. In: *Ecosystems of the World: The Deep Sea* (ed Tyler PA), pp. 81–110. Elsevier Press, Amsterdam, New York.

Tunnicliffe V, McArthur A, McHugh D (1998) A biogeographical perspective of the deep-sea hydrothermal vent fauna. *Advances in Marine Biology*, **34**, 353–442.

Turner TF, Wares JP, Gold JR (2002) Genetic effective size is three orders of magnitude smaller than adult census size in an abundant, Estuarine-dependent marine fish (Sciaenops ocellatus). *Genetics*, **162**, 1329–39.

Tyler PA, Young CM (1999) Reproduction and dispersal at vents and cold seeps. *Journal of Marine Biological Association of the United Kingdom*, **79**, 193–208.

Tyler PA, Young CM (2003) Dispersal at hydrothermal vents: a summary of recent progress. *Hydrobiologia*, **503**, 9–19.

Urcuyo I, Bergquist D, MacDonald I, VanHorn M, Fisher C (2007) Growth and longevity of the tubeworm Ridgeia piscesae in the variable diffuse flow habitats of the Juan de Fuca Ridge. *Marine Ecology Progress Series*, **344**, 143–157.

Urcuyo IA, Massoth GJ, Julian D, Fisher CR (2003) Habitat , growth and physiological ecology of a basaltic community of Ridgeia piscesae from the Juan de Fuca Ridge. *Deep Sea Research Part I: Oceanographic Research Papers*, **50**, 763–780.

Voight JR, Lee RW, Reft AJ, Bates AE (2012) Scientific gear as a vector for non-native species at deep-sea hydrothermal vents. *Conservation Biology : The Journal of the Society for Conservation Biology*, **26**, 938–42.

Vrijenhoek RC (1997) Gene flow and genetic diversity in naturally fragmented metapopulations of deep-sea hydrothermal vent animals. *The Journal of Heredity*, **88**, 285–93.

Vrijenhoek RC (2010) Genetic diversity and connectivity of deep-sea hydrothermal vent metapopulations. *Molecular Ecology*, **19**, 4391–4411.

Young CR, Fujio S, Vrijenhoek RC (2008) Directional dispersal between mid-ocean ridges: deep-ocean circulation and gene flow in Ridgeia piscesae. *Molecular Ecology*, **17**, 1718–31.

Young CM, Vazquez E, Metaxas A, Tyler PA (1996) Embryology of vestimentiferan tube worms from deep-sea methane/sulphide seeps. *Nature*, **381**, 514.

Zelnio KA, Thaler AD, Jones RE *et al.* (2010) Characterization of nine polymorphic microsatellite loci in Chorocaris sp. (Crustacea, Caridea, Alvinocarididae) from deep-sea hydrothermal vents. *Conservation Genetics Resources*, **2**, 223–226.

Zhang D-X, Hewitt GM (2003) Nuclear DNA analyses in genetic studies of populations: practice, problems and prospects. *Molecular Ecology*, **12**, 563–84.

Appendix

Appendix A - Lab protocols

Isopropanol DNA Purification – For DNA isolated from the PrepMan protocol

1. 2 volume of isopropanol (-20°C)
2. Store at -20°C overnight
3. Spin at 8000 rpm for 30 min at 4°C
4. Discard supernatant
5. 500 µL -20°C 70% ethanol wash and vortex
6. Spin at 14000 rpm for 15 min at 4°C
7. Dry for 10-20 min in fumehood
8. Re-suspend pellet in 200 µL sdH_2O
9. Heat at 56 °C for 15 min and vortex

Appendix B - Program scripts

Script used in PAUP* for likelihood analysis and mutation model comparison

Script was from the PAUP* tutorial delivered by David Swofford during the Molecular Evolution Workshop 2013

Heuristic search for optimal tree under the likelihood criteria with default model HKY with transitions over transversion ratio of 2.0 and unequal base frequencies (estimate empirically)
set criterion=likelihood;
hsearch;
describe;

Estimate the ti/tv ratio on the tree found in the previous step
lset tratio=estimate basefreq=estimate;
lscores;

*Combine the **LSet** and **LScores** commands into a single command (convenient when trying alternative models)*
lscores/tratio=estimate basefreq=estimate;

Fix the ti/tv ratio and base frequencies to the values you estimated in the step above and perform another heuristic search using the modified settings
lset tratio=previous basefreq=prev;
hsearch;
describe;

Using the tree topology found in the above search, fit models that assume that rates across sites are (1) gamma distributed, (2) equal rates at variable sites but with some sites invariable, and (3) both gamma-distributed rates and invariable sites.
lset tratio=estimate basefreq=estimate;
lscores/rates=gamma shape=estimate;
lscores/rates=equal pinv=estimate;
lscores/rates=gamma shape=estimate pinv=estimate;

To evaluate whether a simpler DNA substitution rate matrix (e.g., JC, F81, K2P) can explain the data adequately set up the model for among-site rate variation chosen above (i.e. model with the highest likelihood score):
e.g.
lset rates=gamma shape=est pinv=0;

Evaluate the JC+G, F81, and K80 (=K2P) models, respectively
lscores/nst=1 basefreq=equal;
lscores/nst=1 basefreq=estimate;
lscores/nst=2 basefreq=equal tratio=estimate;

Evaluate more complex DNA substitution models, the GTR and Tamura-Nei models, respectively:
lscores/basefreq=estimate rates=gamma shape=estimate nst=6 rmatrix=estimate;
lscores/rclass=(a b a a c a);

Assess models according to a likelihood ratio test

Script to run MIGRATE-N-MPI 3.6 on WestGrid computer clusters for Nestor

```
#!/bin/bash -l
#PBS -N test_migrate
#PBS -M lcpuetz@uvic.ca
#Where to send notifications
#PBS -m bea
#When to send notifications: b(egins), e(nds), a(borts)
#PBS -l walltime=70:00:00
#PBS -l procs=24
##PBS -l nodes=3:ppn=8
##openmp/thread-based programs
#PBS -l mem=20gb
#Total max memory required.

#PBS -j oe
#Combine both standard output and error output

##PBS -q nestor-test
#PBS -q nestor
##PBS -q hermes
#The queue to submit the job to.

cd $PBS_O_WORKDIR
module load migrate

mpirun migrate-n-mpi parmfile -nomenu >& log_${PBS_JOBID}.txt
#export OMP_NUM_THREADS=${PBS_NP}
#mpirun -np 3 -bynode migrate-n-mpi parmfile.testbayes –nomenu
```

Program script to generate multiple runs in for different replicate numbers in MIGRATE-N-MPI 3.6 on WestGrid computer cluster - Nestor

Program was designed to increase the number of replicates defined by the user in a batch run in order to identify the optimum number of replicates needed for data to converge in MIGRATE

```
#!/bin/bash -l
if [ "$1" == "-h" -o "$1" == "-help" -o "$1" == "--help" ]
then
        echo "./runAll_forward.sh strt end [suffix]"
        echo "      Where strt is first replicate number, end is the last replicate number,
                    suffix is the suffix of name of directory."
        echo "     The program generates multiple run for different replicate number in
                    migrate
                    starting from strt ending with end"
        echo  "     and increase replicate number by 10"
        exit
fi
strt=$1
end=$2
suffix=$3
if [ -z "$suffix" ]
then
  suffix="replicateA"
fi
echo $suffix
initwalltime=$((60*3600))
for ((rnum=$strt;rnum<=$end;rnum+=10,initwalltime+=10800))
do
 echo "The directory for the replica $rnum is ${suffix}_$rnum"
# rm -Rf ${suffix}_$rnum
 mkdir -p ${suffix}_$rnum
 cp hf.txt ${suffix}_$rnum/
 cp migrate.pbs ${suffix}_$rnum/
 sed -e "s/replicate=YES:[0-9]*/replicate=YES:$rnum/" parmfile >
${suffix}_$rnum/parmfile
 cd ${suffix}_$rnum
 echo "Submitting job using: qsub -l walltime=$initwalltime migrate.pbs"
 qsub -N hf_$rnum -l walltime=$initwalltime migrate.pbs
cd ../
done
```

Appendix C - Marginal likelihoods used to rank models in MIGRATE

Table A1: Log marginal likelihood values, log Bayes factors and model probabilities used to rank gene flow models among vent fields using High Flux samples

Model	Log marginal likelihood	LBF	Model Probability	Choice
F1: full	-988.69	0.00	0.92	1
F2: N → S	-998.58	-19.77	0.00	3
F3: S → N	-998.90	-20.42	0.00	4
F4: Panmictic	-991.20	-5.02	0.08	2

Table A2: Log marginal likelihood values, log Bayes factors and model probabilities used to rank gene flow models among vent fields using Low Flux samples

Model	Log marginal likelihood	LBF	Model Probability	Choice
F1: full	-1126.63	0.00	0.66	1
F2: N → S	-1131.54	-9.83	0.00	3
F3: S → N	-1131.91	-10.57	0.00	4
F4: Panmictic	-1127.31	-1.37	0.33	2

Table A3: Log marginal likelihood values, log Bayes factors and model probabilities used to rank models among habitat types (grouped high flux samples and grouped low flux samples) at Endeavour.

Model	Log marginal likelihood	LBF	Model Probability	Choice
H1: full	-1381.00	0.00	0.54	1
H2: HF → LF	-1382.14	-2.28	0.17	3
H3: LF → HF	-1388.52	-15.04	0.00	4
H4: Panmictic	-1381.62	-1.25	0.29	2

Appendix D - Microsatellite sequence data

Sample of partial sequence alignment for the R2D12[1] microsatellite locus (ClustalW sequence alignment)

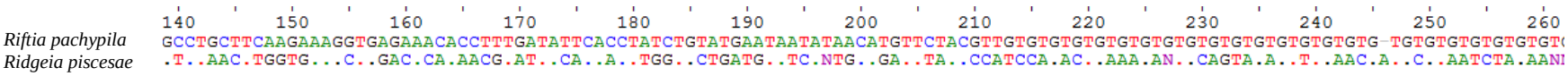

Microsatellite sequences

Sequence labels represent:

> (microsatellite locus)_(specimen ID)_(sequenced in the forward (F) or reverse (R) direction)

> Rpa10CA06[5]_R1138-07-02_F
AANGAGCTGTGCGATTATAACCGCATTTATATTTCTAATTTAAATAAGGATATGCCTAAG
GCGAGGAGACTGCTTGTGTGCATGTGCATGGGAATGTTTATGCTTGTGTTTTGCACTCAT
CTTCACGCANNNNNNNN

> Rpa10CA07[3]_R1138-07-02_F
GANGANGGTGANATNACATTTGTTGACGTATGTGAACAATAGACAAATATATAGTCAAGT
TGATCGTGTCGTCTCTGTTTTGACGTAGGTGTCTACGTGAGCAATACAATCAGATGGACT
CTGATCGCGTCGTCTCTGTTTGCGACTTTGAGGACA

>R2D12[1]_AD4412-2-15_F
GGGCAGTATCTTCAACAGTCTGCTTGGTGAAGCTGGACACAAAACGTATTACACAANNTG
NTGCTGATGTATCAAGCAGATTTAACCCATCCAGACTGAAAGAAAAACTACTGTCACACA
TGCCTAATCTAGAAGCCAACAAAACAACTATGAAGTAATACTCACATTCAATAAGAGACA
GATGCTAGGAAN

> R2E14[2]_AD4412-2-15 _F
ACNNGNACAAGANNGCAAAGTTGACAGCGCTTGAACAAAGATGGGCTGCGTCACTGGCAC
CATTCAACTTCGAGATACGGTATCNNCCTGGTCGAAGTAATGCAAATGCTGATGGATTGT
CACGGCTTGAATCCCACGAAGAGACCAATTTCAGCA

>E310A_AD4412-2-15 _R
NTNAGGTCAGAGGCATTGCCATACAGAAATGGTTAAGCCTGCAGAGTACACATCCATCTT
AGAGATGAGTAGGAAGATGTTGACGATCTCTTGACAGACATCGCTAGTGTCTTCTCTTCC
TTCCGTTGCTCATTGCGTTTCTGACGACGAGCCTTGTACTTAATCGGTTTCAGTTCGTTT
CATACAGATATTTAATTCTTTCTGAGTATCCTCTCTTGATAGATGTCACGGTAGGTGTCA
GTGTTCTTGTCTGTGCCCGTGTGTGCTTGTAAAGGGACGCCACTGTACAAATCAGAAGGA
CCTGCAACACAGATCGGTGACCAACATGCATAAATCAGCATGTATAGAAAAAAGCTATTN
NTCAAGGGATTCCGTTGTGTTGCTGN

> R3D3[3]_AD4412-2-15 _R
NTTNACNNNGNTACGTCGAAAACAGATTNGGNCAACATNTTTACNGTTTCAAANGCACAA
NTAATGTNCATTTCTCANNNTTGNNCGAATGANACACCGTGTATACACACGGGNNNTCCT
CGTNCGATATCAAGNNGTGGCCCNNGAAGAATGCCATCAAGATAGTTGATATAGNGGNTA
ANCAGTNGNGCAGAATACCACNNCTCATACAANCGCA

> ECL3-8D _R1138-07-2_R
NTTGCGTTGCTAACTGCCAAGTGGACGAACCTGTGCCATGATCATAGCAAGGCTCTGGAC
ACACGTCTTGCAATTGGGTGACGGTATCATAGATGCAATGCTTTAATTACGATGTTAAAG
TTGAATAACTTTCATATTCCGGTATGTACTACGACAGTTTATTACATATTGCTTCTAATG
GTCAAAGCATGAGTTCAATGATTTTATAGGGTATTTTGGTGGCCTTTGTTATTTTTAATG
GTGACACAGTTGTCGAATCCTTCCATTCGATTCCGTGTACCTAAAAACCTAGGTTATAAT
AGCCCAACATTACATNTNNNTNNNNGCTAAN